Seeing 3D surfaces: neural stimulation, learning and masking

Vassilis Pelekanos

A thesis submitted to the University of Birmingham

for the degree of Doctor of Philosophy

School of Psychology

College of Life and Environmental Sciences

University of Birmingham

June 2015

Abstract

Our everyday visual perception experience is of a richly detailed world full of bounded objects, slanted and extensive surfaces. Estimating surfaces' depth is critical for visually guided interactions, yet, challenged by the limited two-dimensional input projected on each eye's retina. Binocular disparity, the positional differences that objects project on the two retinae, is a powerful depth cue inducing stereopsis. In the present dissertation, I assessed the neural stages of the visual hierarchy that support the visual perception of disparity-defined three-dimensional (3D) surfaces. In the first experimental chapter (chapter 3), I used fMRI-guided rTMS to probe the cortical areas involved in the perception of slanted surfaces. Results hint at a functional contribution of the dorso-parietal visual stream (posterior parietal cortex; PPC) to slant estimation, however, further work is needed to fully understand the nature of its involvement. In chapter 4, I used fMRI-guided rTMS to show that stimulation-induced disruption of the ventral stream (area LO) eliminates the facilitation observed in 3D surface discrimination when disparity and motion cues inform depth in a congruent manner. This finding indicates that LO encodes signals for the integration of depth cues. In chapter 5, I found rTMS evidence that disparity and orientation signal-in-noise discriminations causally relate to the PPC's function. Interestingly, this relation diminished after training on a visual feature other than the one employed during the rTMS testing (e.g., testing on depth - training on orientation discrimination, or vice versa). This finding indicates that learning generalisation, even across visual features, can influence neuronal organization. In chapter 6, I used metacontrast backward masking to show that brightness masking incorporates the 3D information of disparity-defined slant. This finding suggests that brightness estimation is mediated by mid-level neuronal mechanisms, at a cortical stage where binocular signals have been combined to extract disparity edge structure. Finally, considering the eye-tracking data I acquired during rTMS experiments, I found that neural stimulation did not affect eye movements systematically. These supplementary results provide reassurance that participants' vergence was stable throughout the experiments and there was no stimulation-induced disruption of stereopsis.

Acknowledgements

First and foremost I would like to thank my PhD advisor Andrew Welchman. Thank you for all your contributions of time, guidance and ideas. Your enthusiasm for science and passion for your research have been extremely motivational for me. Even during tough times of my PhD, your professionalism and high quality working standards were strongly stimulating. I appreciate all the skills you taught me. Many of those are skills for life.

I am very grateful to Zoe Kourtzi for her advice and suggestions. Thank you for the insightful comments on my experiments and discussions about their inferences. Thank you for sharing your expertise in vision science in lab meetings and similar occasions. In general, thank you for your continuous support.

Special thanks to Hiroshi Ban. I will forever be thankful to you as a colleague, mentor and friend. Thank you for the endless discussions about my work, your tremendous help throughout my PhD, your astonishing kindness and your support. You have been my best role model as a scientist. Working with you has been a great honour and privilege.

I also thank all the past and present members of the lab. I will never forget the great moments we had in Birmingham for 2,5 years. Still, after the lab's relocation to Cambridge, the same brilliant environment and team-working ethos continued to be strongly influential and stimulating. I want to thank you for all the fruitful scientific discussions and of course for spending several hours to participate in my experiments. Special thanks to Matthew Dexter and Matthew Dyson for managing the lab in Birmingham and Cambridge respectively and providing very helpful technical support.

I thank all my friends, old and new ones. Sorry that I do not name you. You know who you

are! Thank you for sharing great moments and true feelings which I will forever appreciate. I would especially like to thank my parents and brother for always being there to discuss and offer wise advice about every possible aspect of my PhD life in the UK. Thank you for your love, fun and support.

CONTENTS

Page

LIST OF FIGURES

Page

LIST OF TABLES

LIST OF ABBREVIATIONS

2AFC	Two-alternative forced-choice
2D	Two-dimensional
2IFC	Two-interval forced-choice
3D	Three-dimensional
ANOVA	Analysis of variance
ARCMIN	Minute of Arc
ARCSEC	Second of Arc
BOLD	Blood oxygenation level-dependent
cd/m^2	Candela per meter squared
CRT	Cathode ray tube
CZ	The upper point of the skull (vertex)
DEG	Degree
EEG	Electroencephalography
FFA	Fusiform face area
fMRI	Functional magnetic resonance imaging
HZ	Hertz
ISI	Inter-stimulus interval
JND	Just noticeable difference
LCD	Liquid crystal display
LGN	Lateral geniculate nucleus
LO	Lateral occipital
MAE	Motion after-effect

MRI	Magnetic resonance imaging
MS	Millisecond
MSS	Method of single stimuli
MT	Medial temporal
OFA	Occipital face area
P3	The left hemisphere's posterior parietal cortex
P4	The right hemisphere's posterior parietal cortex
PPC	Posterior parietal cortex
PSE	Point of subjective equality
RDS	Random dot stereogram
rTMS	Repetitive transcranial magnetic stimulation
S	Second
SD	Standard deviation
SEM	Standard error of the mean
SOA	Stimulus onset asynchrony
TMS	Transcranial magnetic stimulation
V1	The primary visual cortex

1. General Introduction

The reflected light from the objects around us is captured by the eyes' pupils and directed to the retina at the back of each eye where a projection of the objects impinges. Photoreceptors, one of the retina's layers of nerve cells, convert light to electrical signals which are sent, through the optic nerve, to the brain's lateral geniculate nucleus (LGN) and then to the visual cortex.

The size of a small object's image on the retina (i.e., its visual angle) close to our eyes can be the same as the visual angle of a large object far away. However, we do not normally confound the physical size of an airplane miniature, for instance, and an airplane in the sky. Furthermore, although the raw input signal it receives from each retina is two-dimensional, the brain extracts a detailed three-dimensional (3D) structure of the world. Moreover, although neurons in the retina are sensitive in detecting contrast locally ('ON-type' and 'OFF-type' cells), this information cannot reliably predict properties in a more global context, such as the brightness of a surface, because, as Pessoa and Neumann (1998) note, dark-gray to middle-gray transition can have the same edge contrast as middle-gray to light-gray transition, for instance. Similarly, as Sinha and Adelson (1993) discuss, a change in surface color (a reflectance edge) and a change in surface orientation (that leads to a change in illumination- an illumination edge) can have identical luminance profiles. However, we effortlessly distinguish between the two situations. 'Lightness constancy', which has been studied extensively the last two centuries (Gilchrist, 2006), is another account for a similar phenomenon: it refers to the observation that our perception of the brightness of light and dark surfaces remains more or less the same despite the change in the luminance conditions (see paragraph 1.8 for the relevant terminology).

The above examples highlight the 'inverse problem' that the visual system is challenged by. That is, the visual system has to create a 'global' - complete representation of an image or a scene although the 'local' elements (for instance, the reflectance or

illumination edges) can have different perceptual interpretations. In other words, one of the challenges that the visual system has to respond to is to extract the properties of a scene (e.g., brightness, depth, motion, etc) although, often, these are not explicitly or completely available on the retinal images. Rather, after visual stimuli impinge on the retina, a series of processes is triggered in the brain where the nerve signals are finely processed to inform perception. The rich visual representation of the world seems to be the result of sophisticated dynamic interactions between lower-level visual processes (usually referred to processes at the retinal level) and higher-level ones (including cognitive processes that incorporate knowledge about materials, objects and scenes). In between, there is mid-level vision which involves mechanisms for the perception of surfaces, contours, grouping etc (Adelson, 2000; Cavanagh, 2011).

One means of studying the visual system and probing the mechanisms that support visual perception is to temporally interrupt the conscious awareness of visual stimuli. Such a manipulation allows one to examine the relationship between the perception of a stimulus and the physical substrate that processes the information that the stimulus conveys. As Breitmeyer, Ro, and Ogmen (2004) note, the application of visual mask stimuli to the retinal surface, or the application of transcranial magnetic stimulation (TMS) to the occipital lobe of the brain are two effective techniques for such a manipulation of stimulus awareness. In the experiments of the present PhD thesis, I used both TMS and visual masking, aiming to elucidate the mid-level neuronal mechanisms that support the perception of 3D surfaces.

In chapter 3, I employed TMS to probe the contributions of areas of the ventral and the dorsal pathway of the visual cortex to the estimation of surface slant. I presented surfaces around two baseline slants and measured slant discrimination thresholds while stimulation was applied to the areas of interest. In chapter 4, I investigated whether the neural processing at the ventral stream (area LO) encodes signals for the integration of qualitatively different cues to surface depth (disparity and motion). I tested whether disruptive TMS can diminish the behavioural advantage for estimating near/far surface

displacements when depth is informed congruently by disparity and motion. In chapter 5, I examined the role of visual learning in the cortical organisation that supports the estimation of depth. I compared the disruption that TMS causes in various surface detection tasks (feature difference / signal in noise) and visual features (orientation / depth), between before and after learning, to evaluate the re-organisation of the cortical circuit following visual learning's generalisation across those tasks and visual features. In chapter 6, I used masking to infer whether brightness estimation interferes with surface's slant at the monocular or the binocular stage of the visual pathway and assess whether brightness masking occurs before or after the convergence of binocular signals in the primary visual cortex (V1).

1.1 Depth perception: binocular disparity is a powerful cue

We live in a world full of bounded and occluded objects. Surfaces around us are extended in depth, usually slanted or tilted, and the ability to estimate their depth structure is crucial for visually guided interactions and object manipulation. Thereby, one of the most important missions of the visual system is to use the limited, two-dimensional, signal projected on each eye's retina to recover the scene's 3D geometry.

Since the invention of the stereoscope by Wheatstone (1838), it has been known that, for the human and many other species with frontally located eyes, binocular disparity is a powerful and reliable cue for 3D surface orientation perception (Nguyenkim & DeAngelis, 2003) and the perception of depth in general. Binocular disparity is the positional differences that the objects placed nearer or farther than the point we fixate our sight project on the two retinae, due to the horizontal separation of the two eyes. Depth perception based on binocular disparity is termed stereopsis.

Both horizontal and vertical binocular disparities exist, but it is the horizontal ones that inform the depth of a point relative to the fixation point (Anzai & DeAngelis, 2010). In the

present thesis, I use the term binocular disparity to refer to horizontal disparity. Binocular disparity can be further subdivided in absolute and relative disparity. **Figure 1.1** offers a cartoon illustration of absolute disparity: a point, either nearer or farther than the point where both eyes fixate, (for instance, a nearer point *N* in the figure) produces disparities between the two eyes. Absolute disparity is then defined as the difference in the angles by which the point N (or any other point nearer/farther from fixation) projects on the left and the right eye. As the figure shows, this difference corresponds to the differences in the distance between each eye's fovea (shown in yellow in the figure) and the retinal image of the (nearer/farther) point. Relative disparity, on the other hand, is the difference between the absolute disparities of two points. It, therefore, relies on absolute disparity signals and corresponds to distances between objects irrespectively of where the eyes are fixating (Patten & Murphy, 2012; Roe, Parker, Born, & DeAngelis, 2007).

Although stereopsis is the impressive outcome of the convergence of the two eyes' disparity signals in the brain, yet, other cues, which do not presuppose both eyes' viewing, provide useful information about depth (Boring, 1964). Such monocular cues are texture gradients, perspective, occlusion, relative size, shading and motion, and are successfully used by the visual system to infer depth even when we look a flat canvas like a painting, or when we look a scene with only one eye. For a detailed review of monocular depth cues, see Howard and Rogers (2002).

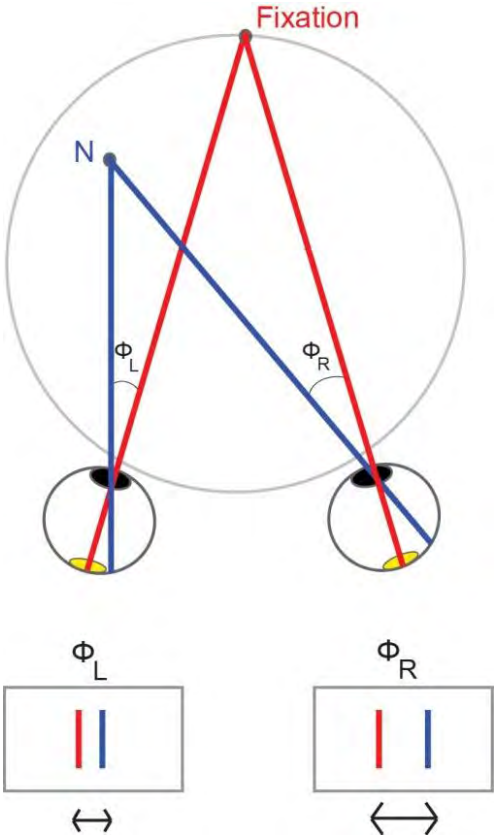

Figure 1.1: Binocular disparity (absolute). A top-down cartoon illustration of a viewer fixating at 'fixation' and an object located at the point N of viewer's left visual hemi field. Point N projects on slightly different anatomical areas on the retinae of the two eyes and binocular disparity of the point N equals ΦL *minus* ΦR. Binocular disparity of any point on the big grey circle (Veith-Muller circle) equals to zero.

1.2 The neurophysiology of binocular disparity

When leaving the retina, neural signals transfer to the visual cortex through the lateral geniculate nucleus (LGN) of the thalamus. Various centers of the visual cortex contain maps of the retina (Wandell, Dumoulin, & Brewer, 2007) and the spatial representation of a scene's features is preserved at the cortex (as well as at the LGN). However, there is no evidence for disparity selectivity in the LGN (e.g., DeAngelis, 2000; Preston, Li, Kourtzi, & Welchman, 2008). Since the information carried by the two eyes converges in individual neurons, for the first time, in the primary visual cortex, V1 is, thus, the first candidate in the visual pathway to process binocular disparity signals.

Indeed, V1 contains neurons selective for binocular disparity, as was first shown in the cat (Barlow, Blakemore, & Pettigrew, 1967) and the monkey (Poggio & Fischer, 1977). Intriguingly, Poggio and Fischer (1977) showed that the 84% of the neurons studied were sensitive in the location in depth of the stimuli used. More importantly, the researchers identified and classified four types of neurons: a) neurons with excitatory activations for stimuli placed nearer/farther than the fixation point b) neurons with inhibitory activations close to the fixation point c) neurons that responded to stimuli placed nearer and d) neurons that responded to stimuli placed farther than the fixation point.

Cumming and Parker (1997) sought to probe the neural basis of stereopsis and address the relationship between disparity selectivity in V1 and the perception of depth. As they reasoned, depth perception requires that image features on one retina are matched with appropriate features on the other retina. They employed the random-dot stereogram (RDS), developed by Julesz (1971), in which the two eyes see randomly positioned but binocularly correlated dots. Critically, though, Cumming and Parker (1997) used an anti-correlated stereogram, where the white dots in one eye are paired geometrically with the black dots of the other eye. The perceptual effect of such an inversion in dots' contrast is dramatic and the perception of stereoscopic depth is destroyed (Parker, 2007). This manipulation allowed for a sophisticated dissociation between the neural responses that a given stimulus triggers (neuronal selectivity for disparity) and the conscious sensation of the stimulus (depth). The researchers recorded activity from V1 neurons and reasoned that if neural processing in V1 is sufficient for stereopsis, then neurons in this area should respond only to the correctly registered geometry of the dots (i.e., only to the correlated RDS) and not to the false matches of the anti-correlated RDS. However, Cumming and Parker (1997) found that the disparity-selective neurons in V1 were activated by the anti-correlated dot stereogram, a result suggesting that neural activity in V1 is not sufficient for the perception of depth.

Neural correlates for stereopsis should be then traced in higher parts of the visual cortex (in extrastriate cortex i.e., beyond the 'striate' V1). Bakin, Nakayama, and Gilbert (2000) showed that neurons in area V2 are strongly activated by correct binocular disparity matches. Interestingly though, Bakin, et al. (2000) found that V2 neurons respond to disparity-defined illusory contours, a finding that sheds light on the neural substrate of surface segregation and modal completion (see paragraph 1.7) and its relationship to depth estimation mechanisms. Furthermore, area V3A, at the parieto-occipital junction (dorsal visual stream - see below), has been found to specialise in the processing of binocular disparity and to support stereopsis in both the human and the monkey (Backus, Fleet, Parker, & Heeger, 2001; Tsao et al., 2003). Other dorsal areas, adjacent to V3A, have also been reported as selective for depth structure and disparity signals (Tyler, Likova, Kontsevich, & Wade, 2006). Preston, et al. (2008) employed a machine learning classifier trained on functional magnetic resonance imaging (fMRI) data evoked by near/far depths. The researchers showed that when provided with fMRI responses from V1, the decoder was able to perform above chance for stimuli defined by both correlated and anti-correlated RDS. However, Preston, et al. (2008) found that there was preferential disparity selectivity in dorsal (V3A, V3B/KO, V7) and ventral (LO) areas for correlated stimuli. This selectivity for the perceptually relevant information of the correct dot matches of the correlated RDS poses to these dorsal and ventral visual stream areas a special role for the perception of depth. Recently, Goncalves et al. (2015) used ultra-high field fMRI to show that neurons in human V3A and V3B/KO are clustered according to their disparity sign preferences. This important finding suggests that disparity processing is supported by a systematically organised cortical architecture in dorsal visual cortex.

Neri, Bridge, and Heeger (2004), in an fMRI study, employed a sophisticated neural adaptation design to address whether distinct brain mechanisms support absolute and relative disparity computations. They found that cortical areas at the dorsal visual stream (V3A, V7 and MT+) were selective for absolute but not relative disparity, while ventral

stream areas V4 and V8 were equally selective for both absolute and relative disparities. Similar to their selectivity for absolute vs. relative disparity signals, another key parameter that probably dissociates the dorsal from the ventral stream is their specialisation in coarse and fine disparities respectively (see paragraph 1.3.2). Before reviewing the studies that suggest such a separation, it is worth referring to the anatomical and functional identity of the two streams.

1.3 The dissociation between the ventral and the dorsal visual stream

1.3.1 'What' versus 'where'

The visual cortex, anatomically, can be decomposed into two main pathways: the ventral which originates from area V1 and connects the primary visual areas with the inferior temporal cortex, and the dorsal pathway which originates from V1 and connects the primary visual areas with the inferior parietal cortex. It is believed that a functional dissociation between the two pathways also exists: the dorsal is supposed to specialise in the encoding of spatial features and relationships among objects locations ('vision for action'), while the ventral one specialises in the recognition of objects ('vision for perception'). The model of the two independent pathways, associating the spatial visual processing with the dorsal stream (usually referred as the 'where' stream) and the processing of objects qualities and features related to the form with the ventral stream ('what' stream), has been a plausible account of empirical findings in neuropsychology, brain imaging and neurophysiology.

In particular, much evidence for the functional separation of the two streams comes from neuropsychology (Goodale & Milner, 1992). In human patient studies, lesions after damage to occipito-temporal areas can result in visual agnosias, where the patient is unable to recognize faces and/or everyday objects. Prosopagnosia, in particular, the face-processing deficit, is the result of damage to the FFA or OFA 'face' areas at the occipito-

temporal pathway of the ventral stream (e.g., Dricot, Sorger, Schiltz, Goebel, & Rossion, 2008). On the other hand, damage to posterior parietal areas at the occipito-parietal stream results in difficulties in navigation and/or hemi-spatial neglect. For example, in optic ataxia, caused by damage to the posterior parietal cortex, patients are unable to accurately reach visual targets, although they have no deficit to recognize them (see Goodale & Milner, 1992 and Bell, Pasternak, & Ungerleider, 2014 for a recent review). Further, experimental support to the two-stream model in the human was first drawn with functional imaging by Haxby et al. (1991). The authors used Positron Emission Tomography (PET) to show bilateral activation of ventral and dorsal areas during a face-matching task and a spatial dot-location matching task respectively.

The separation of the two streams in the human is thought to be homologous to the anatomically and functionally distinct occipito-temporal and occipito-parietal pathways, already known to exist in non-human primates. In particular, lesion of monkeys' temporal (but not parietal) lobe pathway resulted in severe impairments on object discrimination tasks, whereas parietal (but not temporal) lesions resulted in impairments on spatial tasks about the locations of objects (Mishkin, Ungerleider, & Macko, 1983; Ungerleider & Mishkin, 1982). This functional dissociation can be traced back to the separation of the two layers in the LGN, namely the Magnocellular and Parvocellular layers, each carrying different types of signals, which can in turn be traced back to analogous subdivisions on the ganglion cells of the retina (Livingstone & Hubel, 1988). Support for this claim is offered by the fact that Magnocellular and Parvocellular layers remain segregated at the stage of V1, but they are the basic input to the middle temporal area MT and the ventral V4, respectively, which in turn constitute the major input to the posterior parietal cortex and the inferior temporal cortex, respectively (Goodale & Milner, 1992).

However, in recent years, such a one-to-one correspondence between the LGN layers and the cortical visual streams is under controversy. Further, the core assumptions derived from the hypothesis of the functional independency of the two pathways have been

challenged (Schenk & McIntosh, 2010), while the distinction between 'vision for action' and 'vision for perception' has been debated and revisited (Milner & Goodale, 2008).

1.3.2 'Fine' versus 'coarse'

In the domain of binocular depth perception, both pathways have been found to be selective for binocular disparity signals (e.g., Maunsell & Van Essen, 1983; Preston, et al., 2008). However, much attention has been drawn to the hypothesis that a functional dissociation between the ventral and the dorsal visual stream exists in disparity processing. Specifically, there has been recent evidence to suggest that ventral areas specialise in fine stereopsis (processing disparities within the range of 0.3 degrees in the human fovea), while dorsal areas contribute to coarse stereopsis (processing disparities greater than 0.3 degrees in the human fovea, Parker, 2007). Coarse stereopsis is thought to relate to segmentation processes and is often associated with 'coarse tasks' which involve discriminating between absolute disparity signal embedded in noise. Fine stereopsis, on the other hand, is thought to relate to stereoscopic acuity and to laboratory tasks requiring the discrimination of small feature differences in relative disparity, in the absence of noise (e.g., Chang, Kourtzi, & Welchman, 2013; Chowdhury & DeAngelis, 2008; DeAngelis, Cumming, & Newsome, 1998; Uka & DeAngelis, 2003, 2006).

Uka and DeAngelis (2006) found that microstimulation of dorsal MT neurons does not affect fine disparity depth discriminations, but does affect depth judgements in a coarse disparity task where depth signal is embedded in noise. Similarly, Chowdhury and DeAngelis (2008) found that (prior to visual learning; see chapter 5) temporary pharmacological inactivation of dorsal MT caused a dramatic impairment in the discrimination between coarse absolute disparities, but had no effect on fine stereopsis. In a human transcranial magnetic stimulation study, Chang, Mevorach, Kourtzi, and Welchman (2014) recently showed that (prior to visual learning; see chapter 5) neural processing in the left dorso-parietal cortex is

critical for visual discrimination in a signal in noise depth task. In a human fMRI study, Minini, Parker, and Bridge (2010) compared the responses of early occipital, ventral and dorso-parietal areas to different disparity ranges. The researchers found that the dorsal areas showed the greatest response to depth modulations elicited by large changes of disparity magnitude, suggesting that the dorso-parietal pathway may be more sensitive in depth discriminations defined by large-coarse disparities. On the other hand, electrophysiological evidence has suggested that the ventral cortex is selective for fine disparities. Specifically, the disparity-tuned neurons contained in ventral area V4 and in the inferior temporal cortex have been found to selectively respond to feature difference ('fine') depth discrimination tasks (Shiozaki, Tanabe, Doi, & Fujita, 2012; Uka, Tanabe, Watanabe, & Fujita, 2005).

1.4 Seeing 3D surfaces: slant estimation

According to Gibson (1950), surfaces have some essential qualities which can be summarized as follows: edge/contour, solidity to vision and to touch, extended color (brightness, hue and saturation) and slant. Slant is, indeed, a fundamental property of surfaces and its estimation is a necessary skill for the manipulation and estimation of objects' position in three dimensions. Slant can be defined as the angle between the line of sight and the normal to the viewed surface and it corresponds with the angle through which the surface is rotated from the frontoparallel plane (Banks, Hooge, & Backus, 2001; Stevens, 1983).

The estimation of slant can be perceived from the gradient of density of its texture among other cues. As Gibson (1950) notes, a textured image having the same density at all points would give the impression of no slant (i.e., a flat surface in the frontal plane). Gibson further suggested that the impression of the slant of a surface at any point depends on the rate of change of the density of its texture at that point on the retina and (according to the geometry of perspective) texture gets denser as the surface recedes. Indeed, Gibson

(1950) and Gibson and Cornsweet (1952) showed that as the density increases, the perceived optical[1] slant increases correspondingly.

However, the dependency of perceived slant on the density of the texture occurs when vision is monocular and the head is motionless (Gibson & Cornsweet, 1952). In normal binocular vision, disparity is another important cue for the estimation of slant. However, the slant of disparity-defined surfaces cannot be unambiguously estimated solely from horizontal disparities, but more sophisticated computations are taken into account. Specifically, it has been suggested that the vergence of the eyes, the vertical size ratio (VSR) and the horizontal gradient of VSR are signals that the visual system employs in order to extract slant about a vertical and about a horizontal axis (Backus, Banks, van Ee, & Crowell, 1999; Banks, et al., 2001).

Recent studies have examined the optimal ways the visual system uses to combine binocular disparity and monocular cues (like texture and retinal shape) in order to inform unambiguous estimations of surface slant (for example, Hillis, Ernst, Banks, & Landy, 2002; Knill & Saunders, 2003; Sousa, Brenner, & Smeets, 2009). Other researchers have investigated the cortical areas where such a cue combination is encoded: Murphy, Ban, and Welchman (2013) examined the integration of texture and disparity cues to slant discrimination, whereas Welchman, Deubelius, Conrad, Bulthoff, and Kourtzi (2005) investigated the integration of perspective and disparity. Results of these studies suggest that high parts of the visual cortex (for example, dorsal V3B/KO and hMT+, as well as ventral LO) are actively engaged in the combination of cues to slant estimation. Despite this recent interest in decoding the brain mechanisms that support the estimation of slant informed by combined cues, our knowledge of how disparity-defined slant is encoded by the disparity-selective ventral and dorsal cortical areas is still limited. Aiming to address this question, I used fMRI-guided TMS in the first experimental chapter of the thesis (chapter 3).

[1] Gibson and Cornsweet (1952) have made a distinction between optical slant (e.g., that of a bounded surface) and geographical slant (e.g., that of a continuous plane surface which fills most of the visual field).

1.5 Cue integration

As already mentioned, apart from binocular disparity, a number of monocular cues are on the visual system's disposal to recover the depth structure of a scene. The process of integrating different cues to inform depth, although computationally challenging, produces a coherent and robust 3D representation of the environment. In the domain of surface slant for instance, as it was mentioned in the previous paragraph, recent studies have examined the integration of different cues to depth structure (e.g., Knill & Saunders, 2003) and suggested that sensory cues can be combined optimally to result in more accurate depth estimations compared to the presentation of one cue alone (Schiller, Slocum, Jao & Weiner, 2011; but see also Hillis, et al., 2002). Recent neuroimaging studies have investigated the brain mechanisms that support the integration of disparity with other depth cues, as diverse as relative motion (Ban, Preston, Meeson, & Welchman, 2012) shadow (Dovencioglu, Ban, Schofield, & Welchman, 2013) and texture (Murphy, et al., 2013). In chapter 4, I used fMRI-guided TMS to probe the cortical site where disparity and motion integrate to facilitate 3D judgments.

1.6 Visual learning and performance optimization

Experience and practice enhances the ability to make perceptual discriminations in the features of visual stimuli, a phenomenon known as visual perceptual learning (Gibson, 1953). Visual learning is thought to be implicit i.e., it is effective even without awareness and conscious effort during or after training (Gilbert, Sigman, & Crist, 2001). For example, Di Luca, Ernst, and Backus (2010) found that exposure to a vertical disparity gradient which was masked by other depth cues (and hence rendered invisible) influenced the perception of an ambiguous rotating cylinder stimulus. This result indicates that exposure to a novel contingency between an invisible sensory cue (masked disparity gradient) and an established percept (rotation direction of the cylinder) can influence the visual system to

learn a new use for this depth cue and eventually influence the otherwise ambiguous perception. Performance improvement in visual learning has been suggested to involve two separate mechanisms, namely, external noise filtering and stimulus amplification/enhancement (Dosher & Lu, 1998, 1999). Dosher and Lu (2005) further showed that the type of training influences the effectiveness of these mechanisms: training on a high-noise display was found to affect the external noise filtering mechanism only, whereas training on a protocol involving low-level noise affected both external noise filtering and stimulus amplification mechanisms.

In the past decades, it was believed that within a period early in postnatal life, the visual cortex has the capacity to undergo experience-dependent or learning-dependent changes, a period known as critical period (Gilbert, et al., 2001). However, it has been recently shown that neural changes are induced even in the adult cortical circuits as a function of training and practice (Sasaki, Nanez, & Watanabe, 2010). Specifically, visual learning can induce changes in the adult primary visual cortex (although higher cortical areas are believed to undergo practice-induced changes), while the nature of the change has been suggested to depend on the type of task and its difficulty (e.g., Ahissar & Hochstein, 1997; Sasaki, et al., 2010). Recently, visual learning was shown to facilitate recognition and optimize the tuning of neurons in cortical areas of the ventral visual stream in both the human (Li, Mayhew, & Kourtzi, 2009) and the monkey (Adab & Vogels, 2011; Raiguel, Vogels, Mysore, & Orban, 2006; T. Yang & Maunsell, 2004).

Chang et al. (2014) showed that training can cause changes in the circuit that supports visual discrimination in noisy and clear displays: they report a cortical reorganisation as a result of training on a feature differences discrimination depth task. In particular, they found that, after training, neural processing of disparity in the ventral stream (LO) substitutes the otherwise necessary processing in the left parietal cortex during the discrimination of depth signal embedded in noise. In chapter 5, I, similarly, employed the optimization effects of visual learning, together with TMS, to explore whether such a ‘neural

shift' due to training exists not only within depth paradigms, but across visual features as well.

1.7 'Filling-in' and surface perception

The volume of solid objects is delimited by surfaces and the first step in object recognition is to separate surfaces from their background (Gibson 1950). As Gibson stresses, the experience of objects is made possible by the fact that most of the surfaces of the phenomenal world are delimited and they separate from their background by a closed contour/edge. In the physical world, however, objects are very often occluded and degraded. Nevertheless, we do not perceive the sparse information of segmented lines and fragments that fall on the retinae, but our visual sensation of the world is rather rich. How does the brain infer complete surfaces and objects, despite the incomplete input on the retina? One possibility is that 'filling-in' mechanisms interpolate information to areas in which information cannot be measured (e.g., the retinal blind spot) or has not been measured (e.g., internal portions of objects). As Pessoa, Thompson, and Noe (1998) note, perceptual filling-in is a term describing the interpolation of missing information of critical parts of the visual space.

There are many sorts of such 'perceptual completions' and the phenomenon takes place under many occasions and surface configurations. Filling-in the retinal blind spot is a well-studied case, where the visual attributes present in the surrounding visual field fill the center of a stimulus, although the latter falls at the retina's blind spot which lacks photoreceptors (Ramachandran, 1992). During normal vision, as we interact with our environment, we perceive surfaces behind occluding objects as complete and coherent, rather than as pieces and fragments, because the visual system makes an 'amodal' completion. On the other hand, 'modal' (or 'boundary') completion is thought to occur when one view specific laboratory stimuli, like the *Kanizsa* illusory contours (e.g., Anderson,

Singh, & Fleming, 2002; Kanizsa, 1979; Pessoa, et al., 1998). In a typical Kanizsa figure, the co-alignment of incomplete black circles induces the illusory perception of bright contours. Other well-known stimulus configurations that induce illusory perceptions are the *Craik-O'Brien-Cornsweet* and *neon color spreading* illusory surfaces. When viewing the *Craik-O'Brien-Cornsweet illusion*, observers interpret isoluminant areas as having different brightness due to the luminance intensity ramps at their edges. In *neon color spreading*, the color of a real image spreads to create the illusory perception of a colored surface (for a recent review, see Weil & Rees, 2011). In other specifically arranged stimuli, perceptually salient targets in peripheral vision fade away and gradually disappear, following fixation at a central point. This sort of filling-in was first identified in the early 19th century (*Troxler fading)* and can become more striking if the background is replaced by twinkling texture ('artificial scotomas'; Ramachandran & Gregory, 1991), or by a rotating grid ('motion induced blindness'; Bonneh, Cooperman, & Sagi, 2001). All the above visual phenomena demonstrate that, although present only in the surround or borders of a surface, visual features spread to other parts of the visual field and are reported as being present at the centre of the surface. In this respect, the brain is thought to employ a propagation mechanism whereby attributes encoded at one portion of the scene (e.g., contrast edges) influence another portion (e.g., the central part of a surface) (Anstis, 2010).

Such a 'propagation' hypothesis has partially been inspired by the classical studies of Hubel and Wiesel in the cat (Hubel & Wiesel, 1962) and the monkey (Hubel & Wiesel, 1968), which show that, in V1, there are more neurons with receptive fields at the edge of surfaces, and they respond more strongly, than there are neurons with receptive fields at surfaces' interior. (See also more recent studies, e.g., Friedman, Zhou, & von der Heydt, 2003). However, a matter of debate remains relative to the plausible ways that the activity of borders/edge neurons is associated and passed to the interior/filled-in percept. For instance, as Pessoa and Neumann (1998) note, are the bright contours that perceived in a Kanizsa stimulus caused by an associated pattern of firing in topographically organised

visual brain areas, such as cortical area V2? (For a more detailed discussion on this matter, see paragraph 1.9). Furthermore, a discrepancy exists relative to whether a 'featural' completion system exists independently of a 'boundary' completion one, or whether both systems are involved in surface appearance (e.g., Grossberg & Mingolla, 1985). Similarly, it is not fully understood whether a common mechanism underlies both modal and amodal completion (Anderson, et al., 2002; Kellman & Shipley, 1991), but I will not elaborate on these issues further as they are beyond the scope of the present thesis. Nevertheless, all the visual phenomena mentioned above involve completion processes and exhibit a common subjective phenomenology: the visual system forms a coherent representation of surfaces, objects and contours.

1.8 Surface brightness estimation

The estimation of how dim or bright a given surface is involves the translation of objective/physical properties to psychological/perceptual properties. For instance, the physical (and permanent) property of a surface that determines what percentage of light the surface reflects translates to the perceptual term of lightness. Similarly, the physical (but transient) property of luminance (i.e., the absolute intensity of light reflected towards an observer's eye by a surface) corresponds to the perceptual term of brightness (Adelson, 2000; Gilchrist, 2007).

The propagation of visual information from the edge towards the interior of a surface, as introduced in the previous paragraph, can be clearly demonstrated in the domain of brightness. **Figure 1.2** depicts a visual illusion in which the two small central square surfaces appear to have different shades of gray. However, these two patches have exactly the same shade of gray and identical photometric luminance. Different luminance exists only on their surrounding square surfaces. As a result, the central square on the right, which has a bright background, is perceived as darker than the left central square which

has a dark background. Similarly, in the Craik-O'Brien-Cornsweet illusory stimuli, a series of neighboring bars is perceived as having different brightness, although their luminance is the same everywhere except for their edges. Examples like these emphasize that contrast information does not retain at the edge, but spreads and influences the brightness of the entire region (Komatsu, 2008).

Given that early visual processing (e.g., in V1) extracts contrast and edge signals, the visual system is faced with the problem of estimating the continuous brightness of an enclosed surface. One possibility of how the continuous variation of brightness across the visual field is determined, as Pessoa and Neumann (1998) suggest, is that it obtains a unique, smooth brightness distribution from the set of local contrast measurements. At the neural level, this can be accomplished through neural spreading processes (see next paragraph).

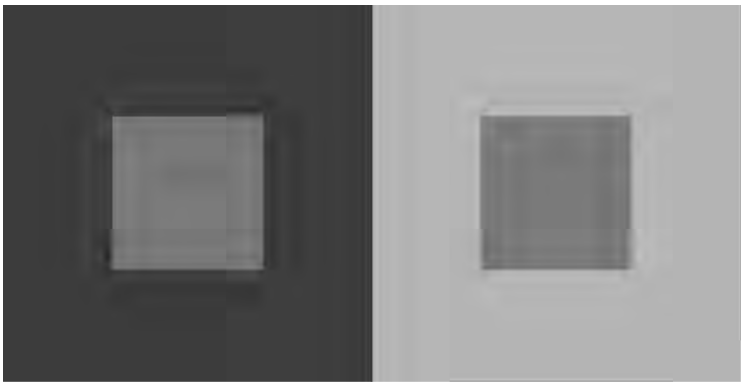

Figure 1.2: Simultaneous brightness contrast (or brightness induction): although they have exactly the same luminance, the small central squares look as they have different brightness due to the difference in the luminance of their backgrounds.

1.9 Neural mechanisms for perceptual completion

A great controversy about perceptual 'filling-in' and completion phenomena relates to (the existence or not of) their neural substrates (e.g., Pessoa, et al., 1998). This controversy

actually reflects a long-standing philosophical debate relative to whether a one-to-one correspondence between neural processes and perceptual states actually exists. In vision science, one view claims that the visual system simply ignores the absence of neural representations and labels the relative region with the information in the surround (symbolic or cognitive theory; see, for example, Anstis, 2010; Pessoa, et al., 1998). On the other hand, the *isomorphic* theory proposes that a spread of activation takes place across the retinotopic map of early visual areas from the border to the interior of the filled-in surface. According to Pessoa and Neumann (1998), such a 'neural filling-in', where an 'active' spreading process occurs in topographically organised early visual areas, is the mechanism that accounts for many well-known completion phenomena. Experimental evidence to support this theory can be drawn, for example by De Weerd, Gattass, Desimone, and Ungerleider (1995): having made a sophisticated correlation between the time course of filling-in and the firing rate of neurons, the researchers showed that, after a few seconds of fixation at an artificial scotoma stimulation, neurons in early visual areas (V2 and V3) increased their activity which gradually became comparable with the activity produced during the viewing of a similar (control) stimulus which did not trigger any filling-in process.

A common finding among behavioral, human neuroimaging and animal electrophysiology studies is that perceptual completion engages early visual areas (mainly V1 and V2), although this is often with some contribution from higher areas (Bartels, 2014; Komatsu, 2006; Weil & Rees, 2011). Nevertheless, it seems that a definite answer relative to whether surface filling-in is associated with isomorphic neural filling-in processes has yet to be given, and probably depends on the surface features each time at hand. In fact, two important questions need to be addressed: Firstly, what are the relative contributions of 'early' and 'higher' visual brain areas? Further, as it is commonly believed that ordinary and filled-in surface perception share common underlying neuronal mechanisms (e.g., Komatsu, 2006) the second question has to do with where in the brain this sharing starts.

Paradiso and Nakayama (1991) examined whether the (neural) interpolation mechanisms that occur during brightness filling-in also play a role in brightness perception during normal vision. The basic idea was that if filling-in involves the spread of activity from the border of a surface towards its interior, then it must be possible to demonstrate the existence of filling-in mechanism by interrupting it. The researchers adopted a masking paradigm in order to achieve such an 'interruption'. They found that the perceived brightness of a uniform target stimulus is dramatically suppressed because of the subsequent presence of a masking contour within the boundaries of the target stimulus. Moreover, the suppressive effect of the mask was greater and more delayed as the target increased in size, indicating that the latest time at which masking is effective increases as the distance between the target and the mask increases. This provides further support to Paradiso and Nakayama's (1991) basic finding that the mask interferes with a process which begins at the target's edge.

Murakami (1995), on the other hand, investigated whether the motion after-effect (MAE)[2] could occur after prolonged observation of filled-in motion at the blind spot. After being adapted to filled-in motion at the one eye's blind spot, participants were presented with a stationary grating in the visual field corresponding to that eye's blind spot, but through the other eye. Murakami found that MAE was experienced even though participants were adapted only to filled-in and not to real motion. This result indicates that filled-in and real motion perception share the same neuronal mechanisms. MAE is thought to occur within retinotopical organization of the visual field adapted (Wohlgemuth, 1911). Also, it "gives rise to interocular transfer" suggesting, thus, that the adaptation takes place in a binocular processing stage (Barlow & Brindley, 1963). Taken together, these two facts suggest that Murakami's results further indicate that filled-in motion perception takes place

[2] A well-known visual illusion where prolonged adaptation to a motion of a particular direction causes a, subsequently presented, stationary scene to be perceived as moving to the opposite direction (e.g., Anstis, Verstraten, & Mather, 1998).

at a stage where there is retinotopic organization, but after the stage where the visual signals of the two eyes converge in V1.

Despite having adopted different methodologies and referring to different aspects of filling-in, if combined, the inferences of Paradiso and Nakayama (1991) and Murakami (1995) studies provide an interesting question that remains to be addressed: what is the stage of visual processing where surface brightness filling-in takes place? In other words, which parts of the visual pathway contribute to both brightness filling-in and brightness perception during normal vision? Could it be the case, for example, that brightness estimation incorporates binocular mechanisms and is mediated by mid-level neuronal mechanisms at a stage where a surface's depth has been extracted? I used masking to investigate this question in the last experimental chapter of the present thesis (chapter 6).

2. General Methods

2.1 Participant recruitment, screening and ethics

All the observers who participated in the experiments of this thesis were students or staff of the University of Birmingham (experiments in chapters 3, 4 and 6) and students of the University of Cambridge (chapters 5 and 6). All participants had normal or corrected-to-normal vision and had not any known history of neurological disorders. They were screened for their stereo vision acuity (ability to discriminate depth positions defined by at least 1 arcmin of horizontal disparity) and/or for any possible contradictions to TMS and fMRI scanning where applicable. They gave written informed consent prior to their participation and received monetary compensation for their time. All studies were conducted according to the protocol ethically approved by the University of Birmingham's STEM ethics committee and the Psychology Research Ethics Committee of the University of Cambridge.

2.2 Monitors configuration and gamma calibration

Stimuli in all experiments were viewed binocularly, through a mirror stereoscope (Wheatstone, 1838). The stereoscope's two mirrors were positioned close to the eyes and had such an angle so that each eye viewed an image from a separate LCD (chapters 3, 4, 5) or CRT (chapter 6) monitor, from a distance of 50 cm. All monitors were gamma corrected and luminance calibration was achieved by linearizing grey-level values using a Minolta LS110 photometer and/or a Brontes spectrophotometer. Actually, the linearized gamma (look-up table) was imported to the stimulus presentation software (Psychophysics Toolbox; see below) on each experiment, and the gamma calibration was applied directly. The presentation monitors' luminance was regularly calibrated to reassure that stimulus luminance was constant across the separate sessions of a project.

2.3 Stimuli and data manipulation

All stimuli used in the experiments of this thesis were generated using Matlab (MathWorks) with extensions from the Psychophysics toolbox (Brainard, 1997; Pelli, 1997). Stimuli were presented via Matlab and Psychophysics toolbox, which allowed for the accurate control of stimulus presentation (e.g., timing, independent manipulation of the images presented to each eye, providing feedback where applicable etc) and recording of participants' responses. Brain imaging data were analyzed using Brainvoyager QX software (see paragraph 2.5). Eye movements were recorded with an EyeLink 1000 eye tracker (SR research; see paragraph 2.7) controlled by the EyeLink toolbox (Cornelissen, Peters, & Palmer, 2002). All data were plotted using Matlab and Adobe Illustrator was used for further, fine tuning of the graphs' appearance. Psychometric functions were fitted to the data using the Psignifit toolbox in Matlab. Statistical analyses were conducted in SPSS (IBM) and power analyses were conducted in GPower (Faul, Erdfelder, Buchner, & Lang, 2009; Faul, Erdfelder, Lang, & Buchner, 2007).

2.4 Transcranial magnetic stimulation

TMS is a technique applied for the non-invasive stimulation of the brain and is widely used in basic and clinical research in the neurosciences. TMS machine delivers a large current in a short period of time. In the magnetic coil, which is placed on one's scalp, a magnetic field is produced which induces an electric field eventually delivered to the brain (Hallett, 2007; Walsh & Cowey, 2000). The electric field is considered sufficient to stimulate neurons of a particular and restricted brain area, so that the normal processing of that area is transiently interrupted. Although there is a debate regarding whether this interruption must be attributed to the decrease of the strength of neurons' signal (e.g., Harris, Clifford, & Miniussi, 2008; Ruzzoli et al., 2011), or to the increase of neural noise (e.g., Ruzzoli, Marzi,

& Miniussi, 2010, but see also Miniussi, Ruzzoli and Walsh, 2010), TMS can successfully manipulate neuronal activity and cortical processing.

Designating the relationship between the brain and the cognitive functions is one of the primary goals in cognitive neuroscience. In vision science, in particular, researchers try to elucidate visual pathways and clarify how visual perception emerges from neural processing. To this end, TMS is a powerful technique: TMS experiments and data are usually treated within a transient 'virtual' brain 'lesion' framework (e.g., Walsh & Cowey, 1998) where an impaired behavioural performance is related and attributed to the transient 'lesion' of a particular cortical area having been TMS-ed. The putative contribution of an area to performing a specific cognitive task can be, thus, revealed (Miniussi, et al., 2010) and causal relationships between the brain and behaviour can be inferred.

However, TMS over an occipital visual area, apart from disrupting the area's function and reducing the sensitivity and neuronal responsiveness to presented stimuli, can also increase the excitatory responses of neurons and even result in the perception of illusory unstructured stimuli known as 'phosphenes' (McKeefry, Gouws, Burton, & Morland, 2009; Meyer, Diehl, Steinmetz, Britton, & Benecke, 1991). Recent studies have shown that the excitation of neurons induced by TMS can facilitate visual detection in some tasks (e.g., Abrahamyan, Clifford, Arabzadeh, & Harris, 2011; Chanes, Chica, Quentin, & Valero-Cabre, 2012). Parameters like the timing of overall stimulation and onset of pulses, the intensity and number of pulses, the area of stimulation, or the coil-to-cortex distance can affect the TMS outcome (Rubens & Zanto, 2012). Essentially, such parameters determine whether TMS will enhance or impair a cognitive function by facilitating or suppressing cortical function respectively. Apart from the above 'technical' parameters of a TMS protocol, neural architecture and biological constrains are also important: as Miniussi, et al. (2010) note, it is the relation of the stimulated area to the general network engaged on a task that really determines whether the final behavioural performance will be impaired or enhanced. Along these lines, as Silvanto and Pascual-Leone (2008) stress, the initial state

of an area also plays a critical role in the neural impact that a stimulus will have on that area.

In the experiments reported in chapters 3, 4 and 5, I used online repetitive TMS (rTMS), where repetitive trains of 5 pulses were applied on each trial. The stimulator output level was at 60% of maximum intensity which is considered sufficient to induce suppression of activity during the first 100-200 ms (Silvanto & Pascual-Leone, 2008). Also, this particular TMS protocol has been shown to successfully induce disruptive effects on a depth discrimination task employed by our group previously (Chang et al., 2014). None of the participants in my experiments reported the perception of phosphenes, which somehow suggests that any excitatory responses of the neural activity due to the application of TMS were unlikely.

2.5 MRI imaging and analysis

In the experiments in chapters 3, 4 and 5, I employed TMS to disrupt the normal neuronal function of the cortical areas of interest, aiming to draw causal links between the stimulated area(s) and depth discrimination performance. However, the accurate targeting of the area must be first ensured in order to identify such a causal relationship and infer the contribution of a cortical area to a cognitive task. One means of achieving an accurate localisation (and ultimately stimulation) is to employ brain imaging before applying TMS: the visual areas are first identified on their retinotopic and/or functional basis with functional brain imaging (fMRI), and then stimulated with TMS. This type of TMS is called fMRI-guided or neuro-navigated TMS (McKeefry, et al., 2009; Sack, Kohler, Linden, Goebel, & Muckli, 2006) and is the type of TMS I used in chapters 3 and 4.

fMRI scans used to localise the visual areas of interest (localizer scans) took place at the Birmingham University Imaging Centre, using a 3 Tesla Philips MRI scanner with an eight-channel radiofrequency head coil. A multi-slice 2D gradient echo planar imaging

sequence [repetition time (TR) was 2 s, 32 slices per volume, 1.5X1.5X2 mm voxel size resolution] was used to measure blood oxygenation level-dependent (BOLD) signals. For each participant, T1-weighted 3D anatomical images (1X1X1 mm resolution) were used for co-registration.

During the fMRI localiser scans, I mapped the visual cortex both retinotopically and functionally using standard fMRI procedures. Irrespectively of the areas I was interested in stimulating in each experimental chapter (i.e., PPC, V3A, LO, in chapter 3; LO in chapter 4), retinotopic areas V1, V2, V3d, V3v, V3A, V7 and V4 were identified for each participant using rotating wedge stimuli (Sereno et al., 1995) to identify visual field position. Area V3B/KO was mapped retinotopically as the region with a full hemifield representation in the lateral direction from the foveal focus of V3A (Tyler, et al., 2006). Because V3B/KO is also defined functionally using the voxels that respond to kinetic boundaries more than to transparent motion or to luminance-defined gratings, as area KO does, (Van Oostende, Sunaert, Van Hecke, Marchal, & Orban, 1997 -but see also Zeki, Perry & Bartels, 2003) we call it V3B/KO (Ban, et al., 2012). Area V5/MT was defined as the set of voxels at the occipito-temporal cortex responding more to coherently moving dots relative to a static set of dots (Zeki et al., 1991). Finally, area LO was defined as the area in lateral occipito-temporal cortex having greater response to intact than scrambled images of objects (Grill-Spector, Kushnir, Hendler, & Malach, 2000; Kourtzi, Betts, Sarkheil, & Welchman, 2005; Malach et al., 1995). For detailed reviews on the functional specialization of the visual areas and the contemporary methods for dissecting them, see Grill-Spector and Malach (2004); McKeefry, et al. (2009); Press, Brewer, Dougherty, Wade, and Wandell (2001).

For the analysis of brain imaging data, I used Brainvoyager QX software, version 2 (Brain Innovation). Data from functional scans were preprocessed using three-dimensional motion correction, slice time correction, linear trend removal and high-pass filtering. The anatomical scans were transformed into Talairach space, with inflation of the cortex to create flattened surfaces of both hemispheres. The functional runs of each participant were

aligned with their anatomical scan and transformed into Talairach space. Both left and right hemispheric coordinates were assessed.

2.6 fMRI-guided TMS protocol

In all the experiments involving TMS, biphasic magnetic pulses were delivered through a 70 mm figure eight-shaped coil connected to MagStim rapid magnetic stimulator (MagStim Company). For each TMS session, the position of the coil was held constant by a coil holder, and TMS pulses were initiated using Matlab (Mathworks). To navigate the magnetic coil to the functionally localized areas V3A and LO (chapters 3 and 4), I used Brainsight (Rogue Research Inc): it is a neuro-navigation system which tracks the head's and the coil's positions and overlays this information on the anatomical MRI scan of the participant. Magnetic coil's position over the posterior parietal cortex (PPC; chapters 3 and 5) was identified and guided through the 10-20 EEG coordinate system (P3 corresponds to left PPC and P4 corresponds to right PPC). The vertex (area CZ) was defined and localized as the upper point of the skull, at the middle point between nasion and inion, halfway between the two ears. The coil was placed over CZ in parallel to the scalp.

On each trial, I delivered 5 successive pulses at 10 Hz (i.e., each pulse lasting for 100 ms) administered either simultaneously with, or just before, the visual stimulus onset. Whether TMS pulses are, or are not, synchronized with the visual stimulus' onset has been a critical factor to determine the effect of TMS on a cortical function (see above). Therefore, the timing of the pulses was manipulated according to the research hypothesis of each individual experiment. Each rTMS session was split in two parts, in the intermission of which I replaced the TMS coil. The rationale for replacing the coil was twofold: (a) to avoid the coil's overheating and conform to safety standards for TMS stimulation; (b) to allow some rest time to the participants. After placing the coil over the area of interest, and prior to starting an experimental session, I delivered to every participant a few single pulses.

This was done, at first, in order to examine whether stimulation induced the perception of phosphenes. Secondly, in order to evaluate whether the coil-to-head distance and the participant's sensation of the pulses were appropriate.

2.7 Eye tracking

Visual processing of the incoming stimuli relies on precise movements of the eyes. Through the sophisticated coordination of the visual and the motor system, eye movements provide the brain with the necessary (and constantly updated) visual information. For instance, the encoding of different portions of the scene in high resolution is allowed through saccades where the eyes move rapidly to guide portions of the scene to the fovea. Another major type of eye movements is vergence eye movements (Henderson, 2006). Vergence is the simultaneous movement of the two eyes in opposite directions in order to direct the two eyes' foveae to a common point in depth and maintain single binocular vision. Fixation of near objects is termed 'convergence' and fixation of far objects 'divergence'. Therefore, vergence is important for accurate binocular vision in 3D tasks and stereopsis (Welchman & Harris, 2003b - but see also Lugtigheid, Wilcox, Allison & Howard, 2014).

A wide network of cortical brain areas is involved in eye movement control (Pierrot-Deseilligny, Rivaud, Gaymard, Muri, & Vermersch, 1995). Stimulating the cortex with TMS may disrupt eye movement control and fixation because of possible side-effects on the eye-muscles control. The posterior parietal cortex (PPC) has been reported to be involved in the control of vergence eye movements in particular (e.g., Gnadt & Beyer, 1998; Q. Yang & Kapoula, 2004). In the experiments reported in chapters 3 and 5, I applied rTMS over the PPC. Therefore, in order to control for any possible TMS-induced vergence disruptions, I recorded the participants' eye movements on-line during TMS (and during some no TMS sessions).

I recorded binocular eye movements using an EyeLink 1000 eye tracker (SR research) on a sampling rate of 500 Hz. Participants' eyes were viewed by the eye tracker camera, through the mirrors of the stereoscope, by infrared transmission. Eye position was calibrated at the beginning of a session where participants were gazing at a calibration target which was drifting on 9 default (chapter 3) or customized (chapter 5) positions around the screen. During each experiment, participants were instructed to maintain fixation at the centre of the screen, on a square marker, which was, however, shifting horizontally (1 deg to the right, back to the centre, 1 deg to the left and back to the centre) every 10 trials to regularly re-calibrate and inform the eye tracker for eyes' position. Eye movements were not recorded for participants who wore glasses, because glasses often cause the distortion of reflections of the cornea. I removed any eye-tracking data in which the eye tracker failed to determine pupil-corneal reflections, as was, for example, the case with some participants wearing contact lenses. Further, I discarded the data in which tracking signal was lost for any of the two eyes or both.

I pre-processed and excluded data that contained blinks and saccades (as identified by EyeLink's default functions) via a custom Matlab script and MS Excel functions. I defined horizontal vergence as the difference between the two eye's horizontal positions (right minus left) at each sample, with regard to the fixation at the centre of the screen (e.g., Chang, et al., 2014; Lugtigheid, Wilcox, Allison, & Howard, 2014; Q. Yang & Kapoula, 2004), and converted the raw X coordinate data (screen's pixels) to degrees of visual angle. Vergence data were parsed into time frames corresponding to each trial within a session, and the data from every single trial were automatically plotted by the same Matlab script I also used for pre-processing. Subsequently, I averaged and plotted vergence data across all trials within a session to assess whether parietal stimulation (as compared to CZ stimulation and to no TMS sessions) induced any systematic differences in vergence. Visual inspection of the data (both on the individual-trial and the average-of-all-trials basis) did not show any systematic differences in the vergence eye movements induced by TMS,

in accordance with Kapoula, Isotalo, Muri, Bucci, and Rivaud-Pechoux (2001). In particular, vergence for most of the participants showed similar fluctuation patterns between PPC stimulation sites and the control sessions. For representative graphs and further discussion on the eye tracking data, see the appendices of chapters 3 and 5.

2.8 Method of single stimuli

The method of single stimuli (MSS) is a psychophysical method variant of the method of constant stimuli and the two-alternative forced-choice (2AFC): instead of explicitly presented with a reference stimulus-to-be-compared with the test stimulus on each trial, participants are presented with the test stimulus only and required to compare it with the (mentally preserved) mean intensity of the set of all stimuli. Previous studies have successfully employed this method: Morgan, Watamaniuk, and McKee (2000), in a task requiring the estimation of separation between horizontal lines, found that the thresholds measured with the MSS were as precise as the ones measured with the method of constant stimuli (at least, if 20 practice trials were provided). The test stimulus was presented for 1 s in a single interval alone and observers judged whether the test was larger or smaller than the implicit mean of the set. Nachmias (2006), in a paradigm where observers judged the ratio of spatial extents in simple visual patterns, found that performance in one-interval trials using the MSS was even better compared to the method of constant stimuli.

However, the method of single stimuli can have some drawbacks and limitations. At first, the first few presentations of the stimulus set may be thought of as learning trials where participants develop some concept of the stimulus continuum (Rambo, 1961). Indeed, it is reasonable to expect that, during the first trials, participants try to estimate where the mean intensity of the stimulus set is and their responses, therefore, might not be reliable. In chapters 3 and 4, where the MSS was used, participants were trained

extensively on the MSS task before taking part in the main experiments. The training phase of the experiments has provided reassurance that participants could reliably perform the MSS task throughout the main experiments (see chapters 3 and 4).

Additionally, the MSS can be prone to serial effects depending on the order that stimuli are presented. As Rambo (1961) discusses, for example, judgments made in a series in which the lower extreme of stimulus intensity precedes the remainder of the stimulus series would generally be higher than those obtained from judgments of a series in which the higher end of the stimulus range was presented first. Indeed, Parducci (1959), in a study where stimuli presented and judged in ascending and descending series, found that responses were shifted towards the end of the stimulus series presented first and this finding was consistent with the results that Rambo (1961) obtained as well. To overcome such a potential order-effect bias, in the experiments in chapter 3 and 4, the whole range of intensities of the testing stimuli was presented randomly.

Furthermore, the implicit reference in the MSS may bias the responses of the observers who may compare the test stimulus with a misremembered reference stimulus. Nevertheless, Vreven (2006), in a 3D-shape discrimination task using the MSS, discusses that this is an unlikely explanation of her results. Another potential shortcoming of the MSS could be the difficulty to intersperse different experimental conditions in a block/run. In order for multiple references and conditions to be presented in a single block, participants must keep in memory as many reference stimuli as the number of conditions. Further, they must compare any given test trial with the appropriate reference. Performance is, thus, prone to noise and mistakes. In chapters 3 and 4, it was therefore important to establish a unique characteristic for each condition, to ensure that participants did not confuse the stimuli between conditions. (For details, see *Methods* in chapters 3 and 4).

2.9 Visual masking and the stimulus onset asynchrony

Visual masking refers to the phenomenon where the visibility of a briefly presented stimulus (target) is suppressed because a second stimulus (mask) is presented soon afterwards. This type of masking is known as backward masking (Breitmeyer & Ogmen, 2000; Breitmeyer & Ogmen, 2006). In the domain of brightness, the reduction that the backward mask causes to the brightness of the target is called metacontrast (Alpern, 1953). Exchanging the temporal order of the target and the mask, so that the target follows after the mask, results in paracontrast forward masking (Breitmeyer & Ogmen, 2006). In the present thesis, I use the term masking to refer to backward masking.

Although the spatial aspects of backward masking are considered to be critically important (e.g., Hermens and Ernst, 2007; Polat, Sterkin & Yehezkel, 2007), an extensive research concerning its temporal characteristics has designated the well-known 'U-shaped masking'. This refers to the shape of the curve depicting target's visibility as a function of the stimulus onset asynchrony (SOA; Alpern, 1953). In particular, this function is usually portrayed with a U-shaped curve, since target's visibility is not impaired when either very short or very long SOAs are used, but is reduced in between. Indeed, Paradiso and Nakayama (1991) adopted metacontrast to show that not only the presence of the mask dramatically interrupts and suppresses the brightness perception ('filling-in') of a briefly presented target, but that the mask is maximally effective with an SOA of 50-100 ms between the target and the mask. Although different SOA time-windows are used in the literature, it seems that an SOA between 30 and 150 ms is generally a reliable range for reduction effects in target's visibility (Breitmeyer & Ogmen, 2006, p.38; Polat et al., 2007). For the experiments in chapter 6, the SOA was tailored to every participant: to reassure that observers' SOA thresholds would lie in the range 30-150 ms, prior to attending a main experiment, all observers completed an estimation-of-SOA session consisted of three five-minute blocks (50 trials each). I, thus, tailored SOA thresholds for every participant individually and the mean estimated SOA was 116.7 ms (*SEM* = 4.4).

3. Seeing slanted surfaces: probing the contributions of dorsal and ventral visual brain areas

Abstract

Our ability to estimate the slant of nearby objects (such as a table top) is critical for visually guided interactions. Estimating surface slant involves inferring information about 3D structure from 2D retinal images and the cortical circuits that support this ability are not fully understood. Here, I sought to test for the involvement of cortical areas in slant judgments by perturbing their activity using repetitive transcranial magnetic stimulation (rTMS). Participants (n=8) viewed slanted surfaces defined by binocular disparity rendered in random-dot stereograms. I presented two baseline slants (10 deg, 50 deg) and measured slant discrimination thresholds around these values using the method of single stimuli. Stimuli were presented for 850 ms, and 5 online rTMS pulses were synchronised with every stimulus presentation. In different testing sessions, I targeted stimulation to the posterior parietal cortex (PPC) and functionally-localised areas V3A and LO in both hemispheres. I obtained control measurements by applying rTMS to CZ. I failed to observe any significant effect of rTMS over V3A or LO on slant discrimination performance. However, I found that performance for the high and low slants became similar when stimulating left PPC. Finally, order analysis showed that, irrespectively of the area of stimulation, there was a considerable learning effect, with participants improving across testing days. These results hint at a functional contribution of the PPC to slant estimation, however, further work is needed to fully understand the nature of its involvement.

3.1 Introduction

Tilt is an angular quantity used to describe orientation or direction measured in the frontoparallel image plane (Stevens, 1983). 'Oblique effect' (e.g., Furmanski & Engel, 2000) is the phenomenon where sensitivity for discriminating stimuli oriented along the vertical or horizontal axis ('cardinal' stimuli) is observed to be greater relative to 'oblique' orientations (45 or 135 degrees oriented stimuli). In particular, such a cardinal salience has been observed at both the behavioural level (enhanced visual discrimination for vertical and horizontal orientations; Campbell & Kulikowski, 1966) and the neural level (greater fMRI responses in V1 for 'cardinal' oriented, compared to 'oblique' oriented stimuli; Furmanski & Engel, 2000). Other studies have investigated another, similar, effect regarding the visual perception of orientation in the frontoparallel plane: Sasaki et al. (2006) showed that gratings of orthogonal oblique orientation activate complementary quadrants in the visual cortex. In other words, this 'radial bias' demonstrates that oblique (tilted) orientations, corresponding to radial (i.e., emanating from a common central point) orientation in a given quadrant of the visual field, triggered greater fMRI responses, than tangential orientations, in all the retinotopic areas in both the human and the monkey. Therefore, the study suggests that there is a neural link between orientation sensitivity and the retinotopically organized visual areas. Further, the researchers supported their fMRI findings with human psychophysics which showed greater sensitivity for the radial orientations.

Although the visual mechanisms for the perception of orientation in the frontoparallel plane (2D orientation) have been extensively studied in the past decades, little is known about the cortical mechanisms that support the perception of surfaces' 3D orientation, i.e., their slant. While tilt is an angle measured in the image plane, slant is an angle measured perpendicular to the image plane (Stevens, 1983 -see also General Introduction). Furthermore, slant can be defined by the gradient of density of its texture (Gibson, 1950) and/or by binocular disparity (see *General Introduction*). Although recent studies have investigated the neural mechanisms that support the cue combination to slant in the human

(Murphy, et al., 2013; Welchman, et al., 2005), and the disparity-defined slant in the monkey (Nguyenkim & DeAngelis, 2003), relatively little is known about the role of disparity-selective cortical areas in the perception of slant defined by disparity only.

The aim of the present study was to investigate the cortical sites that support the perception of disparity-defined slanted surfaces. I used stimuli defined around rotation axes of two slant magnitudes: a 'high' (rotated around 50 deg) and a 'low' (rotated around 10 deg) one. The preliminary psychophysical data I collected showed that the discrimination of stimuli slanted around the 10 deg axis (the individual surfaces were increased or decreased in step sizes of 3 degrees around the 10 deg axis on each trial) was enhanced, relative to those which were similarly jittered in step sizes of 3 degrees around the 50 deg reference rotation axis (see *below*). This is not surprising in the context of the 'oblique effect' discussed above, or more generally, in the context of Weber's law. Simply stated, according to Weber's law, the just noticeable difference (*jnd*) is a constant proportion of the original stimulus' intensity value (Levine & Shefner, 2000). Applied in the domain of binocular disparity-defined slant, the further away a surface is from the frontoparallel, the bigger the step should be for the *jnd* to be detected. In other words, various slants rotated, with step sizes of 3 degrees, around the 10 deg reference axis would be expected to be more easily discriminated compared to slants rotated, with step sizes of 3 deg, on a bigger reference axis (50 deg).

In the main experimental part of this study, I sought to investigate the contribution of areas of the dorsal and the ventral visual pathway to the perception of slant. In particular, I was interested in examining whether the discrimination of slant defined by low (10 deg slant) versus high (50 deg slant) disparity is supported by the same or different cortical mechanisms. I used fMRI-guided rTMS to transiently disrupt the regions of interest and evaluate their causal relationship to slant perception. The main hypothesis was that since behavioural discrimination was worse within the 50 deg than within the 10 deg condition, then the TMS-induced disruption of the critical area(s) should be greater within the 10 deg.

Simply stated, it was tempting to assume that since performance in the 50 deg condition was already noisy anyway, then stimulation should have a more profound disruptive effect on the 10 deg condition because there was 'more room' for interruption in this condition.

3.2 Methods

3.2.1 Participants

Eight participants (5 female, 3 male), students at the University of Birmingham, participated for money compensation. All had normal or corrected-to-normal vision and were naïve to the purpose of the study.

3.2.2 Regions of interest

Regions of interest were the dorsal area V3A, the higher ventral stream area LO and the posterior parietal cortex (PPC). I was interested in assessing V3A because, at first, this area has been found to be highly selective for disparity and depth information in both the human and the monkey (e.g., Backus, et al., 2001; Preston, et al., 2008; Tsao, et al., 2003, see General Introduction). Also, Ban, et al. (2012) recently showed that, together with V3B/KO, V3A also contains fMRI signals used for the accurate decoding and prediction of depth from the concurrent combination of depth cues by a machine learning classifier. In a similar study, Ban and Welchman (2015) used slanted surfaces to find that fMRI signals in V3A can be used for the accurate decoding of slanted surfaces with different angle magnitudes, by a machine learning classifier. Specifically, signal information in V3A was sufficient to explain the greater behavioural sensitivity in discriminating surfaces slanted near the frontoparallel (7.5 or -7.5 deg), compared to those slanted far away from the frontoparallel (>40 deg). On the other hand, I was interested in stimulating area LO, given that this area specialises in the perception of objects' 3D shape and structure (Kourtzi, Erb,

Grodd, & Bulthoff, 2003; Kourtzi & Kanwisher, 2001). Finally, I was interested in stimulating the PPC, based on evidence that this part of the dorsal cortex is involved in the visual selection of salient information (Mevorach, Humphreys, & Shalev, 2006, 2009) and also in encoding the spatial information about objects locations (e.g., Haxby, et al., 1991; see General Introduction). Area CZ was stimulated as a control for the possibility of nonspecific effects associated with TMS experiments, such as the sound generated by the rTMS pulse administration and the tactile-muscle stimulation artifacts (for a recent review about effective controls in brain stimulation studies, see Davis, Gold, Pascual-Leone, & Bracewell, 2013). I stimulated CZ twice in order to compare CZ data with the data acquired from the rest areas of interest (which were stimulated bilaterally), and also in order to get a more objective and accurate control index.

3.2.3 Stimuli

Stimuli were grayscale random-dot stereograms of planar circular surfaces with slant (rotation about the horizontal axis). Slanted surfaces were presented inside a rectangular aperture and were defined by disparity. Stimuli were presented on a mid-grey background, whereas the dot density of the stimulus differed significantly from the background to allow figure-ground segmentation. Stimuli were viewed through a laboratory stereo set up where the two eyes viewed separate LCD monitors from a distance of 50 cm through a mirror stereoscope. Screens resolution was 1680 x 1050 pixels at a refresh rate of 100 Hz. When both eyes viewed the stereogram, a single slanted surface was perceived (**figure 3.1**)**.**

To control for low-level covariates, which participants could potentially rely on for their slant judgments, I varied both the depth displacement and the size of the stimuli. The rationale for this manipulation was because one could potentially judge surfaces' slant based on the depth differences between two surfaces existing at their top or bottom parts, and not based on their slant *per se*. To minimize this potential bias, I randomised the

displacement of the surfaces in depth, which was jittered between +/-1 cm around a mean distance of 50 cm at the point of fixation. (For a similar control, to minimize low-level cues' effectiveness, see Knill & Saunders, 2003). Moreover, in order to further attenuate possible low-level biases, I randomized the size of the stimuli, which were taking the values 5.25, 6.0, or 6.75 degrees of visual angle randomly.

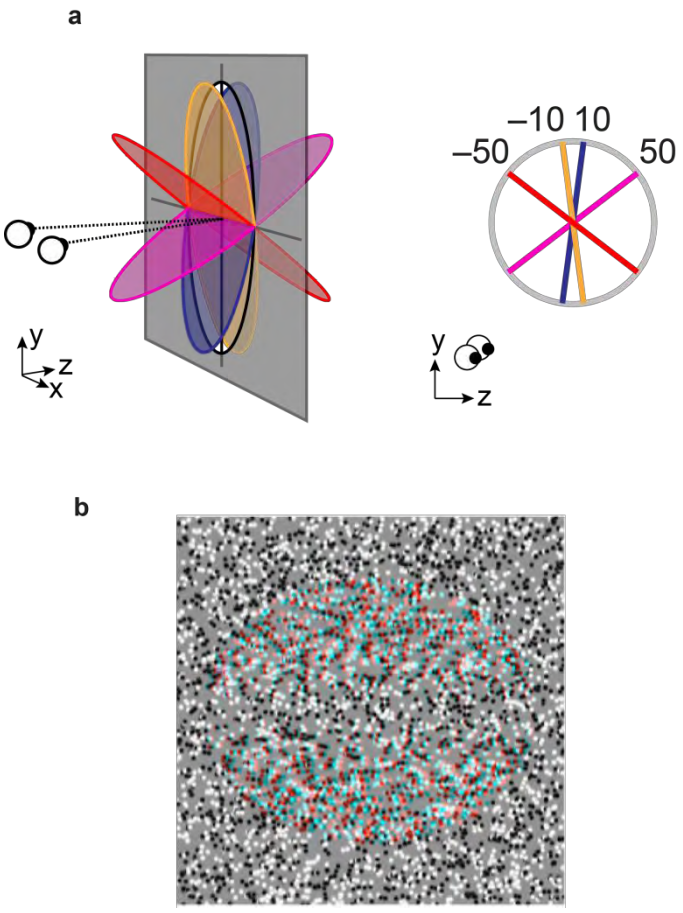

Figure 3.1: (a) Cartoon illustration of the 'TopNear' and 'TopFar' views of the two conditions' slant: 10 and 50 degrees. **(b)** Red-green anaglyphic stereogram to show the 3D representation of the 50 deg slant.

3.2.4 Design of the method of single stimuli

Although the MSS has been reported to be as precise as other psychophysical methods (see *General Methods*), it might be problematic when employed in tasks using multiple conditions. The present study used two conditions interleaved in a block (see

Psychophysics, below). Morgan (1992) employed the MSS to ask participants to make judgments about the separation of simple lines in four different conditions. The conditions differed relative to the orientation of the reference stimulus (87.75, 89.25 deg and so on), or relative to the quadrant of the screen in which it was presented. Interestingly, the resulting thresholds were not significantly different than the ones obtained in a paradigm where each separation took place in isolated blocks. However, the number of interspersed implicit references was a critical factor for this accuracy in thresholds. Specifically, increasing the number of references to 8 resulted in a decline of precision in the separation judgments. In their second experiment, Morgan et al. (2000) adopted a variation of the paradigm that Morgan (1992) used, to assess the ability of trained observers to select among similar targets when asked to generate multiple implicit references: all targets had the same orientation and position, but differed relative to an accompanying symbolic cue. That cue was used in order to designate the appropriate reference.

Here, in order to achieve a reliable performance, I aimed to reassure that perceptual discrimination would be accurate and that participants would correctly assign each stimulus to its appropriate category before they respond. Similarly to Morgan, et al. (2000), I could technically employ a symbolic cue to accompany each of the references-to-be-recalled. However, Morgan et al.'s (2000) task was different relative to the one used here: they simulated a simple task involving the separation between straight lines, whereas I was measuring the discrimination of fine differences among surfaces with varying slants. Given that I used two interspersed implicit references/conditions (10 and 50 deg reference slants), I decided to establish a unique characteristic for each one of them, that is, to present each condition with a unique direction: each condition's/slant's top part was pointing either near or far relative to the viewer (see **figure 3.2** and below). Furthermore, to overcome the possibility that, during the first few presentations of stimuli, participants would try to estimate the mean intensity of the stimulus set (learning trials), the main experiments were preceded by a training phase (see below). Finally, to rule out the possibility of any serial

effects in participants' judgments during the main experiments (see General Methods; Parducci, 1959; Rambo, 1961) testing slants were fully randomised on each trial (see below).

3.2.5 Psychophysics

Participants were presented with slanted surfaces belonging to two conditions. One condition consisted of slants jittered around the 10 deg horizontally sheared reference axis: the reference itself was 10 deg, and another 6 testing slants (each with a constant step size of 3 deg -either increasing or decreasing from 10 deg) were presented randomly in every block. Therefore, 3 surfaces were more slanted (taking values 13, 16, 19 deg) and the other 3 were less slanted (7, 4 and 1 deg) than the reference. The second condition consisted of the same number of slants and step sizes (presented randomly), but the base/reference slant was at 50 degrees. Therefore, within each condition, the discrimination among surfaces of fine slant differences was required.

On each trial, participants were presented with a single surface alone and were asked whether it was more, or less, slanted relative to the (implicit) mean of its own condition's set. Surfaces belonging to the two conditions were presented randomly. One group of participants viewed the 10 deg condition's slants with their top parts being near ('TopNear') and the 50 deg condition's slants with their top parts being far ('TopFar'). The other group viewed stimuli in the opposite permutation (see **figure 3.2**). In the preliminary behavioural experiments, where training on the task with the two conditions interleaved was provided, participants could do the task adequately and produce reasonable psychometric functions after training (see **figure 3.3**).

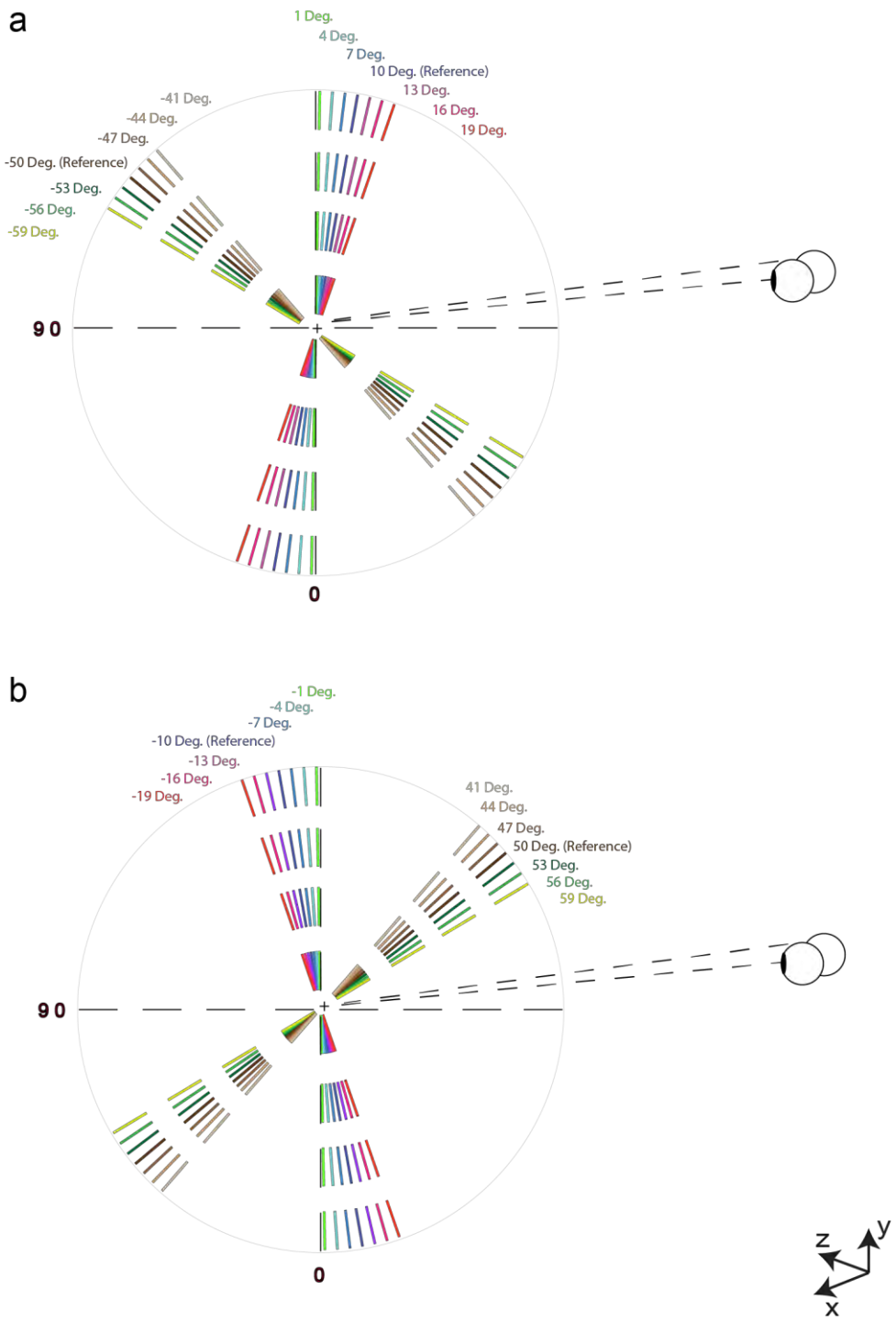

Figure 3.2: (a) First group's main experiment: 10 (TopNear) and -50 (TopFar) reference slants presented in the same block. **(b)** Second group's main experiment: -10 (TopFar) and 50 (TopNear) reference slants presented in the same block. The seven different levels of slants (step sizes -9 -6 -3 0 3 6 9) for each condition and group appear in different colour.

The study was completed in two different phases: the training and the main TMS phase. The training phase was designed to train participants on the task so that they can reliably make fine discriminations of slant. In the main phase, the aim was to identify the brain areas whose function is necessary for the visual discrimination of slant. During the behavioural-only experiments (prior to the application of any TMS) I found a 'slant oblique effect' (see *Results*) similar to the one referred in the introduction. I then used rTMS to evaluate whether disruption of the disparity-selective regions of interest would be greater within the 10 deg than the 50 deg condition.

3.2.6 Procedure

3.2.6.1 Training phase (behavioural only)

Day 1

Pre-Training

The training phase of the study started with a pre-training session. No feedback was provided for correct/wrong responses, and the rationale for this session was to get a baseline performance - index. Participants were assigned to two different groups, differing as for the main experiment group they belonged to: half of them were presented with the 10 deg (TopNear) & -50 deg (TopFar) conditions interleaved in the same block. The other half of participants were assigned in the 50 (TopNear) & -10 (TopFar) conditions main experiment/group. Each session consisted of 280 trials (20 repetitions of each one of the 7 step sizes, i.e., 140 trials for each slant direction) and lasted for around 12 minutes.

Training

After completing the pre-training session, participants were trained on the same task, with feedback, but were presented with the opposite slant directions than the ones constituting their group's main experiment. The rationale for this manipulation (i.e., preserving slants' magnitude but changing slants' direction) was to minimise the viewers' exposure to the specific stimuli used in the main experiment, and ensure that psychophysical improvement would not be stimulus-driven and restricted. Each condition was presented alone in a block of 140 trials and feedback was provided for correct/incorrect responses. Each participant attended each block twice.

Post-training

After training, participants attended a block consisted of their main experiment's conditions (both interleaved in the block). The number of trials and duration were the same as in the pre-training phase, while no feedback was provided.

Day 2

On a subsequent day, participants attended the post-training block again, so that I could evaluate the efficacy of the training phase.

I plotted psychometric functions as the proportion of 'more slanted' responses against the constant stimuli step values. The participants' performance indicated that the training phase was effective (see **figure 3.3** for representative graphs depicting clear improvements after training). All participants could easily do the task after training. As expected, their performance was enhanced (steeper psychometric functions) for the 10 deg relative to the 50 deg condition. This general 10-deg advantage indicates an 'oblique effect' for slant

discrimination and is consistent with Weber's law in the context of disparity-defined slant (see *Introduction* and below).

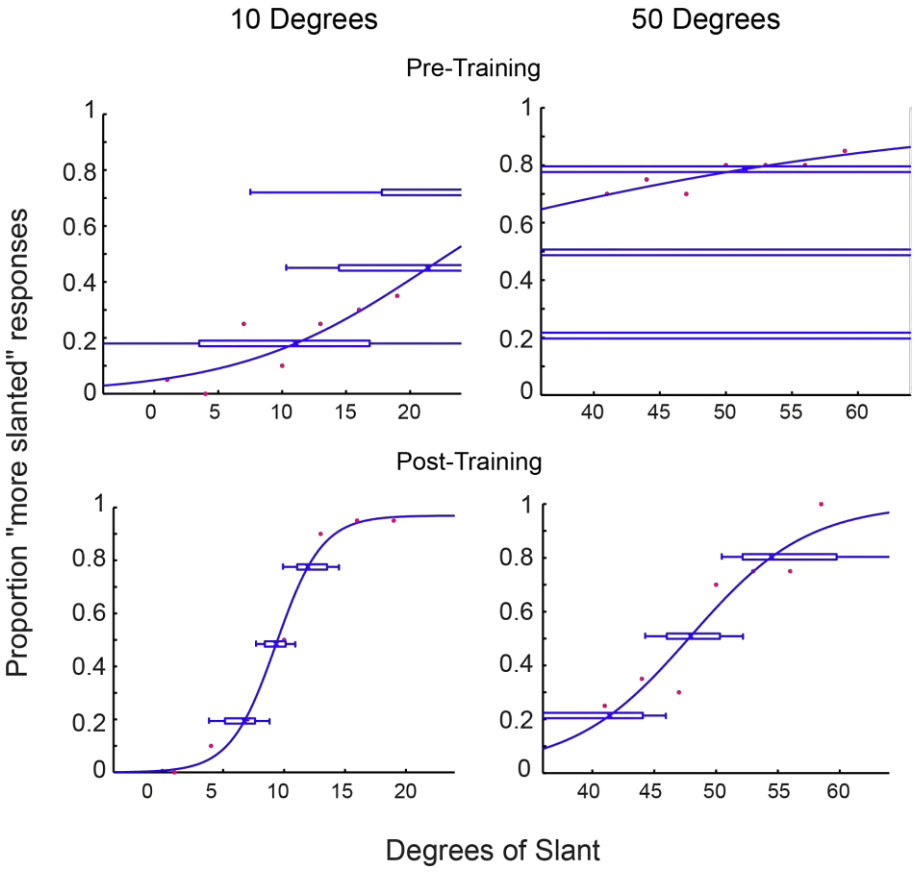

Figure 3.3: Slant discrimination performance in the 10 and 50 deg conditions, both pre- and post-training, for participant *LR*. Proportion of judging trial surfaces as 'more slanted (than the mean slant)' is plotted against stimulus intensity (degrees of slant). After training, performance extremely improved as the reasonable slopes of the psychometric functions indicate.

3.2.6.2 Main phase (TMS)

TMS Protocol

In the beginning of each TMS session, in order to provide a practice platform and 'warm up' participants, all viewers completed two practice blocks with feedback. Each block contained a single reference slant (either the 10 or the 50 deg) whose individual surfaces were presented 20 times each. Surfaces were again slanted in the opposite directions than the ones appearing in the participant's main experiment. After this practice, participants

attended a 196-trial behavioural-only block, without feedback, which contained their main experiment's conditions and slant directions. A concatenation and average of all the behavioural blocks of this stage informed each participant's overall 'behavioural' performance (see *Results* below). Subsequently, participants completed the main experiment of their group, without feedback, while rTMS was applied concurrently with the stimulus onset.

On each trial, 5 successive pulses were delivered at 10 Hz (i.e., each pulse's duration was 100 ms), synchronized with the onset of the visual stimulus. This rTMS protocol, over LO and the PPC, has previously been used to successfully disrupt depth judgments (Chang et al., 2014). Pulses lasted for 500 ms, while the stimulus remained on screen for 850 ms. After participant's response, there was a 2500 ms interval (**figure 3.4**). None of the participants reported the perception of phosphenes. I followed the fMRI-guided TMS approach and used BrainSight (Rogue Research Inc) to navigate and place the coil over the functionally localized areas V3A and LO bilaterally. PPC and CZ were identified and guided through the 10-20 EEG coordinate system (see *General Methods*). Each rTMS session consisted of 196 trials (14 repetitions per stimulus/step size, i.e., 98 trials for each slant direction; see table 1) and was split in two parts.

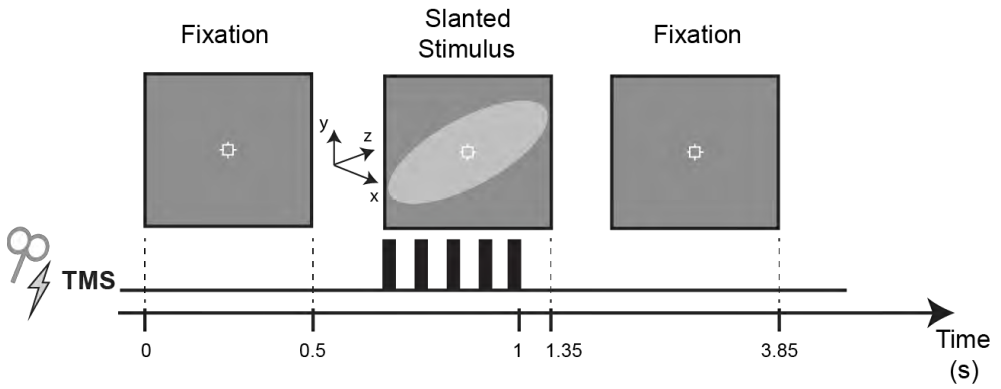

Figure 3.4: Schematic view of the rTMS procedure and parameters.

Table 3.1: Summary of the procedure in the TMS phase of the study. The order of stimulating the different areas on separate days during the main TMS phase was randomised. The order illustrated here is just an example.

Day						
1	**2**	**3**	**4**	**5**	**6**	**7**
Practice on the 10 & -50, **OR** the -10 & 50 (the opposites than the ones presented in the main experiment) in **separate blocks**, **with feedback.** 140 Trials	Practice… " " 140 Trials	Practice.. " " 140Trials	Practice.. " " 140Trials	Practice.. " " 140Trials	Practice.. " " 140Trials	Practice.. " " 140Trials
Behavioural main session–**No feedback** 280 trials	" " 280 trials	" " 280 trials	" " 280 trials	" " 280 trials	" " 280 trials	" " 280 trials
Break	**Break**	**Break**	**Break**	**Break**	**Break**	**Break**
Main & CZ 98 Trials	Main & P3 98 Trials	Main & P4 98 Trials	Main & R.V3A 98 Trials	Main & L.V3A 98 Trials	Main & R. LO 98 Trials	Main & L. LO 98 Trials
Break	**Break**	**Break**	**Break**	**Break**	**Break**	**Break**
Main & CZ 98 Trials	Main & P3 98 Trials	Main & P4 98 Trials	Main & R. V3A 98 Trials	Main & L. V3A 98 Trials	Main & R. LO 98 Trials	Main & L. LO 98 Trials

3.3 Results

Ban and Welchman (2015) observed that viewers' sensitivity was highest for low slant angles (that is, close to the frontoparallel; 7.5 and -7.5 deg) and declined as the slant angle increased ('slant oblique effect'). During the training phase of the present study, I observed a similar facilitative effect which was further confirmed during the main behavioural experiments. Inspecting each condition's psychometric functions (**figure 3.5** depicts representative graphs from 2 participants) indicates that the rate at which performance improves as stimulus intensity increases (slope) is greater within the 10 deg than the 50 deg condition.

I employed sigmoidal psychometric functions (logistic and cumulative Gaussian) to fit to the data, using the Psignifit toolbox in Matlab. Psignifit uses the observed values/data to generate 4999 simulations of the psychometric function (bootstrap resampling) and returns the median values of the estimations it makes for each variable. To quantify performance and perform statistical analyses for both the behavioural and the TMS data, I retrieved and analysed the threshold at 50% (PSE) "more slanted" discrimination level and the standard deviation variables as they derived from the estimates of the psychometric functions (see *TMS data* below).

3.3.1 Behavioural data

Comparison of the averaged slope values across participants revealed that the psychometric functions for the 10 deg condition were significantly steeper (greater slope values) than those for the 50 deg condition [$t(7) = 7.484$, $p < .001$]. This indicates that participants, in the 10 deg condition, were able to discriminate among the fine differences in slant with greater accuracy (Frund, Haenel, & Wichmann, 2011) compared to the 50 deg condition.

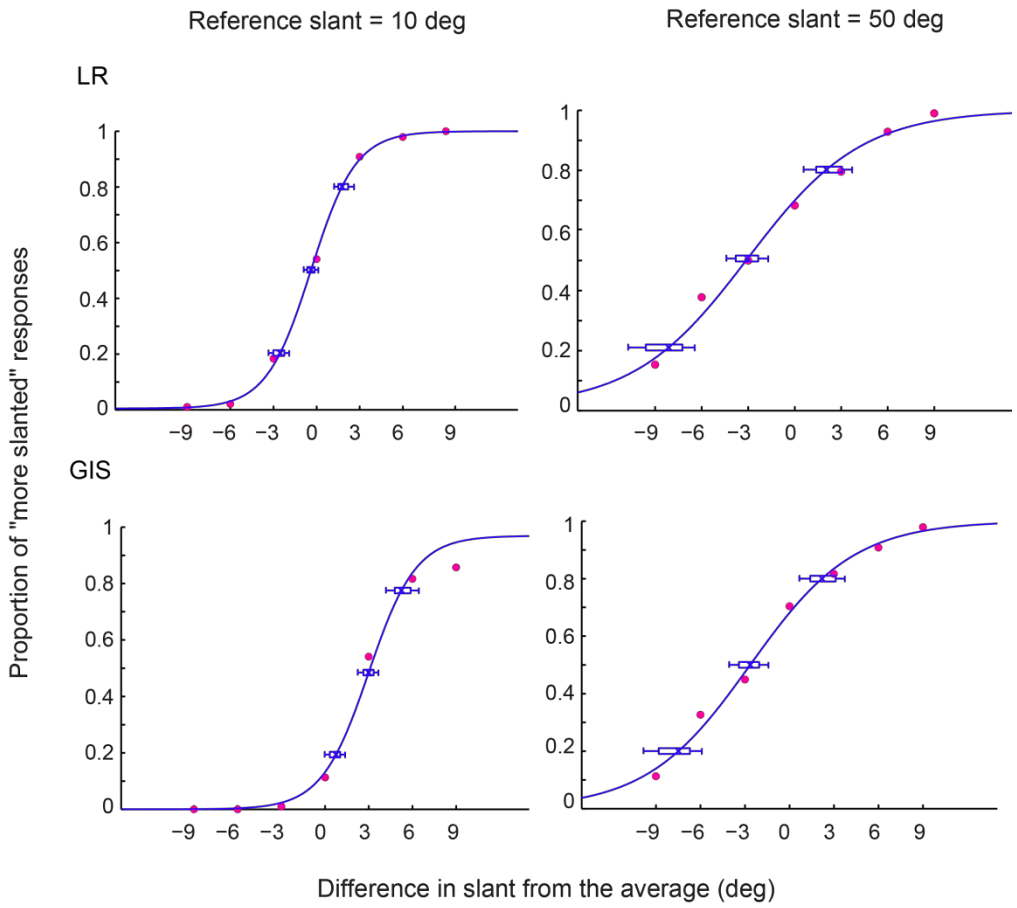

Figure 3.5: Concatenated slant discrimination performance (behavioural only) of two representative participants *LR* and *GIS*. Proportion of judging trial surfaces as 'more slanted (than the mean slant)' is plotted against the number of degrees away from the average/reference slant. Positive values on the x axis indicate more slant. Left column graphs depict performance in the 10 deg condition which produced much steeper psychometric functions than the the 50 deg condition (right column).

3.3.2 TMS data

The graphs in **figure 3.6** show psychometric functions for each participant in each condition. Each brain area noted on the graph refers to bilateral data (the two hemispheres pooled together, while, for CZ, the two times this session was run are pooled together). Thus, functions are fitted for 28 trials/repetitions per stimulus level. Both the 10 deg and 50 deg conditions were considered. The graphs show how the curves of the psychometric functions fitting the rTMS data shift as a function of the stimulated area. Visual inspection of the graphs does not reveal any systematic effect. Data neither suggest that any of the stimulated cortical areas support slant perception directly, nor explain the 10 deg vs 50 deg

discrimination differences observed behaviourally. A potential systematic shift of the curves of the psychometric functions, or a change in the slope values would probably be sufficient to indicate an important contribution of a stimulated region to the perception of slant. However, the graphs suggest neither a specific pattern in the slopes, nor any systematic shift of the curves within conditions.

As it derives from signal detection theory, the mean of the Gaussian distribution represents the bias, while the standard deviation represents the sensitivity (Green & Swets, 1974). To quantify bias, I thus used the point of subjective equality (PSE) expressed as the threshold at 50% “more slanted” discrimination level. Furthermore, to quantify sensitivity, I used the just noticeable difference (JND) expressed as the standard deviation of the psychometric functions (calculated as 84.1% threshold *minus* 50% threshold). Statistical analyses of these variables follow in the next paragraph.

Positive values of slant indicate ‘more slant’ than the average slant of the whole set of the testing surfaces, in other words, ‘more slant’ than the implicit reference (which is denoted by 0 deg) for both the 10 deg and the 50 deg conditions (see *Psychophysics*).

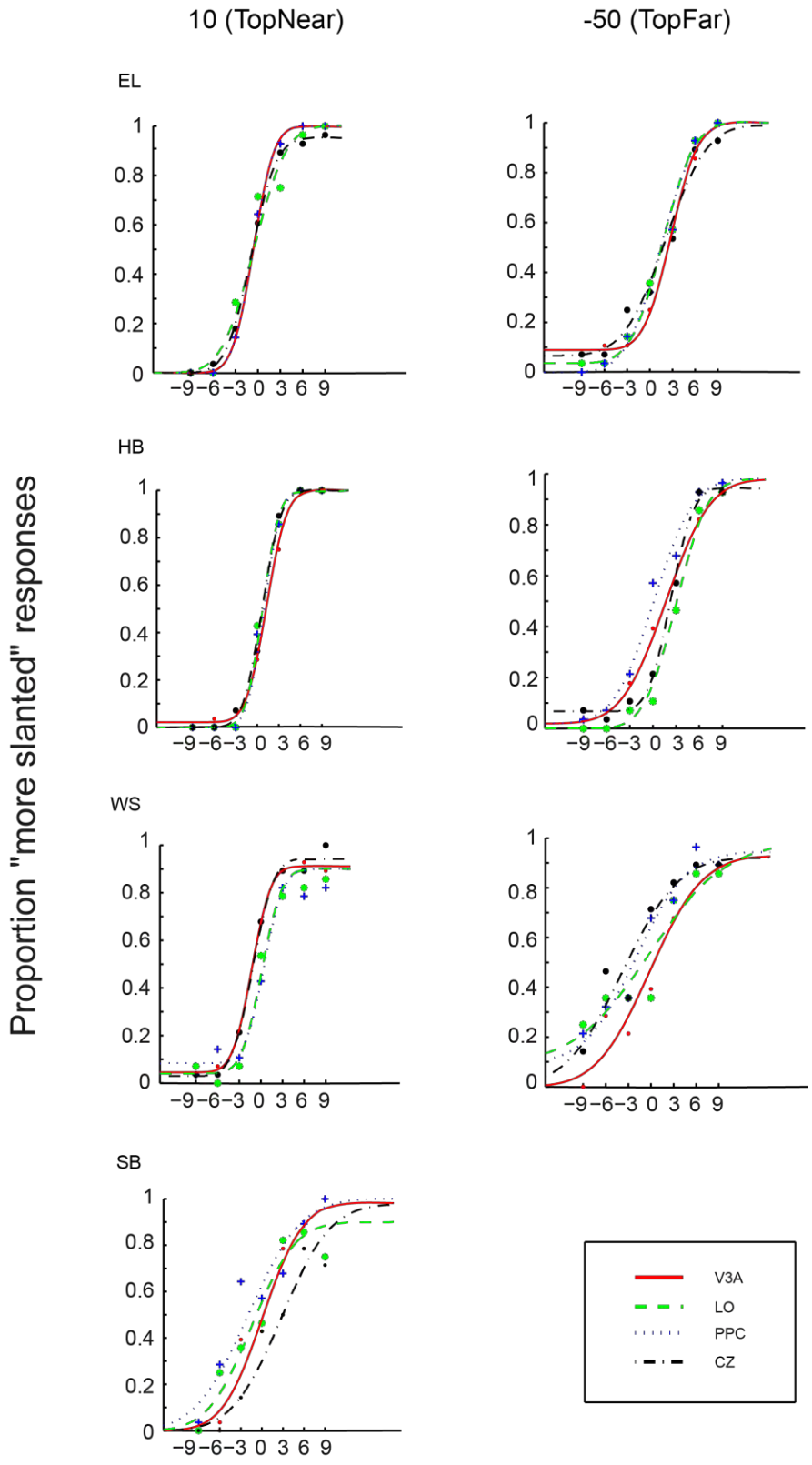
10 (TopNear)
-50 (TopFar)
EL
HB
WS
SB
Proportion "more slanted" responses
Difference in slant from the average (deg)
V3A
LO
PPC
CZ

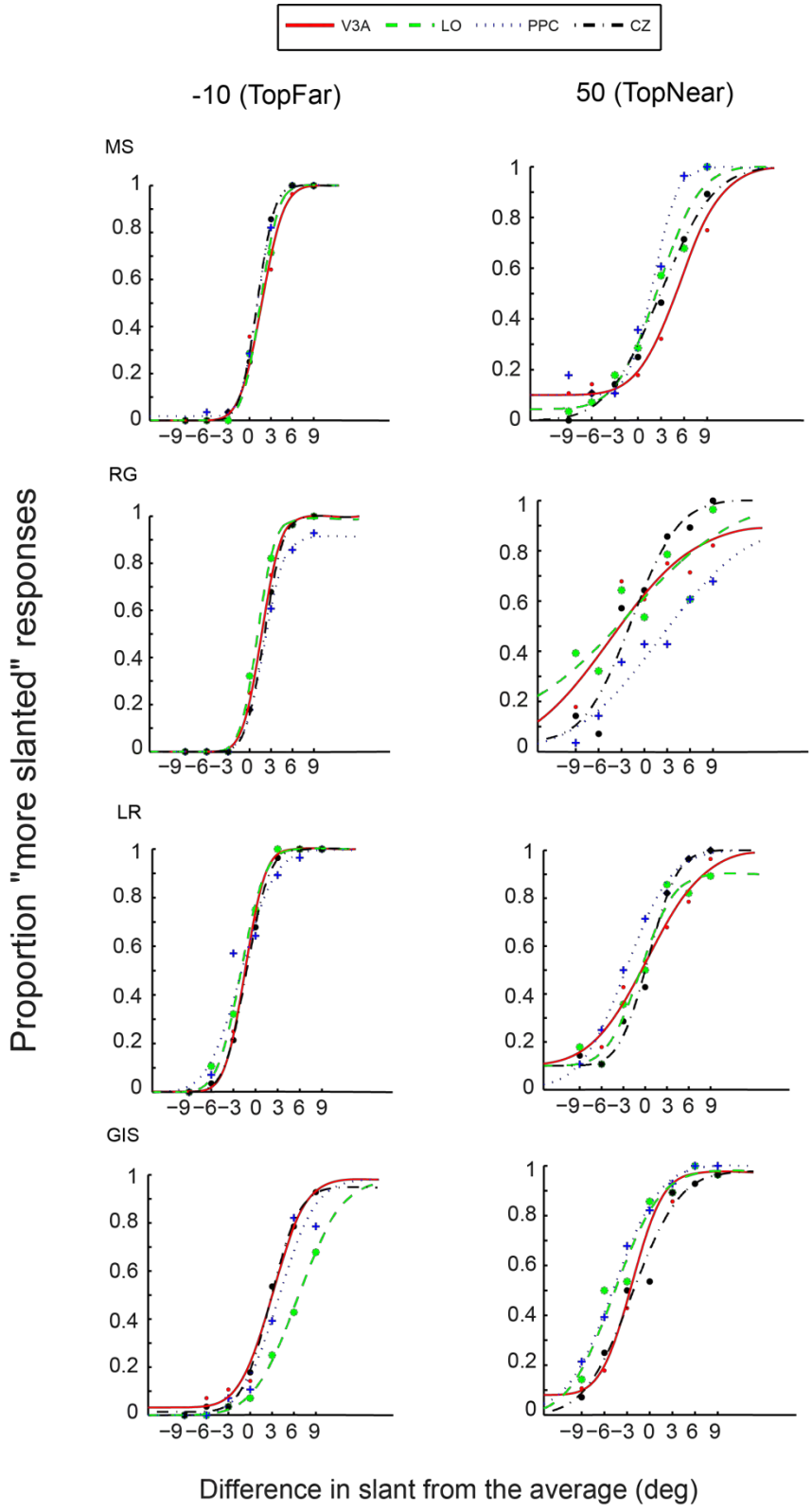

Figure 3.6: Slant discrimination performance across all the areas of stimulation (concatenated for the two hemisheres). Each curve indicates the best fit of the cumulative Gaussian function for each of the experimental conditions, across participants. Proportion of judging trial surfaces as more slanted (than the mean slant) is plotted against the number of degrees away from the average/reference slant. Irrespectively of the area of stimulation though, in the 50 deg condition

(both for the 'TopNear' and 'TopFar' groups), performance was generally worse than the 10 deg condition.

Threshold (PSE) analysis

A 2 (slant: 10/50 deg) X 4 (area: CZ/V3A/LO/PPC) X 2 (hemisphere: left/right) repeated measures ANOVA for the threshold/PSE values revealed a non-significant main effect of slant [$F(1,7) <1$, $p = .478$, partial $\eta^2 = .074$] and a non-significant main effect of the area of stimulation [$F(3,21) = 1.17$, $p = .345$, partial $\eta^2 = .143$]. Post-hoc power analyses (Cohen, 1988) for the slant factor revealed a power (1-*β error probability*) level of 0.13, whereas for the area factor, power (1-*β*) was 0.24. Results indicate that for both conditions, there was no systematic contribution of any of the stimulated areas to the discrimination of slant, although the power analyses suggest that statistical power was low. Data are shown in **figure 3.7a**.

PSE values for the clustered conditions (bilateral areas pooled together) are shown in **figure 3.7b**. Thresholds were lower (actually slightly below zero) in the 50 deg condition compared to the 10 deg condition for all the areas of stimulation, except for the V3A where thresholds became almost equal for both conditions. However, this interaction was not significant [$F(3,21) < 1$, $p = .772$, partial $\eta^2 = .051$, power (1-*β*) = 0.06], as a 2 (slant: 10/50 deg) X 4 (area: CZ/V3A/LO/PPC) repeated measures ANOVA revealed. Also, there was a non-significant main effect of slant [$F(1,7) < 1$, $p = .587$, partial $\eta^2 = .044$, power (1-*β*) = 0.06) and a non-significant effect of the area of stimulation [$F(3,21) <1$, $p = .70$, partial $\eta^2 = .064$, power (1-*β*) = 0.07].

I analysed the data further in order to probe the effects that the particular direction of slant might had. A 4 (area: CZ/V3A/LO/PPC) X 4 (condition: TopNear_10 / TopFar_50 / TopFar_10 / TopNear_50) repeated measures ANOVA revealed a non-significant main effect of the particular condition [$F(3,9) < 1$, $p = .527$, partial $\eta^2 = .210$, power (1-*β*) = 0.48] and a non-significant interaction [$F(9,27) < 1$, $p = .903$, partial $\eta^2 = .127$, power (1-*β*) = 0.12].

These results indicate that the particular slant direction that the test surfaces had did not bias participants' discrimination of slant.

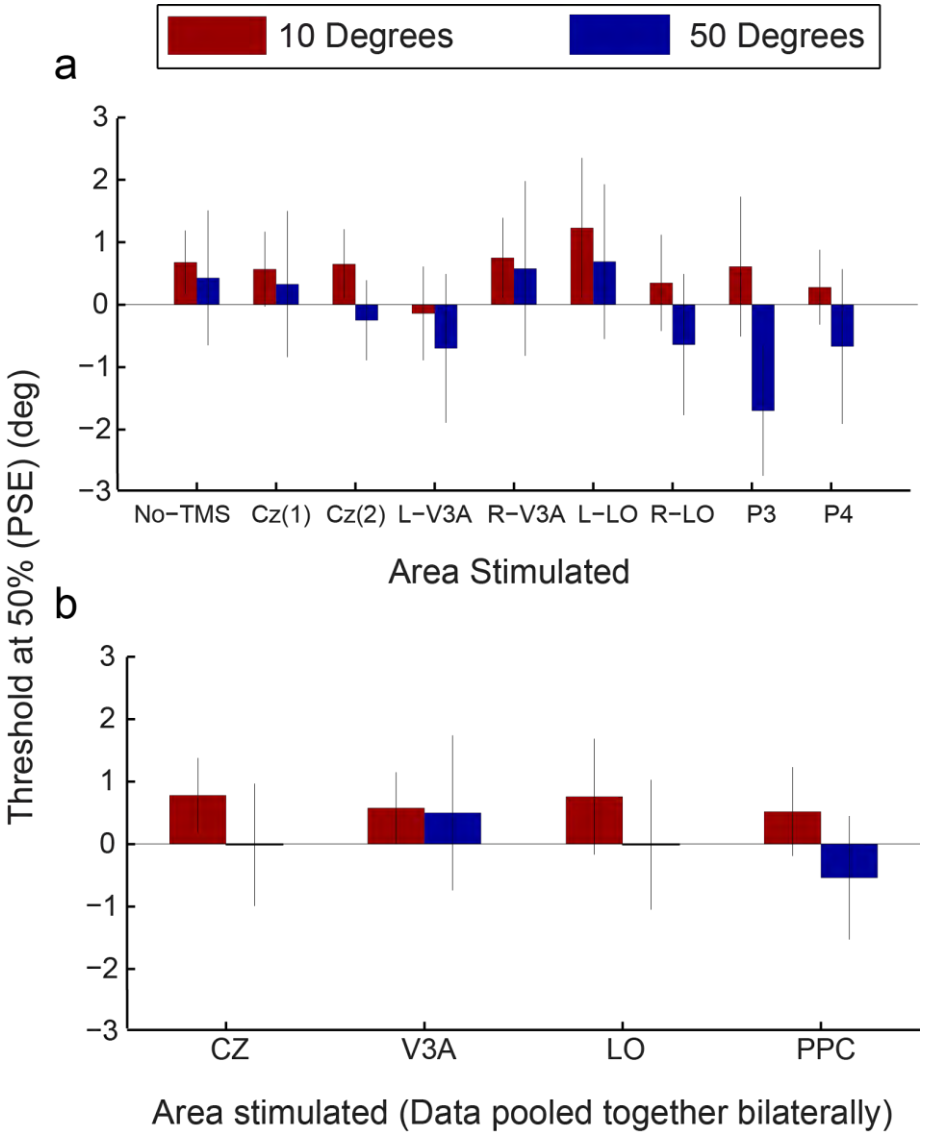

Figure 3.7: (a) Averaged threshold (PSE) values across participants for the 10 and 50 deg conditions as a function of the stimulated brain areas individually and **(b)** the clustered areas of stimulation (bilaterally). Error bars indicate standard error of the mean.

Standard deviation (JND) analysis

A 2 (slant: 10/50 deg) X 4 (stimulated area: CZ/V3A/LO/PPC) X 2 (hemisphere: left/right) repeated measures ANOVA for the standard deviation (SD) of the psychometric functions revealed a significant main effect of slant [$F(1,7) = 12.848$, $p = .009$, partial $\eta^2 = .647$, power

(1-β) = 0.99] with the 10 deg condition having, on average, decreased SD (indicating greater sensitivity) than the 50 deg one (**figure 3.8**). However, I did not find a significant effect of the area of stimulation [$F(3, 21) = 2.053$, $p = .137$, partial $\eta^2 = .227$, power (1-β) = 0.56]. This result indicates that, for both conditions, there was no systematic contribution of a specific area to the discrimination of slant. Finally, there was a non-significant effect of the hemisphere stimulated [$F(1,7) < 1$, $p = .946$, partial $\eta^2 = .001$, power (1-β) = 0.05].

To investigate the results further, I pooled data from the two hemispheres together. SD values for these clustered conditions are shown in **figure 3.8b.** As expected from the individual conditions' analysis above, SD decreased in the 10 deg condition compared to the 50 deg condition for all the stimulated areas [main effect of slant; $F(1,7) = 9.629$, $p = .017$, partial $\eta^2 = .579$, power (1-β) = 0.99]. However, data clustering failed to reveal a main effect of any of the areas stimulated [$F(3,21) < 1$, $p = .808$, partial $\eta^2 = .044$, power (1-β) = 0.06] indicating that there was no systematic contribution of an area to the discrimination of slant. Finally, there was a non-significant interaction between slant and area [$F(3,21) < 1$, $p = .637$, partial $\eta^2 = .076$, power (1-β) = 0.07].

To probe the effects that the particular direction of slant might have, I analysed the data further. A 4 (area: CZ/V3A/LO/PPC) X 4 (condition: TopNear_10 / TopFar_50 / TopFar_10 / TopNear_50) repeated measures ANOVA revealed a non-significant main effect of the particular condition [$F(3,9) = 3.804$, $p = .052$, partial $\eta^2 = .559$, power (1-β) = 0.99] and a non-significant interaction [$F(9,27) < 1$, $p = .832$, partial $\eta^2 = .153$, power (1-β) = 0.16]. Although these results indicate that the combination of the upwards/downwards ('TopNear'/'TopFar') direction for the two slants did not affect performance during the TMS stimulation of the areas of interest, however, the p value for the main effect of condition was found to be close to the α significance level ($p = .052$). Pairwise comparisons showed that there was a significant difference between the "Top Near" 10 deg condition and the "Top Near" 50 deg condition ($p = .011$). Therefore, it seems that in the case that the surfaces were slanted with their top part being near to the participant, participants were

more sensitive in discriminating slant within the low slant condition (10 deg) compared to the high slant condition (SD decreased in the 10 deg group).

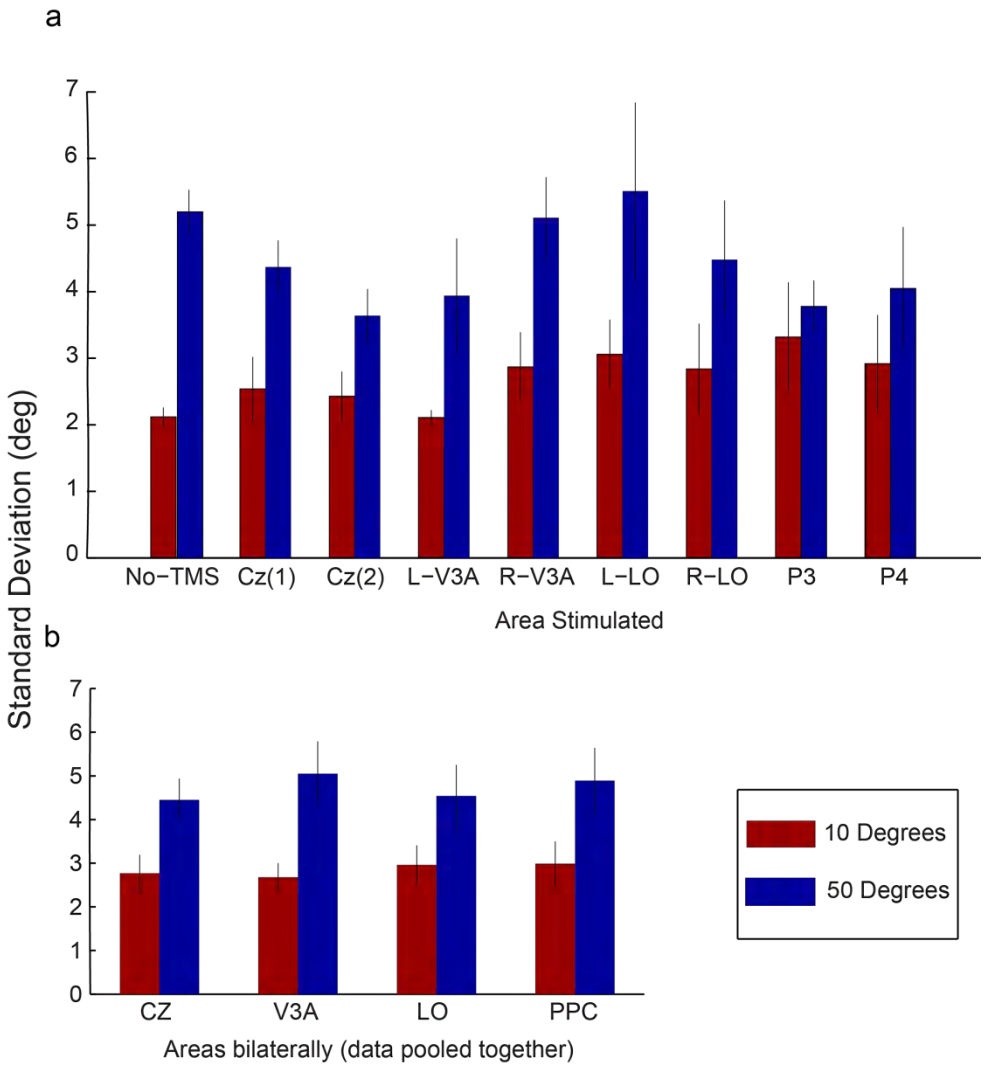

Figure 3.8: (a) Averaged standard deviation values across participants for the 10 and 50 deg conditions as a function of the stimulated brain areas individually and **(b)** the clustered areas of stimulation (bilaterally). Error bars indicate standard error of the mean.

3.3.3 Effect of order/training

Figure 3.9 shows standard deviation plotted as a function of the different days of experimentation. The plotted data are averaged across participants independently of the area that was stimulated on each day (stimulation of different areas was randomised across participants). Inspecting the graph suggests that performance was facilitated (as the decrease in SD indicates) as the days of experimentation passed.

The effect failed to reach statistical significance for the 10 deg condition [correlation between SD and the day: r = -.164, p (one-tailed) = .10]. However, within the 50 deg condition, correlations between the SD and the day were significant [r = -.318, p (one-tailed) = .008].

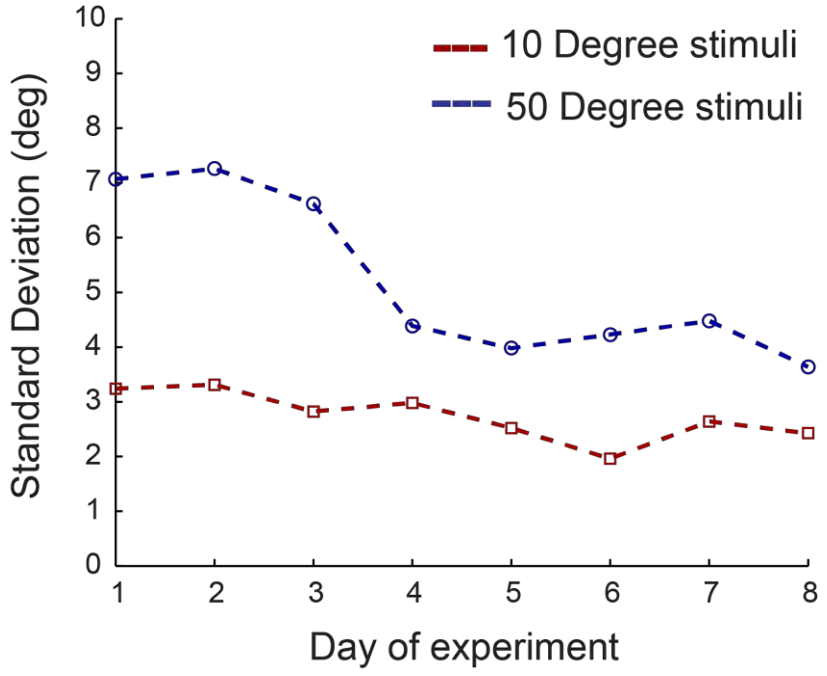

Figure 3.9: Standard deviation (JND) values for the 10 and 50 deg conditions as a function of the days of experimentation in a row. Data averaged across participants, irrespectively of the TMS-ed area on each individual.

3.4 Discussion

Behaviourally, I observed a robust difference in the discrimination of slant defined by 'low' disparity (slanted surfaces around 10 deg), compared to the discrimination of slant defined by 'high' disparity (50 deg slant). Specifically, slant/depth discrimination was facilitated for the former. I sought to explore the neural basis of this difference by applying rTMS over areas known to be selective for disparity-defined depth. I stimulated the higher ventral stream area LO, the dorsal area V3A and the PPC aiming to reveal the cortical locus of slant estimation. Standard deviation analysis suggested that slant discrimination around the 10 degree axis was facilitated (decreased SD), compared to the 50 deg, during all TMS sessions indicating that none of the stimulated areas was found to contribute to the discrimination of slant. However, as **figure 3.8a** suggests, the difference in sensitivity between the two slants was minimised after P3 stimulation where discrimination became comparable between the two conditions and the '10 deg advantage' attenuated.

How can this result be accounted for? One might be tempted to assume that rTMS over the PPC attenuated the salient spatial differences between the high and the low slant, resulting, thus, in the equivalence in performance between the two. Even though the two conditions were controlled for low-level covariates (by varying the depth displacement and the size of the surfaces -see *Stimuli*), they still had a profound aspect ratio difference whose spatial encoding may engage the parietal cortex. In other words, it could be the case that the PPC, and more specifically area P3, encodes the aspect ratios of varying magnitude stimuli and thus explains the differential behavioural performance between low and strong slants (Weber's law) at the first place. Even if this hypothesis was valid, however, it cannot suggest a contribution of the PPC to the fine discrimination of slant *per se*, but, instead, suggests the PPC's involvement in the discrimination between coarse spatial differences in the broader sense. This is in accordance with the specialisation of the visuo-parietal dorsal stream in encoding spatial information about objects locations (e.g., Goodale & Milner, 1992; Haxby, et al., 1991; see General Introduction) and with the

involvement of the PPC in inhibiting high-salience distracting stimuli (Mevorach, et al., 2006, 2009). Nevertheless, the above argument is just a speculation since the effect of the area of stimulation did not reach statistical significance.

Moreover, the analysis of the order/training effects, which showed that participants kept on improving on the task during the TMS phase of the study, challenges the data's inference as attempted in the previous paragraph. In particular, no matter the area of stimulation, data showed an important learning-related facilitation pattern (especially in the 50 deg condition) as the days of experimentation passed. A sensible explanation for this learning effect could be that participants (most of whom where experienced in psychophysical experimentation) had already become familiar enough with the task due to the extensive testing during the training phase and the behavioural-only blocks with feedback on each TMS day (see *Procedure*). Thus, there was probably 'no room' for rTMS to disrupt performance, since learning was already very strong. This observation highlights the need of a careful manipulation of training in psychophysical experiments. In the next two chapters, I, indeed, took this into account and sought to get a deeper understanding of the role of visual learning in psychophysical performance. Below, I discuss a few alternative approaches to the present study and I acknowledge possible shortcomings of the current experimental design which may have affected the results I obtained.

Firstly, one obvious design artifact could be the small number of participants used in the experiment. As the post-hoc power analyses (Cohen, 1988) showed (see *Results*), most of the statistical tests lacked sufficient statistical power to detect any significant effects even if they actually exist. Since statistical power is positively correlated with the sample size, the failure to find significant effects is probably because the sample size was too small ($n = 8$).

Additionally, it is possible that the regions of interest selected for stimulation were not sufficient. rTMS was applied over areas of the dorsal and the ventral stream which are

known to specialise in stereo vision: V3A is strongly activated by disparity signals in both the human and the monkey (e.g., Tsao, et al., 2003), whereas LO specialises in the perception of objects' 3D shape and structure (e.g., Kourtzi & Kanwisher, 2001). However, disparity-tuned neurons have been found in many areas of the cortex (e.g., Parker, 2007) including V1. Additionally, given that the neural correlates of the oblique effect in a 2D display are constrained in V1 (Furmanski & Engel, 2000), it would not be surprising if the application of TMS in the primary visual cortex did reveal a functional contribution of that area to disparity-defined slant. On the other hand, as Nguyenkim and DeAngelis (2003) note, depth estimation based on disparity information is unlikely to be coded in areas as early as V1 or V2. (Experimental evidence supporting this statement is reviewed in *General Introduction)*. Instead, Nguyenkim and DeAngelis (2003), following previous studies which have shown that area MT is sensitive in disparity signals, found that a great deal of cells in monkeys' area MT are tuned for 3D surface orientation (tilt and slant) defined by disparity. Taking everything into consideration, there are reasons to believe that a possible TMS application over additional areas in the human (V1 or MT+ for instance) might shed more light on how the visual system discriminates slant.

Furthermore, it might be the case that the timing of the pulses or/and the stimulus onset/duration I used was not optimal. Specifically, since the pulses were synchronized with the onset of the visual stimuli, it is possible that there were not enough carry over effects of the rTMS within each trial. Recently, this TMS protocol effectively disrupted depth judgments under LO and the PPC stimulation (Chang et al., 2014), but the present and Chang et al.'s studies have used different stimuli and visual tasks. In order to examine whether the administration of TMS pulses prior to the stimulus onset can induce greater disruptive effects, in the second experiment of the next chapter the pulses preceded the stimulus onset.

Given the differential effects that various TMS protocols induce (Rubens & Zanto, 2012) and also given the fact that the effects from TMS protocols are prone to high levels of

inter-individual variability (Maeda, Keenan, Tormos, Topka, & Pascual-Leone, 2000), it is possible that the rTMS protocol I used was not suitable for the specific participants. It is worth noting, for example, that the observers that participated in this study had been exposed to TMS experiments many times in the past. It is possible, therefore, that their sensitivity in brain stimulation had already significantly decreased. To overcome this potential methodological artifact, most of the participants I recruited for the experiments in the next chapters were not previously exposed to TMS experiments.

As far as the psychophysical parameters and design of the study are concerned, I will now discuss the pros and cons of the current design, as well as of some potential alternative psychophysical designs. At first, I presented each stimulus/step value 14 times in each session. 14 repetitions per stimulus are probably not enough in order to adequately fit a psychometric function to the data obtained. However, because of the tradeoff between reliability and fatigue/safety, I chose this number of trials in order to conform to the rTMS safety restrictions and not exceed the 1000 pulses per session (7 stimuli per condition X 2 conditions X 14 repetitions each X 5 pulses on stimulus onset).

Moreover, although none of the participants reported a difficulty in performing the MSS task, there is a possibility that this method has constrained performance (see *General Methods*). Sousa, et al. (2009), in a slant discrimination paradigm, employed a visual search task to examine the role of individual cues in slant perception. The visual search task requires the fast identification of a different (target) stimulus among other (similar) stimuli. Obviously, the more salient the target is, the faster its identification will be. Banks, et al. (2001), in a similar slant discrimination study, asked participants to adjust the test plane's slant about a horizontal axis until it appeared perpendicular to the line of sight. A visual search task similar to Sousa et al. or an adjustment task similar to Banks et al. could be employed as alternative psychophysical designs in the present paradigm. Further, one could employ the traditional two-interval forced-choice (2IFC) design: two slanted surfaces would be presented on each trial sequentially -one being the reference stimulus with a

constant slant value, while the other one would be the test, whose slant would vary. This method, though, would entail the disadvantage of applying rTMS on the onset of each interval/stimulus per trial, which might result in the over-stimulation of the target area. Further, stimulation during the first stimulus' presentation might result in an interruption of processing during the second stimulus presentation. In order to avoid such overstimulation and uncontrolled carry over risks, the reference and the test stimulus could be simultaneously presented in the left and right halves of the screen, in a 2AFC manner. However, this manipulation would probably make the task very easy. The option of a 3AFC or even 4AFC could be alternatively possible, but still, it would entail the problem of having several potentially uncontrolled covariates (attention and/or saccadic eye movements towards wide distances on the screen). Taking everything into consideration, in the next chapter, the MSS was again chosen as the appropriate method to avoid the risk of applying TMS over multiple intervals. In those experiments however, I took into account the possibility that the MSS may incommode participants, and thus sought to ensure the method's suitability by conducting some pilot experiments.

3.5 Appendix for chapter 3: eye movement data

The PPC has been reported to be involved in the control of vergence eye movements (e.g., Gnadt & Beyer, 1998; Q. Yang & Kapoula, 2004). In order to control for the possibility of TMS-induced disruptions of vergence, I recorded eye movements online with the TMS experiments reported above. In this section, I present representative graphs depicting vergence eye movement data for a few participants. I obtained vergence movements by substracting the left eye's horizontal position from the right eye's horizontal position with regard to the centre of the screen (see *General Methods*). Hence, negative vergence values correspond to eye positioning for near stimuli (being closer than the fixation point at the centre of the screen - on the screen's plane). Vergence during posterior parietal cortex (P3 or P4) stimulation, and CZ (or no TMS) as controls, are plotted as a function of time.

The graphs presented in the first section of the appendix refer to vergence data averaged across all trials within each session and, as denoted on the figures, refer to some 50 ms before rTMS stimulation and last for some 50 ms following the last TMS pulse. Visual inspection of the graphs for the majority of the trials for all the participants showed no systemic differences in vergence across the experimental sessions. Indeed, as the graphs below indicate, eye movements followed almost identical fluctuation patterns between PPC stimulation sessions and the control sessions.

3.5.1 Data averaged across trials

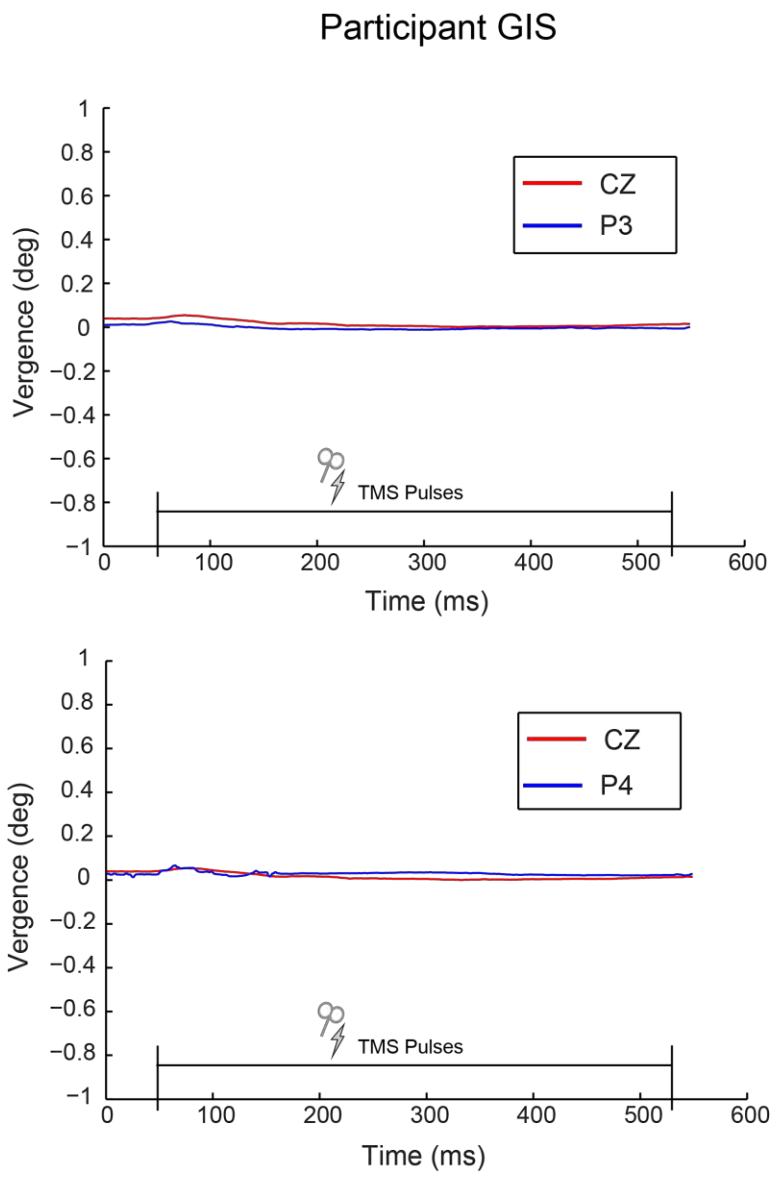

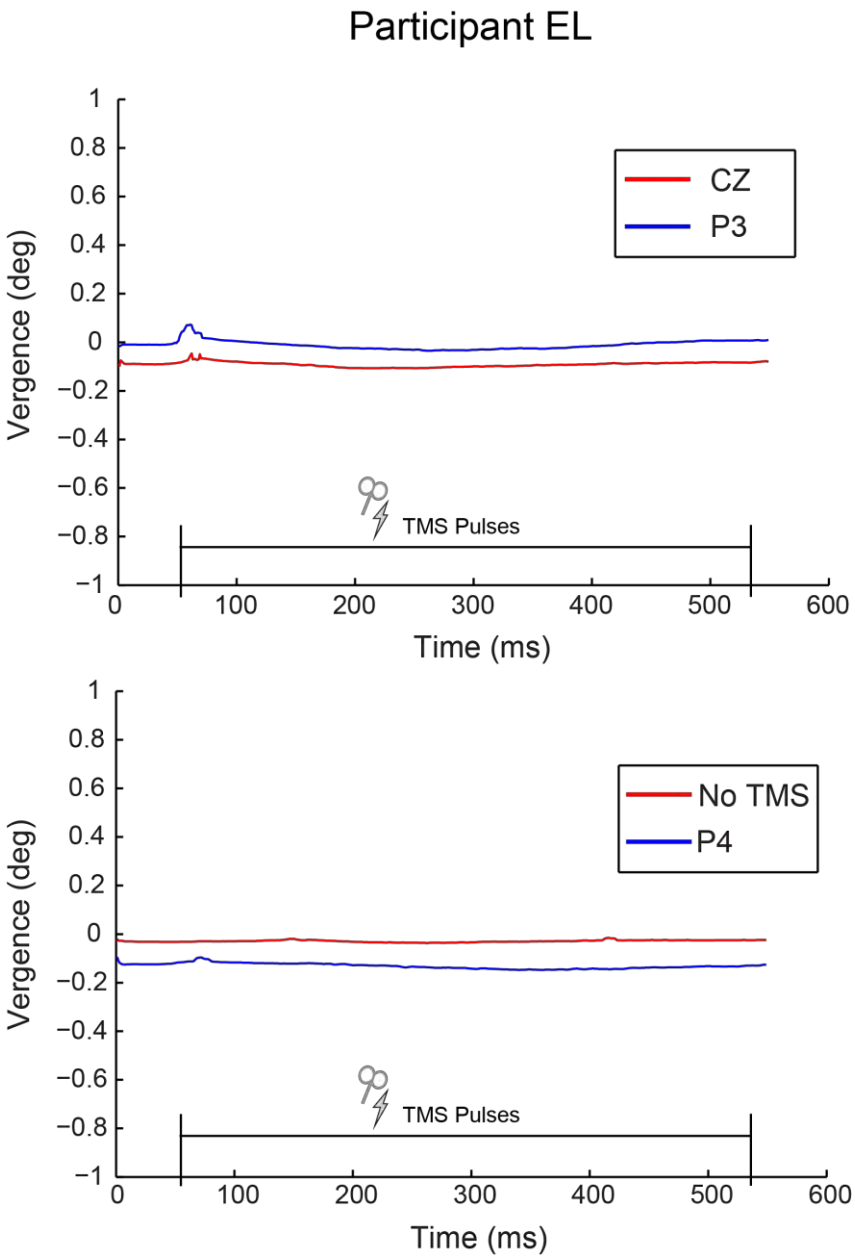
Participant EL
Vergence (deg)
Time (ms)
CZ
P3
TMS Pulses
No TMS
P4
TMS Pulses

Participant HB

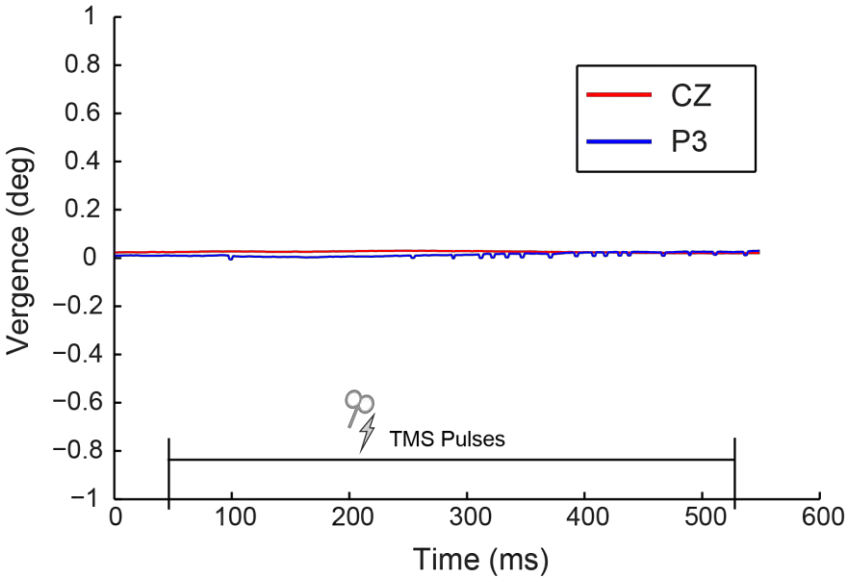

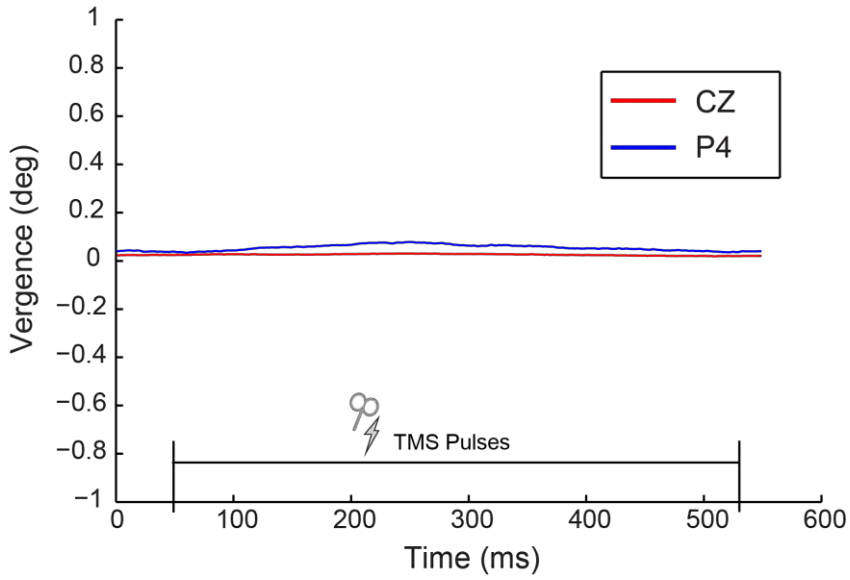

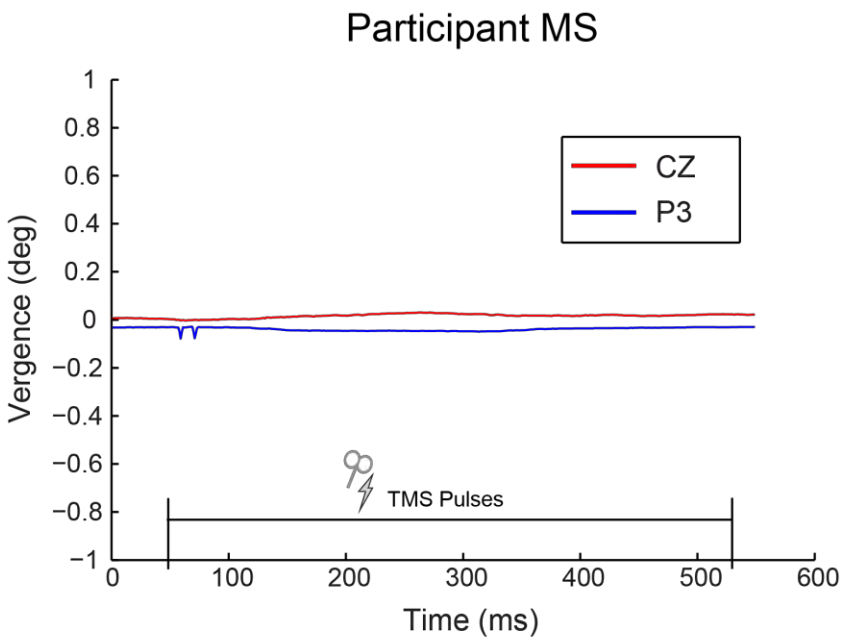
Participant MS
Vergence (deg)
1
0.8
0.6
0.4
0.2
0
−0.2
−0.4
−0.6
−0.8
−1
CZ
P3
TMS Pulses
0
100
200
300
400
500
600
Time (ms)

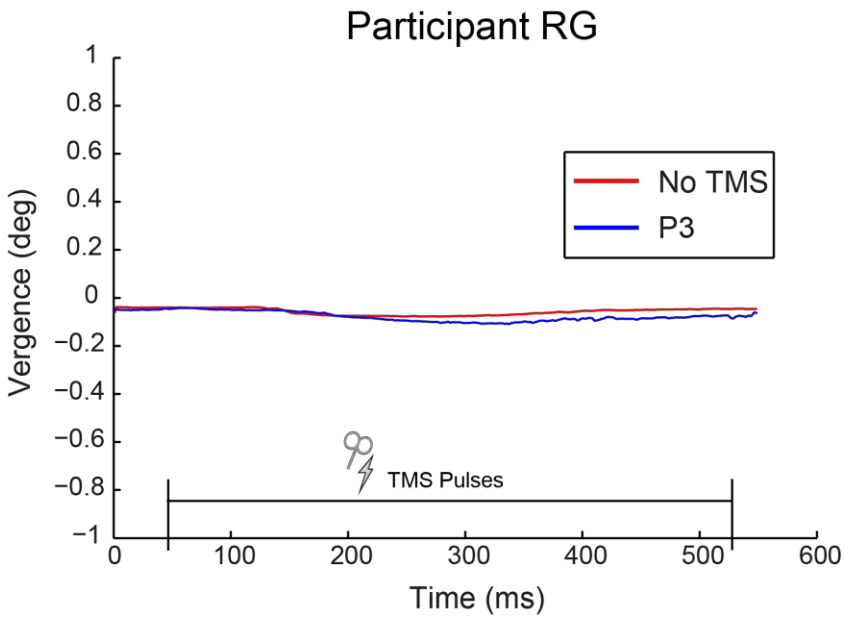
Participant RG
Vergence (deg)
1
0.8
0.6
0.4
0.2
0
−0.2
−0.4
−0.6
−0.8
−1
No TMS
P3
TMS Pulses
0
100
200
300
400
500
600
Time (ms)

3.5.2 Single trial raw data

The above eye-tracking data are averaged across tens of trials. Therefore, it is reasonable to assume that the overall variability between trials has been defused due to averaging, resulting thus in the smooth curves of eye movements across time. However, the majority of the raw eye movement data derived from individual trials showed similar, smooth, flactuations of vergence. Below, I present a few representative graphs from individual trials for the same participants.

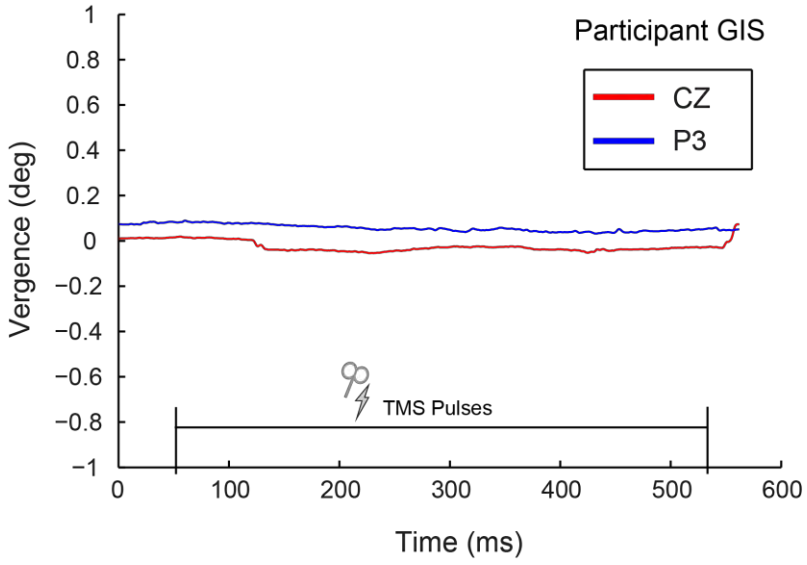

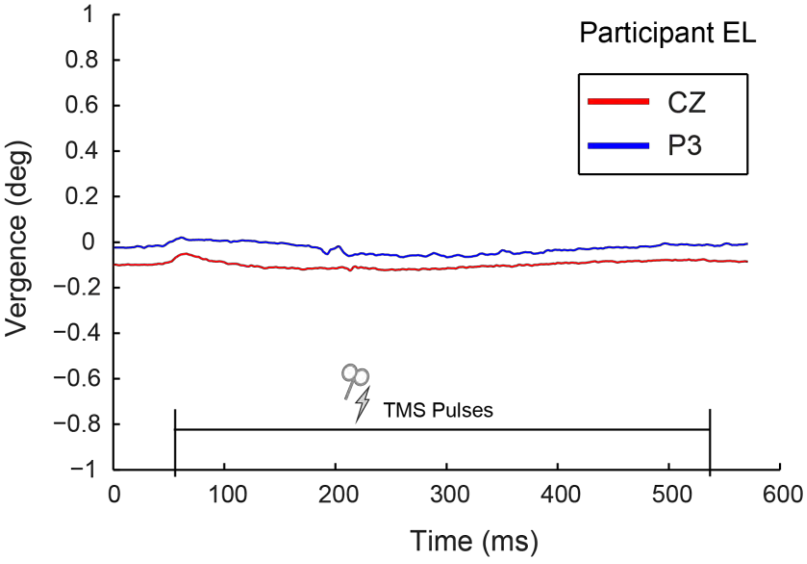

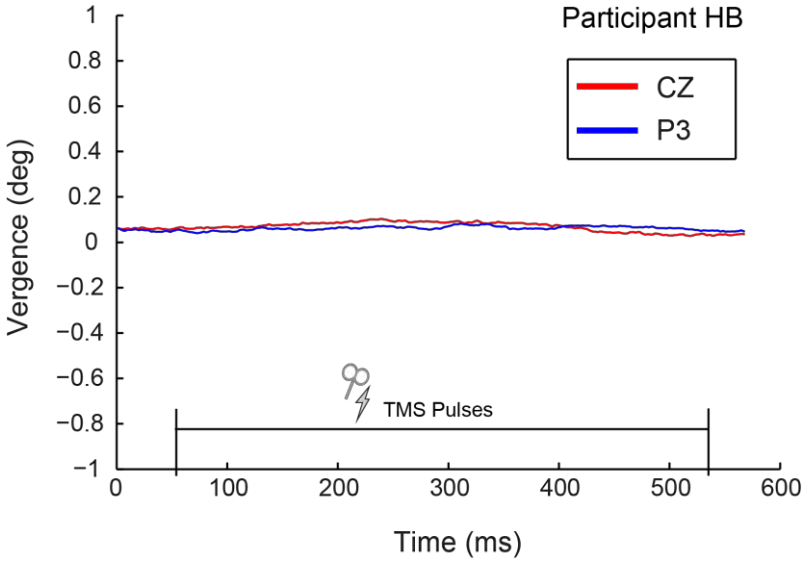
Participant HB
CZ
P3
Vergence (deg)
1
0.8
0.6
0.4
0.2
0
−0.2
−0.4
−0.6
−0.8
−1
0
100
200
300
400
500
600
TMS Pulses
Time (ms)

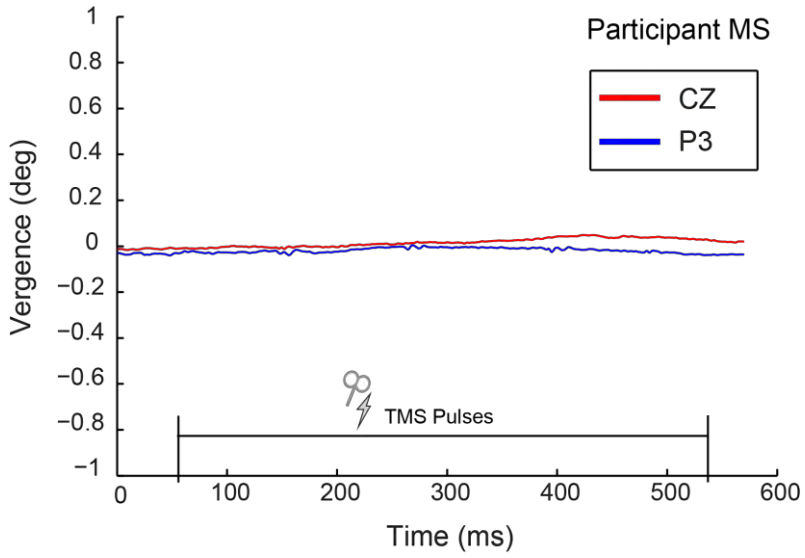
Participant MS
CZ
P3
Vergence (deg)
1
0.8
0.6
0.4
0.2
0
−0.2
−0.4
−0.6
−0.8
−1
0
100
200
300
400
500
600
TMS Pulses
Time (ms)

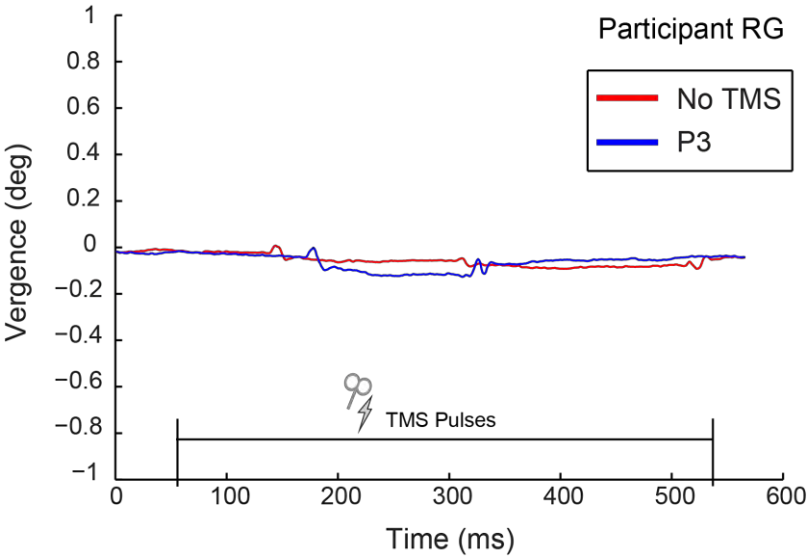
Participant RG
No TMS
P3
Vergence (deg)
1
0.8
0.6
0.4
0.2
0
−0.2
−0.4
−0.6
−0.8
−1
0
100
200
300
400
500
600
TMS Pulses
Time (ms)

4. Integration of motion and disparity cues to depth in ventral visual cortex

Abstract

Apart from binocular disparity, the visual system is exposed to several depth cues in addition to disparity. When the available cues are combined by the brain, a more accurate representation of depth is perceived, compared to the presentation of one cue alone. However, the computational mechanisms that allow the integration of qualitatively different cues remain largely unknown. Here, I used repetitive transcranial magnetic stimulation (rTMS) to examine the involvement of (the functionally localised) cortical area LO, which specialises in 3D object recognition, in 3D cue integration. Participants (n=16) viewed a rectangular moving stimulus whose inner part (target) was displaced farther than the surround in fine steps. Critically, the target's depth was informed either by disparity alone, or by disparity and motion where the two cues signalled depth in a congruent manner. Perceptual judgments, during preliminary behavioural-only sessions, were more accurate and facilitated for the latter (disparity & motion) condition, confirming the advantage of cue integration. In the TMS sessions of the study, rTMS was administered over area LO in both hemispheres, while control measurements were obtained by stimulating area CZ. After manipulating the timing of the rTMS pulses, I found that stimulation over right LO, preceding the stimulus onset for 500 ms, eliminated the advantage of the fused disparity & motion condition. This finding indicates that neural processing in LO is nesseacary for the integration of disparity and motion cues to surface depth perception.

4.1 Introduction

A mosaic of extrastriate visual areas extending in both the occipito-parietal (dorsal) and the occipito-temporal (ventral) streams are engaged in the processing of binocular disparity and in stereo vision. For example, the retinotopic dorsal areas V3A/B have been found to be selective for disparity signals and stereopsis in both the human and the monkey (Backus, et al., 2001; Tsao, et al., 2003; Tyler, et al., 2006), while the ventral stream, and specifically area LO, specialises in the perception of objects' 3D shape and structure (Kourtzi, et al., 2003; Kourtzi & Kanwisher, 2001). In our complex environment, however, the visual system is exposed to several other depth cues which are qualitatively different to binocular disparity, but signal depth in addition to it. The brain then combines texture, shading, occlusion or perspective (to name a few "pictorial" or monocular cues) with disparity and extracts a coherent 3D representation of the scene (Landy, Maloney, Johnston, & Young, 1995) (see *General Introduction*).

When a viewer translates, the images of objects at different distances move across the retina with different velocities (Nadler, Angelaki, & DeAngelis, 2008). This motion parallax is another reliable and powerful depth cue (Rogers & Collett, 1989; Rogers & Graham, 1982). Contrary to the pictorial cues mentioned above, motion-parallax relies on extraretinal (non-visual) signals, since it is associated with the integration of self-induced visual motion and pursuit eye movements (Nadler, Nawrot, Angelaki, & DeAngelis, 2009).

Although the integration of multiple cues results in more accurate depth estimations compared to the presentation of one cue alone (Schiller et al., 2011; Hillis, et al., 2002), it was only recently that attention was brought to the brain mechanisms that support depth cues integration. To this end, dorsal area V3B/KO was identified as the main cortical region where disparity and other cues, as diverse as relative motion (Ban, et al., 2012) shadow (Dovencioglu, et al., 2013) and texture (Murphy, et al., 2013), integrate to facilitate depth judgments in a range of 3D estimation paradigms. In the present study, I adopted Ban et

al.'s (2012) stimuli, defined by disparity only or by disparity and motion parallax, to implement a fine stereoscopic discrimination task and investigate the cortical mechanisms of 3D cue integration by using fMRI-guided TMS.

Pasalar, Ro, and Beauchamp (2010) used TMS to investigate the causal relationship between multisensory integration across modalities and the brain: they showed that TMS over the posterior parietal cortex eliminates the advantage of visual-tactile multisensory integration. Here, in order to probe the cortical locus of the integration of disparity and motion during surface fine depth judgments, I used rTMS in a stereoacuity task requiring near vs far surface discriminations. Similarly to Pasalar, et al. (2010), I assumed that the behaviourally facilitated performance for discriminating depth in a disparity and motion congruent condition should diminish due to TMS-induced cortical disruption. I manipulated the timing of stimulation and pulses were delivered either concurrently (experiment 1) or prior (experiment 2) to the visual stimulus onset. I report evidence that rTMS over area LO shortly (500 ms) preceding the visual stimulus onset changes the behavioural performance and suffices to eliminate the disparity and motion cue integration advantage.

4.2 Methods

4.2.1 Participants

Sixteen observers (7 female, 9 male), students at the University of Birmingham, took part in the two experiments. Two of the participants were excluded because of their poor performance on the depth discrimination task (see below). From the fourteen remained, twelve participated in experiment 1, nine in experiment 2, while seven observers were common in both studies. All participants had normal or corrected to normal vision and were naïve to the purpose of the study.

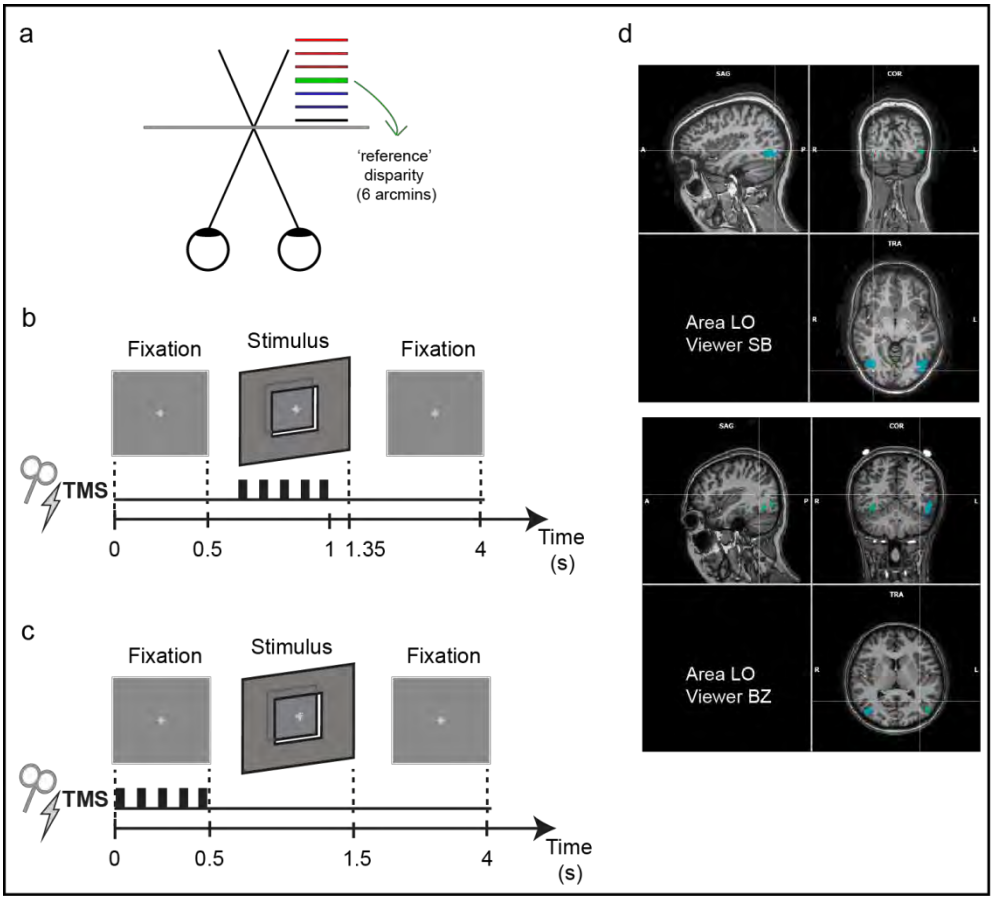

Figure 4.1: (a) Top-down view of the fine depth discrimination task in this study. The disparity of the central target varied in seven steps. Participants reported whether the target was farther or nearer than the average of all the stimuli's disparity (denoted in green here). Five TMS pulses, each lasting for 100 ms, were applied on each trial of experiment 1 and experiment 2: **(b)** Schematic view of the rTMS design and timing parameters for the 'concurrent pulses' study (experiment 1): the first pulse was simultaneous with the onset of the testing visual stimulus which remained on screen for another 350 ms after the last TMS pulse. **(c)** In the 'prior' study (experiment 2), the first pulse was applied 500 ms before the stimulus onset, while the last pulse was almost simultaneous with the visual stimulus onset. **(d)** The brain region that responds significantly more when intact than scrambled versions of images of objects are viewed (area LO) is bilaterally stamped for two participants/viewers.

4.2.2 Regions of interest and TMS protocol

I applied four experimental rTMS conditions, each in a separate session: stimulation over left LO, right LO, area CZ and no TMS. The no TMS session always took place first to avoid potential accumulative effects carried over from previous stimulations. The three sessions involving rTMS took place in a random order, each on a separate day.

I was interested in the bilateral stimulation of LO, to test for depth cues integration specificity, for the following reasons: although fMRI data have suggested a significant involvement of V3B/KO in disparity and motion cue integration to depth (Ban, et al., 2012), in a previous (unpublished) pilot rTMS study in our group we failed to find evidence that stimulation of V3B/KO can attenuate the behavioral enhancement of the integrated disparity and motion. The difference in the methodologies used (fMRI vs TMS) might explain this difference in results. However, this discrepancy could also be accounted for by the differences in the task employed in each study, in light of the functional dissociation believed to exist between the dorsal and the ventral streams: specifically, it has been demonstrated that the dorsal stream is not causally related to fine disparity judgments. In contrast, the ventral stream has been shown to selectively respond to small disparities and fine stereopsis (Chowdhury & DeAngelis, 2008; Shiozaki, et al., 2012; Uka & DeAngelis, 2006; Uka, et al., 2005) -see *General Introduction*. In Ban et al.'s study, viewers were required to judge whether the target of the test stimulus was nearer (in 'near' trials) or farther (in 'far' trials) than the standard stimulus (constant at ±6 arcmin). In contrast, in the task employed here, participants discriminated among several small steps of fine disparity (see below). Therefore, it was reasonable to expect a critical neural contribution of ventral area LO to the execution of the present task. Area CZ was stimulated as a control for the possibility of nonspecific effects associated with rTMS experiments, such as the sound generated by the TMS pulse administration and the tactile-muscle stimulation artifacts.

On each trial, I delivered 5 successive pulses at 10 Hz (i.e., each pulse lasting for 100 ms) administered either simultaneously with (experiment 1; **figure 4.1b**) or 500 ms before (experiment 2; **figure 4.1c**) the visual stimulus onset. None of the participants reported the perception of phosphenes. After response, there was a 2500 ms interval before the next trial. Similarly to the previous chapter, I have followed the fMRI-guided TMS approach and used Brainsight (Rogue Research Inc) to place the coil over the functionally localized left and right LO. For CZ, the coil was guided through the 10-20 EEG coordinate system.

4.2.3 Stimuli and psychophysics

I adopted Ban et al.'s (2012) grayscale random-dot stereograms which I presented against a mid-gray background. The presentation region of the stereogram was surrounded by a grid of black and white squares to provide an unambiguous background reference and promote a stable vergence posture. Stimuli were viewed through a laboratory stereo set up where the two eyes viewed separate LCD monitors from a distance of 50 cm through a mirror stereoscope. Screens resolution was 1680 x 1050 pixels at a refresh rate of 100 Hz. When both eyes viewed the stereogram (each eye viewing each of stereogram's part at the corresponding monitor) a single surface in the plane of the screen ('surround') was seen, having a size of 12.5 x 12.5°. The inner/central part ('target') of the surround frame, a square of 8.5 x 8.5° size, was varied in seven fine steps of far depth relative to the flat surround (**figure 4.1a**). At the center of the stimulus there was a square of 1° where participants were fixating.

Ban et al. (2012) employed a two-interval forced-choice (2IFC) paradigm where the disparity magnitude of the test stimulus was controlled by a staircase. However, here, the implementation of a 2IFC paradigm would be inappropriate. Specifically, applying rTMS to alter the initial brain state during the presentation of one stimulus (the reference for example) would have a strong neural impact on the processing of the second stimulus (the test for example). As Silvanto and Pascual-Leone (2008) note, the initial state of a brain region plays a critical role in the neural impact that a stimulus will have on that region (see *General Methods*). In a potential 2IFC methodology, therefore, I would not be able to evaluate the contribution of the targeted area to an observed behavior, if rTMS effects were carried from one interval over the other. Hence, similarly to the previous chapter, I used the method of single stimuli (MSS): participants were asked to indicate whether the target on each trial was farther away ('more depth') or closer ('less depth') than the average depth of all the targets' magnitude levels presented in the set. (For more details on the MSS, see *General Methods*).

Binocular disparity and motion were manipulated in two experimental conditions: in the 'Disparity Only' condition, depth of the target was defined solely by disparity, while in the 'Disparity & Motion' condition, depth was informed congruently by disparity and motion parallax (**figure 4.2**). In both conditions, the surround and target planes were moving horizontally following a sinusoidal velocity profile (duration 1 s), and the target was taking the following horizontal disparity magnitudes: 2.5, 4, 5.5, 6, 6.5, 8, 9.5 arcmin. The surround surface had constant disparity (appearing on the screen's plane) and constant motion (at 0.9° amplitude), while the target surface was moving with amplitude that (in the disparity & motion condition) ranged from 0.29° to 1.32° depending on its disparity magnitude. In the disparity only condition, both the target and the surround produced a rigid horizontal movement (0.9°) irrespectively of the disparity magnitude of the target. On the other hand, in the 'disparity & motion', the relative motion was perceived as a pattern of deletion and accretion of the surround or target as they moved across the screen. Thus, motion parallax, 'the relative image motion between objects in different depths that normally results from the observer's movement' (Nadler, et al., 2008; Nadler, et al., 2009), was perceived. As an example of motion parallax, one could imagine being on a moving train where the near objects, relative to a point of fixation, seem to move faster than those being far away. Stimuli in the combined disparity & motion condition here simulated the above natural environment situation: when assigned with the smallest disparity (appearing near) the target's motion amplitude was 1.32°, whereas when assigned with the biggest disparity (appearing far) its motion was 0.29°.

To rule out the possibility of any serial effects in participants' MSS judgments during the main experiments (see General Methods; Parducci, 1959; Rambo, 1961), all testing stimuli (both conditions and the depth amplitudes within each condition) were randomly interleaved. Each stimulus/disparity level was presented 14 times so that each session had a total of 196 (7 stimulus levels x 14 times each x 2 conditions) trials.

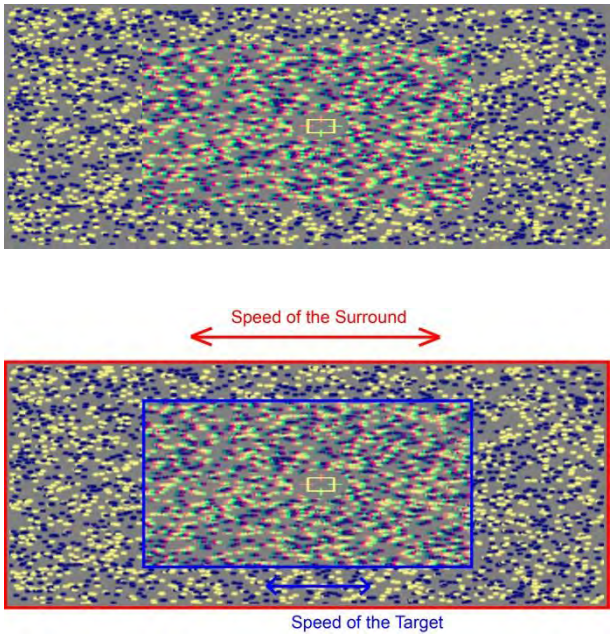

Figure 4.2: Red-green anaglyphic stereograms to illustrate the 'Disparity Only' (upper part) and the 'Disparity & Motion' (lower part) stimuli. In the disparity only condition, the target and the surround surfaces moved rigidly with a constant movement. In the 'disparity & motion', the surround and the target were moving with different velocities (producing patterns of deletion and accretion to simulate motion parallax) depending on the disparity magnitude of the target.

4.2.4 Preliminary observations and rationale

The study was completed in two different phases: The first phase, similarly to the previous chapter, was the training (solely behavioural) phase, designed to train participants on the 3D stimuli and the MSS task. Results from the experiments in this phase provided reassurance that participants could reliably perform near/far discriminations at the motion parallax apparatus and produce reasonable psychometric functions.

I employed sigmoidal psychometric functions (cumulative Gaussian) to fit to the data, using the Psignifit toolbox in Matlab. Psignifit uses the observed values/data to generate 4999 simulations of the psychometric function (bootstrap resampling) and returns the median values of the estimations it makes for each variable. Similarly to the previous chapter, to quantify performance and perform statistical analyses for both the behavioural and the TMS data, I retrieved and analysed the threshold at 50% (PSE) "farther"

discrimination level and the standard deviation variables as they derived from the estimates of the psychometric functions.

During the no TMS preliminary sessions, I observed an improved depth discrimination performance at the 'Disparity & Motion', compared to the 'Disparity Only' condition. This behavioural improvement for almost all the participants, due to the accumulated depth cues of disparity and motion, is qualitatively revealed by a visual inspection of the sample psychometric functions depicted in **figure 4.3**: the curves fitting the Disparity & Motion data are either steeper or leftward shifted compared to the Disparity Only, indiacting a more accurate and easy perceptual discrimination for the former condition (e.g., Frund, et al., 2011). Quantitatively, significant behavioural differences between the two conditions were revealed, across all participants, in terms of standard deviations (SD) (decreased in the Disparity & Motion; [$t(20) = 4.885$, $p < .0001$]) and thresholds (decreased in the Disparity & Motion; [$t(20) = 5.354$, $p < .0001$]).

In the main phase of the study, I used rTMS aiming to identify the brain mechanisms that support the behavioural difference between the two conditions. I hypothesised that neurostimulation of the critical cortical area should attenuate the behavioural enhancement observed at the Disparity & Motion condition as a result of cue fusion.

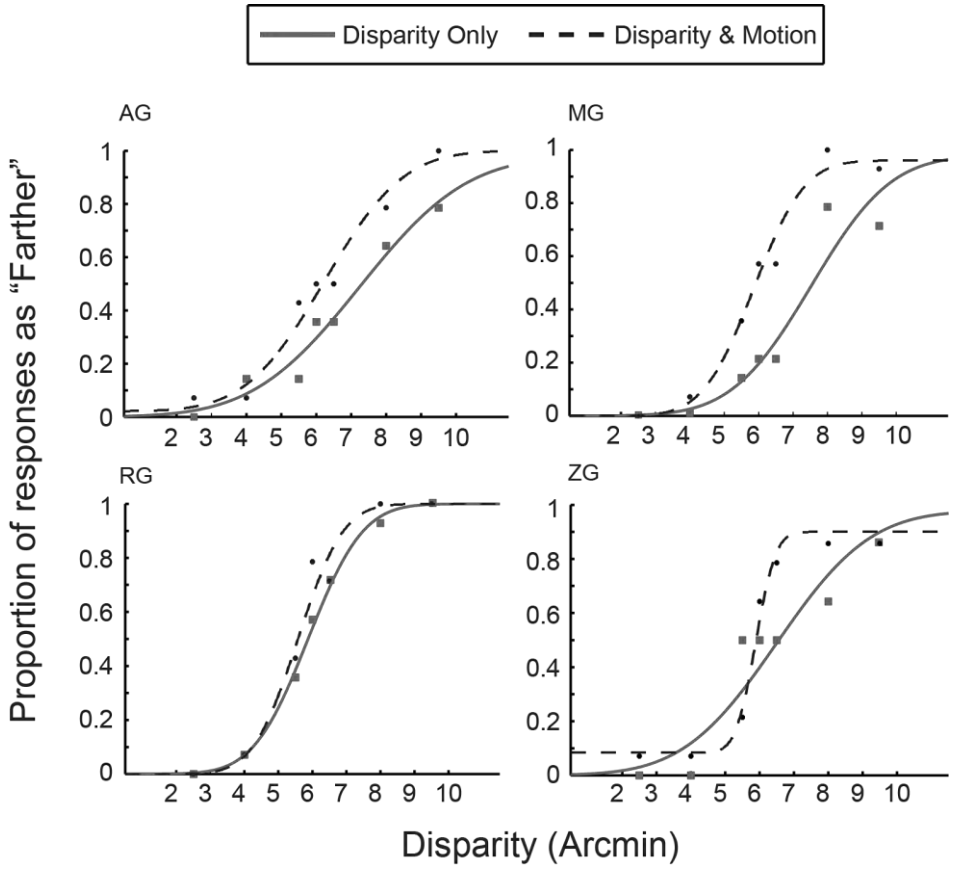

Figure 4.3: Psychometric functions for the depth discrimination performance under the two experimental conditions at the behavioural (no TMS) session regarding four representative participants (*AG, RG, ZG* and *MG*). The proportion of judging trial surfaces as 'farther' than the implicit reference (the mean of the whole set) is plotted against the various depths (in arcmin) of the stimuli presented. The curves indicate the best fit of the cumulative Gaussian function. Either steeper or leftwards shifts of the curve indicate improved performance at the Disparity & Motion compared to the Disparity Only condition.

4.2.5 Pilot training experiments on the method of single stimuli

Because five participants (*MG, CL, DP, AG* and *ZG*) were not experienced with psychophysics tasks, before their training on the 3D stimuli in the stereoscope, they were trained on a simple behavioural paradigm with 2D stimuli. The main rationale for this training experiment was to reassure that the participants were familiarised with the psychophysical aspects of the experiment. On each trial, a pair of horizontal lines being slightly separated to each other was presented in a single interval alone, for 1 second. Viewers judged whether each given pair was more or less separated relative to the average separation distance of the whole set (see Morgan, 1992). There were 7 different step levels

of separation between the lines (i.e., 7 different pairs/stimuli) and the exact distance between each pair was determined based on the (normalized) disparity levels of the 3D stimuli in the main experiment. I presented each stimulus level 14 times and fitted cumulative Gaussian functions to the proportion of “bigger separation” responses (**figure 4.4**).

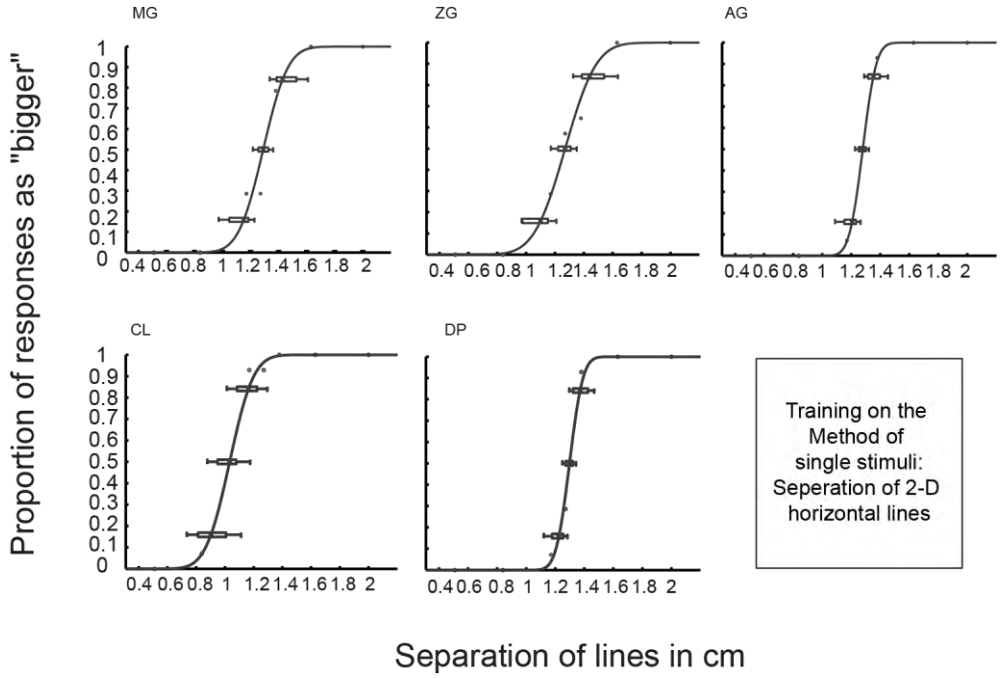

Figure 4.4: Psychometric functions obtained from the 5 participants who were trained on the method of single stimuli (MSS) task, requiring the discrimination of 2D separated lines. The curves, indicating the best fit of the cumulative Gaussian function, have been fitted nicely to the data, reassuring participants’ familiarisation with the MSS.

4.3 Results

4.3.1 Experiment 1: pulses concurrent with the visual stimulus onset

Fourteen observers in total took part in experiment 1 (mean age = 22.3, SEM = 0.58, 6 females), but data obtained from 2 of them were excluded from further analysis since the estimates of their psychometric functions were outside the range of the tested stimuli. Four participants (*JH, BZ, RG and AP*) were naïve to the 3D motion parallax stimuli (the rest of

the participants participated in the 'prior pulses' version of the study in a previous testing). Therefore, these four observers were trained on the experimental stimuli and procedure as follows: they firstly attended the depth discrimination task without feedback. Consequently, they repeated the same task, but feedback (fixation cross turning to green for correct responses -turning to blue for incorrect ones) was provided for the trials belonging to the Disparity Only condition. Participants attended this feedback training session between 3 and 5 times, depending on how much training each one needed to produce reasonable psychometric functions.

After training, participants attended the main no TMS session and, subsequently, the TMS sessions in a random order. During rTMS, pulses were administered concurrently with the visual stimulus onset and were applied over left LO, right LO and CZ, each on a separate day. Similarly to the previous chapter, I used the threshold at 50% performance level (PSE) and the standard deviation (JND) to quantify performance. Below I present the results as acquired by fitting cumulative Gaussians to the data.

Threshold (PSE) analysis

As **figure 4.5** shows, thresholds at 50% performance level decreased in the Disparity & Motion condition compared to the Disparity Only condition during both LO and CZ stimulation sessions. A 2 (area stimulated: Concatenated LO / CZ] X 2 (Condition: Disparity Only / Disparity & Motion) repeated measures ANOVA showed a non-significant main effect of the area [$F(1,11) = 1.53$, $p = .24$, partial $\eta^2 = .122$, power ($1-\beta$) = 0.13]. However, there was a significant main effect of the condition [$F(1,11) = 14.88$, $p = .003$, partial $\eta^2 = .575$, power ($1-\beta$) = 0.97] indicating that, no matter the area of stimulation, observers were more biased in discriminating depth in the Disparity & Motion condition than in the Disparity Only. There was a non-significant interaction effect between the area and the condition [$F(1,11) = 2.16$, $p = .170$, partial $\eta^2 = .164$, power ($1-\beta$) = 0.20].

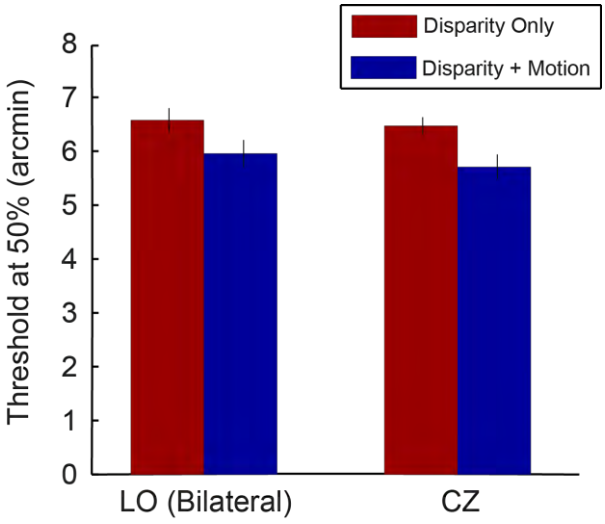

Figure 4.5: Averaged threshold at 50% "farther" responses across participants for the Disparity Only and the Disparity & Motion conditions as a function of the concatenated bilateral LO and CZ sessions for the concurrent rTMS pulses. Error bars indicate standard error of the mean.

Standard deviation (JND) analysis

a. All areas and conditions individually

Standard deviation decreased in the Disparity & Motion condition compared to the Disparity Only condition, indicating that participants were more sensitive in discriminating depth in the former. Intriguingly, this predominance existed in all the sessions except for CZ (**figure 4.6, left part**). I subtracted the mean SD of the Disparity & Motion condition from the mean SD of Disparity Only and found that, indeed, all sessions (no TMS, left LO and right LO), except for CZ, had a positive signed mean. One-way repeated measures ANOVA for this differential standard deviation between the two conditions across sessions revealed a significant main effect of the session [$F(3,33) = 4.494$, $p = .009$, partial $\eta^2 = .29$, power $(1-\beta) = 0.33$], but all post hoc comparisons were non-significant. These results suggest that rTMS was sufficient to slightly minimize the perceptual discrimination difference observed at the no TMS session, but there was no systematic effect of any of the areas stimulated. In the no TMS session, one-sample t-test against zero confirmed that the differential standard deviation between the two conditions was significantly different than zero [$t(11) = 3.63$, $p =$

.004]. However, one-sample t-tests against zero for the remaining sessions did not reveal any significant differences. [Left LO: $t(11) = .73$, $p = .48$; Right LO: $t(11) = 1.8$, $p = .10$; CZ: $t(11) = -.73$, $p = .48$].

b. Concatenated bilateral LO and CZ

In order to reduce the variability of the data, I pooled the two unilateral LO stimulation sites together and analysed them against CZ. The analysis after fitting psychometric functions to the bilateral LO and (single) CZ clusters' data follows. Standard deviation decreased (indicating greater sensitivity/facilitated performance) in the Disparity & Motion condition compared to the Disparity Only during the LO stimulation sessions, while this pattern reversed and SD decreased for Disparity Only under CZ stimulation (**figure 4.6, right part**). This is a difficult result to account for, but most probably indicates that brain stimulation, concurrent with the visual stimulus onset, failed to disrupt the integration of depth cues and to attenuate the facilitative effect that disparity and motion integration normally has on depth discrimination. A 2 (area stimulated: Concatenated LO / CZ) X 2 (Condition: Disparity Only / Disparity & Motion) repeated measures ANOVA showed non-significant effects of the area [$F(1,11) = 2.057$, $p = .179$, partial $\eta^2 = .158$, power $(1-\beta) = 0.19$], condition [$F(1,11) < 1$, $p = .782$, partial $\eta^2 = .007$, power $(1-\beta) = 0.05$] and the interaction between area and condition [$F(1,11) = 2.623$, $p = .134$, partial $\eta^2 = .193$, power $(1-\beta) = 0.26$].

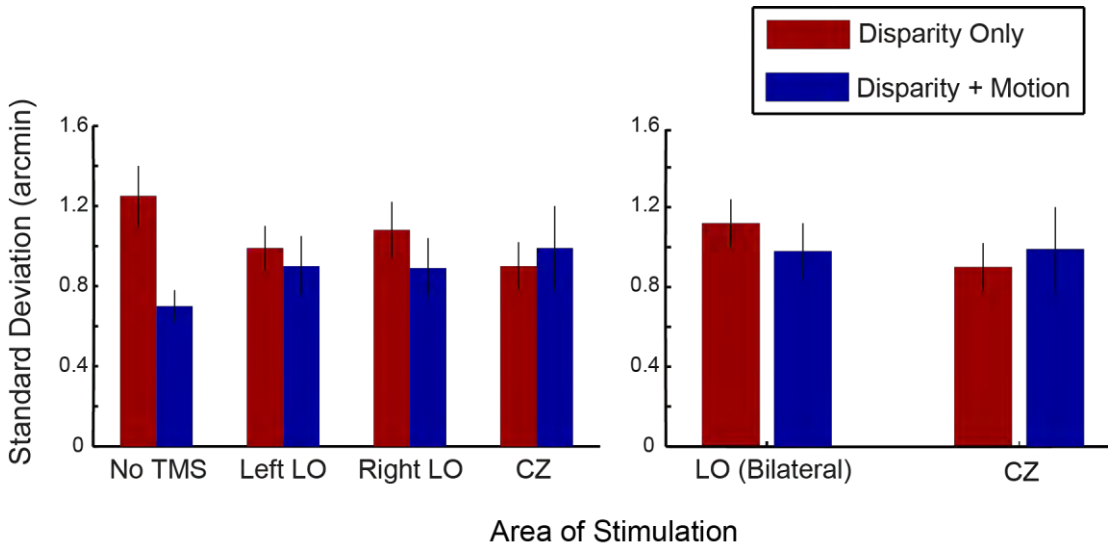

Figure 4.6: Averaged standard deviation values across participants for the Disparity Only and the Disparity & Motion conditions as a function of the different sessions individually (left part) and the concatenated bilateral LO and CZ sessions (right part), for the concurrent rTMS pulses. Error bars indicate standard error of the mean.

4.3.2 Experiment 2: pulses prior to the visual stimulus onset

The improved depth estimation in the Disparity & Motion condition, during no TMS sessions, indicates that when visual depth cues aggregate to signal depth simultaneously, then perceptual judgments are facilitated (Dosher, Sperling, & Wurst, 1986; Landy, et al., 1995). However, the concurrent timing of the rTMS pulses failed to reveal the cortical locus of this cue integration and its 'predominance' in behaviour. In experiment 2, seeking to identify the optimal timing of pulses in order to establish a transient 'virtual lesion' (Walsh & Cowey, 1998) and reveal the contribution of the stimulated areas to the behavioural observations, I used nine observers (mean age = 22.1, SEM = 0.89, 1 female) and administered the rTMS pulses 500 ms before the visual stimulus' onset. In the following graphs (**figure 4.7**), raw data (where the two controls (no TMS and CZ) and the two LO areas (right and left) have been pooled together) are presented for each condition for all the participants. For most of the participants, stimulation of LO resulted in an attenuation of performance for the combined motion and disparity condition (psychometric function either

less steep or with higher SD). All the raw data (each rTMS session plotted individually) are presented in the chapter's appendix.

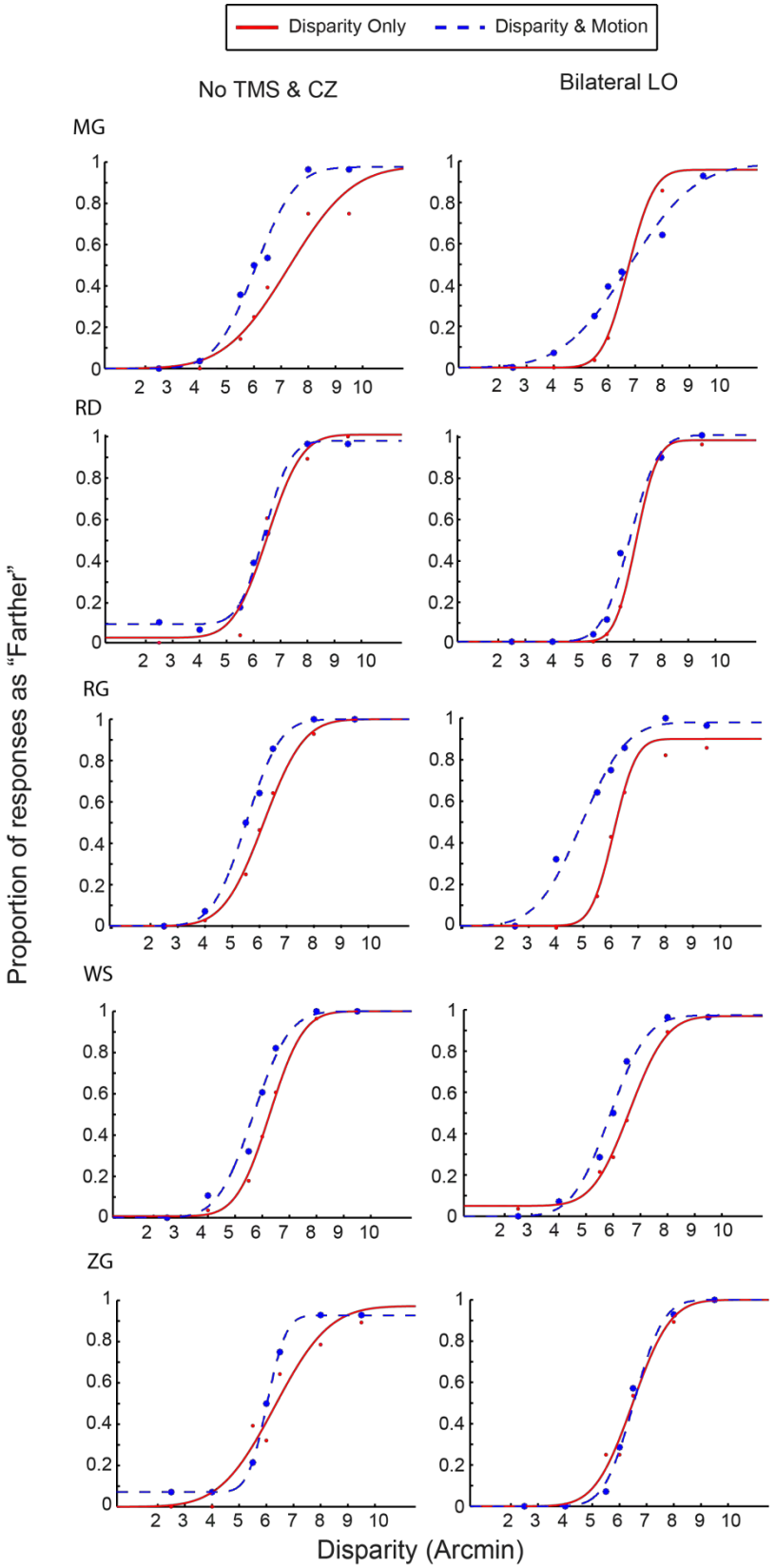

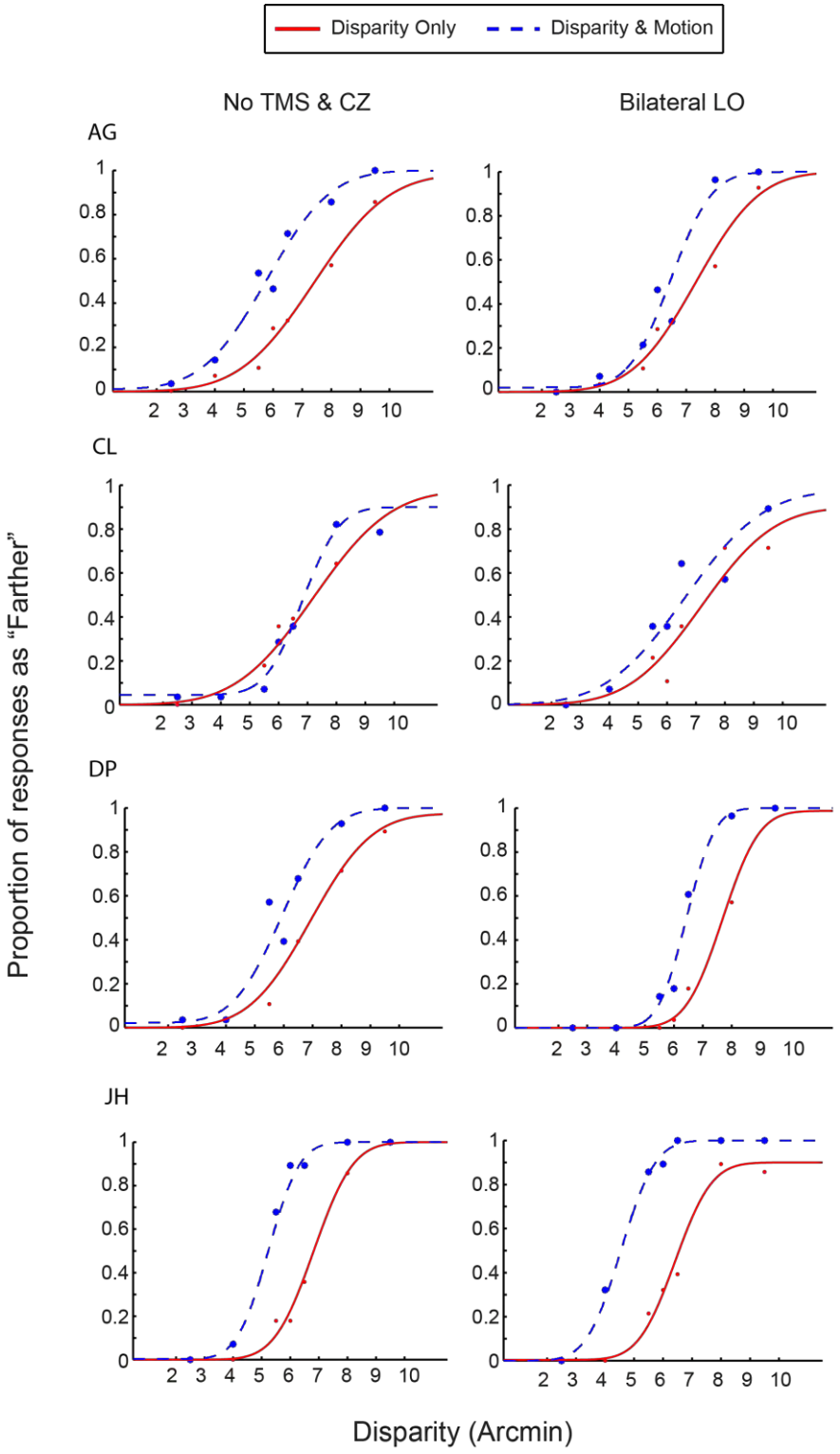

Figure 4.7: Psychometric functions for control (no TMS and CZ pooled together) and LO sessions, across conditions, for all participants of experiment 2. Each curve indicates the best fit of the cumulative Gaussian function for the Disparity Only and Disparity & Motion conditions. Visual inspection of the graphs reveals a quite systematic leftward shift or steeper psychometric function curves for the fused 'Disparity & Motion' compared to the 'Disparity Only' condition at the control sessions, but not LO. For all the raw data (each TMS session plotted individually), see the appendix.

Threshold (PSE) analysis

I analysed threshold data at the 50% performance level as estimated by fitting the psychometric functions. As **figure 4.8** shows, thresholds decreased in the Disparity & Motion condition compared to the Disparity Only condition during both LO and CZ stimulation sessions. A 2 (area stimulated: Concatenated LO / CZ] X 2 (Condition: Disparity Only / Disparity & Motion) repeated measures ANOVA showed a non-significant main effect of the area [$F(1,8) < 1$, $p = .41$, partial $\eta^2 = .085$, power $(1-\beta) = 0.08$]. However, there was a significant main effect of the condition [$F(1,8) = 12.45$, $p = .008$, partial $\eta^2 = .61$, power $(1-\beta) = 0.94$] indicating that, no matter the area of stimulation, observers were more biased in discriminating depth in the Disparity & Motion condition than in the Disparity Only. There was a non-significant interaction effect between the area and the condition [$F(1,8) < 1$, $p = .958$, partial $\eta^2 = .00$, power $(1-\beta) = 0.05$].

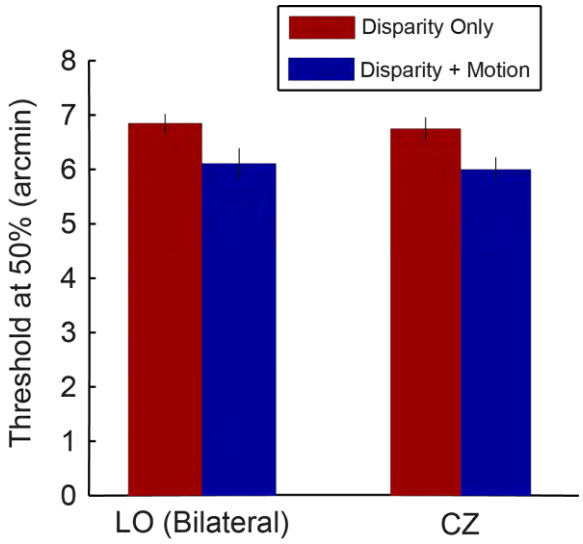

Figure 4.8: Averaged threshold at 50% "farther" responses across participants for the Disparity Only and the Disparity & Motion conditions as a function of the concatenated bilateral LO and CZ sessions for the concurrent rTMS pulses. Error bars indicate standard error of the mean.

Standard deviation (JND) analysis

a. All areas and conditions individually

Depth discrimination improved (decreased standard deviation) during no TMS, CZ and left LO sessions for the Disparity & Motion, relative to the Disparity Only condition. This facilitation changed (the pattern was actually reversed indicating an interaction effect; see below) only during right LO stimulation (**figure 4.9; left part**).

As I did in experiment 1, I subtracted the mean SD of the Disparity & Motion condition from the mean SD of Disparity Only, which resulted in a positive signed number for all sessions, except when TMS was delivered to right LO. One-way repeated measures ANOVA for this differential standard deviation between the two conditions across sessions revealed a significant main effect of the session [$F(1.8,14.7) = 4.46$, $p = .033$; Greenhouse-Geisser correction, partial $\eta^2 = .358$, power $(1-\beta) = 0.37$]. Indeed, the facilitated behavioural discrimination of depth in the Disparity & Motion condition compared to Disparity Only condition vanished only after the stimulation of right LO: pairwise comparison between no TMS and right LO was also significant [$t(8) = 4.38$, $p = .002$). One-sample t-tests against zero confirmed that the differential standard deviation between the two conditions was significantly different than zero in the no TMS [$t(8) = 3.09$, $p = .015$] and CZ sessions [$t(8) = .584$, $p < .001$], but not in the left LO [$t(8) = .273$, $p = .79$] and right LO sessions [$t(8) = -1.72$, $p = .123$].

b. Concatenated bilateral LO and (single) CZ

In order to reduce the variability of the data, I pooled the two unilateral LO stimulation sites together and analysed them against CZ. The analysis, after fitting psychometric functions to the bilateral LO and (single) CZ data, follows. SD decreased in the Disparity & Motion condition compared to the Disparity Only condition during stimulation of CZ. Interestingly, this enhanced sensitivity in Disparity & Motion vanished during LO stimulation, where SD pattern reverses in favour of the Disparity Only (**figure 4.9; right part**). Although this result

suggests that rTMS over LO disrupted the integration of depth cues and attenuated the facilitative effect that disparity and motion integration normally has on depth discrimination, statistical analysis failed to reach significance: a 2 (area stimulated: Concatenated LO / CZ) X 2 (Condition: Disparity Only / Disparity & Motion) repeated measures ANOVA showed non-significant effects of the area [$F(1,8) <1$, $p = .882$, partial $\eta^2 = .003$, power $(1-\beta) = 0.05$], condition [$F(1,8) <1$, $p = .824$, partial $\eta^2 = .007$, power $(1-\beta) = 0.05$] and the interaction between area and condition [$F(1,8) = 2.592$, $p = .146$, partial $\eta^2 = .245$, power $(1-\beta) = 0.30$].

c. Concatenated bilateral LO and concatenated control sessions

I analysed the clustered LO (right and left pooled together) and the clustered control session (CZ and no TMS pooled together), each consisted of 28 trials per stimulus level presented. The analysis, after fitting a cumulative Gaussian to the bilateral LO and grouped control sessions' data, showed the following: not surprisingly, the difference in SD between Disparity & Motion and Disparity Only in the control concatenated cluster was greater than the LO one (**figure 4.9; right part**). This facilitated performance for Disparity & Motion during the control sessions diminished during LO stimulation sessions, where the standard deviation pattern reversed in favour of the Disparity Only. This interaction between the area and the condition was significant, as a 2 (Session: Concatenated LO / Concatenated control) X 2 (Condition: Disparity Only / Disparity & Motion) repeated measures ANOVA [$F(1,8) = 6$, $p = .040$, partial $\eta^2 = .428$, power $(1-\beta) = 0.70$] revealed. This result suggests that when disparity and motion cues are seamlessly (during no TMS and CZ) integrated, depth perception is enhanced. This enhancement vanishes after stimulation of LO, rendering this area, thus, a highly probable cortical site for the optimal fusion of disparity and motion cues.

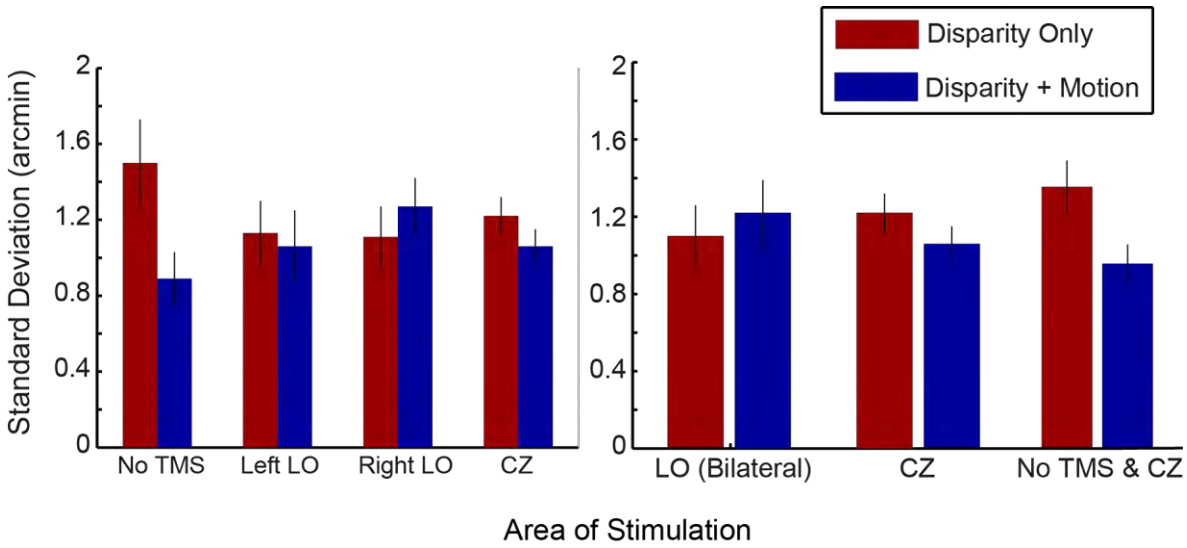

Figure 4.9: Averaged standard deviation values across participants for the Disparity Only and the Disparity & Motion conditions. The two conditions are plotted as a function of the different sessions individually (left part) and the concatenated bilateral LO, CZ alone and the concatenated control (no TMS + CZ) sessions (right part), for the prior TMS pulses experiment. Error bars indicate standard error of the mean.

4.3.3 Effect of order/training

Similarly to chapter 3, I analysed the data for order effects, to examine whether participants' performance improved as a result of the successive exposure to the task (irrespectively of the TMS session they were undertaking each day). **Figure 4.10** represents the days of experimentation plotted as a function of performance (as quantified with standard deviation). Correlation analysis showed that the day of experimentation was not significantly related to the standard deviation in disparity only [r = -.239, p (one-tailed) = .080] nor disparity & motion [r = .239, p (one-tailed) = .080] condition.

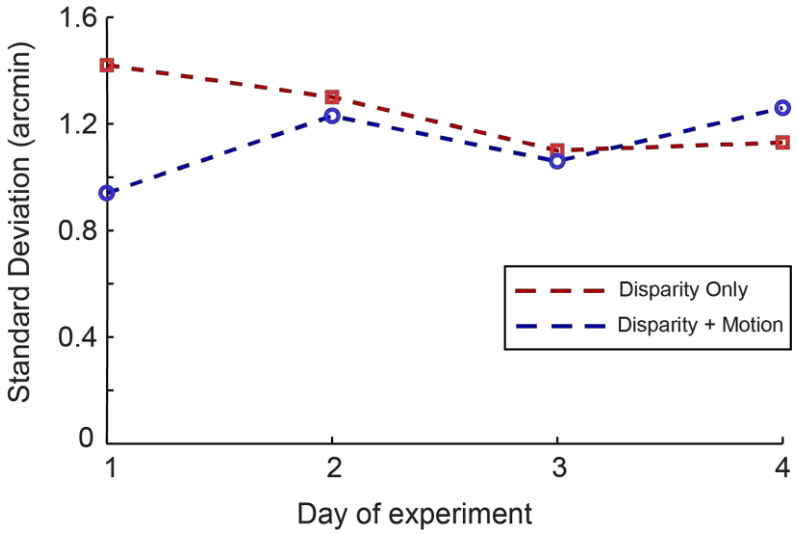

Figure 4.10: The days of experimentation as a function of standard deviation. Both conditions are assessed and data are averaged across participants.

4.3.4 Common participants of experiments 1 and 2

To fully evaluate the factors that affect depth cues integration, I analysed the data acquired from the 7 observers who participated in both the prior and the concurrent timing versions of the study. As **figure 4.11** shows, in the case that the TMS pulses were preceding the visual stimulus, depth discrimination was significantly facilitated (decreased standard deviation) in the Disparity & Motion condition of the control (no TMS & CZ) sessions, compared to the Disparity Only condition. However, during LO stimulation sessions, this pattern was reversed and standard deviation was slightly increased in the 'Disparity & Motion'. However, this significant interaction (see analysis of the concatenated data above) between session/area and condition was the case only when TMS pulses were administered prior to visual stimulus and not for the concurrent version (see right part of the graph), as a 2 (Timing: Prior / Concurrent) X 2 (Session: LO / control) X 2 (Condition: Disparity Only / Disparity & Motion) repeated measures ANOVA revealed: there was a significant interaction among all three factors (timing, session and condition) [$F(1,6) = 6.45$, $p = .044$, partial $\eta^2 = .518$, power $(1-\beta) = 0.97$].

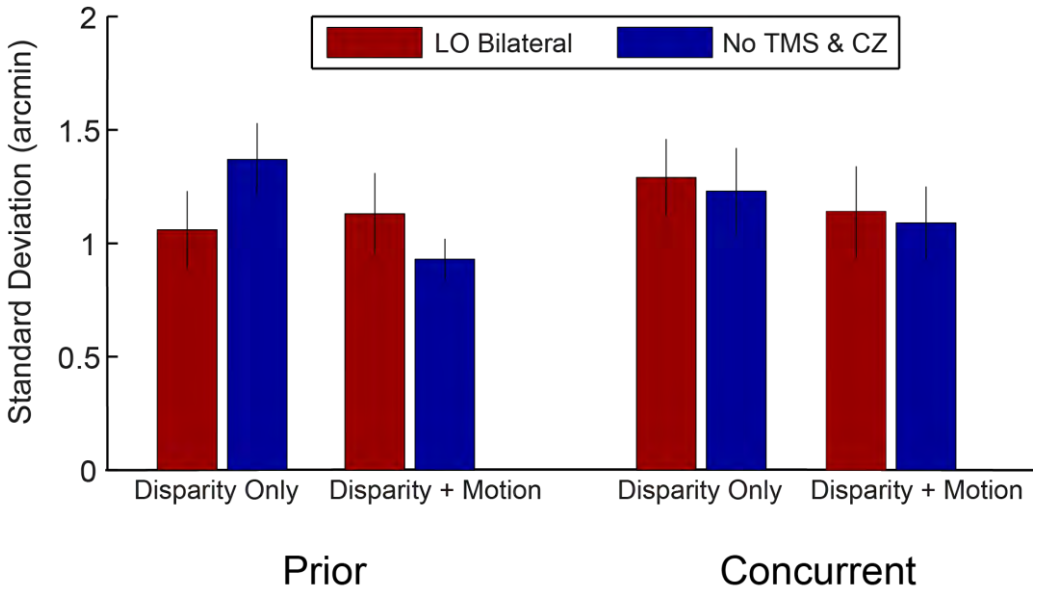

Figure 4.11: Standard deviation data from the 7 common viewers having participated in both experiments 1 ('concurrent' rTMS timing) and 2 ('prior' timing), as a function of the session (concatenated LO vs concatenated control), the condition (disparity only vs disparity & motion) and the TMS timing (prior vs concurrent). A significant interaction among all three factors indicated that the interaction of session and condition was not equally present in experiments 1 and 2: only when the pulses were applied prior to the stimulus onset, the area of stimulation was significantly interacting with the condition. Error bars indicate standard error of the mean.

4.4 Discussion

As indicated by the preliminary data of this study, in almost all the no TMS sessions, perceptual judgments in a fine discrimination task controlled by the method of single stimuli were more accurate and facilitated in the condition where depth was informed by both disparity and motion parallax cues, compared to disparity alone. This enhancement in sensitivity, revealed by decreased standard deviation in the Disparity & Motion condition compared to the Disparity Only condition, was the result of the aggregation of two depth cues signalling depth congruently and concurrently. Aiming to identify where in the brain the optimal fusion of depth cues is localised, I conducted a series of rTMS experiments and found that stimulation of area LO significantly eliminates the behavioural enhancement that disparity and motion integration normally gives rise to. Importantly, the present study shows that this effect highly depends on the timing of the pulses administration and that different

rTMS timings are not equally effective: specifically, magnetic pulses delivered concurrently with the visual stimulus to-be-perceived were insufficient to disrupt the neural mechanisms that support disparity and motion cues integration. On the other hand, when TMS pulses preceded the visual stimulus onset for 500 ms, a complete attenuation of the predominance of the Disparity & Motion condition and a reverse of the effect in favour of Disparity Only took place. Taken together, these results ascribe to LO a special role in the fusion of depth cues, suggesting that neural processing in at least right LO (as the analysis for individual hemispheres showed) is neccessary for the integration of disparity and motion information.

In accordance to the result reported here, a similar integration of 3D cues in LO has been reported by Welchman, et al. (2005). The researchers used fMRI to show that activity in LO supports the combination of cues to slant, resulting in the perception of global 3D shapes. However, Welchman, et al. (2005) reported that, in addition to LO, dorsal activity, in area MT+, is also critical for the combination of cues to slant. This latter result is, somehow, in agreement with Ban et al. (2012) who also found that dorsal processing, (in area V3B/KO), supports the integration of motion and disparity. Specifiaclly, Ban et al. (2012) showed that fMRI activity in V3B/KO was effectively used by a machine learning classifier to reliably discrimiante stimuli extended in near or far depth, but sensitivity and decoding performance in area LO was not found to be equally significant.

How can this discrepancy between the fMRI and the present rTMS study be accounted for? One possibility is that the depth discrimination task that each study requires is supported by fundamentally separate neural mechanisms. Critically, although stimuli in the two studies were very similar (central targets extended in depth, defined by disparity and/or motion), in Ban et al.'s study viewers judged whether the target of the test stimulus was nearer (in 'near' trials) or farther (in 'far' trials) than the standard stimulus (constant at $\pm$6 arcmin). In contrast, in the present study, the target stimulus took one of seven horizontal disparity magnitude levels. It appeared either nearer or farther than the implicit reference disparity and the participants made 'more fine' depth judgments: they completed

a fine stereopsis task of relative disparity, requiring to compare each given stimulus with the whole set's average depth (set at 6 arcmin and always appeared farther than the frontoparallel surround). Previous studies employed very similar 'fine' tasks, where the presented dispairty varied in several small steps. They found that the ventral –and not the dorsal- visual pathway causally relates and significantly contributes to fine depth discriminations (e.g., Chowdhury & DeAngelis, 2008; Shiozaki, et al., 2012; Uka, et al., 2005) (see *General Introduction*). This specialisation of the ventral stream in fine depth tasks and relative disparities could theoretically predict that the neural processing ventrally may indeed support the integration of 3D cues in fine stereopsis. However, I cannot exclude the possibility that cue integration for fine stereopsis may involve a broader network of areas and that rTMS over LO disrupts just a part of this network and not the cortical locus of the integration *per se*. In other words, the impaired behavioural performance due to the transient 'lesion' of an area due to TMS does not highlight that this area is necessary and sufficient for the behaviour under question. It could be the case, for example, that cue integration evokes activity in both the dorsal and the ventral streams which together encode different aspects of the perceptually relevant information (Preston, et al., 2008).

Apart from perceptual processing, the psychophysical method (MSS) I have employed requires a good amount of visual memory resources. Xu and Chun (2006) showed that the visual objects held in the visual short-term memory (VSTM), as well as their spatial locations, are represented in the lateral occipital complex. Given the nature of the MSS, I cannot exclude the possibility that my findings may simply support the critical role that LO has been found to play in VSTM's encoding and maintenance. However, for such an interpretation, one would expect a decline in performance in both the Disparity Only and the Disparity & Motion conditions under LO stimulation, an expectation not supported by the data acquired though.

4.5 Appendix for chapter 4: raw psychometric functions

The following graphs depict the raw data for each condition and area of stimulation individually for every participant. For most of the participants, under right LO, the sensitivity at the combined motion and disparity condition is attenuated (psychometric function becomes either less steep or with bigger SD).

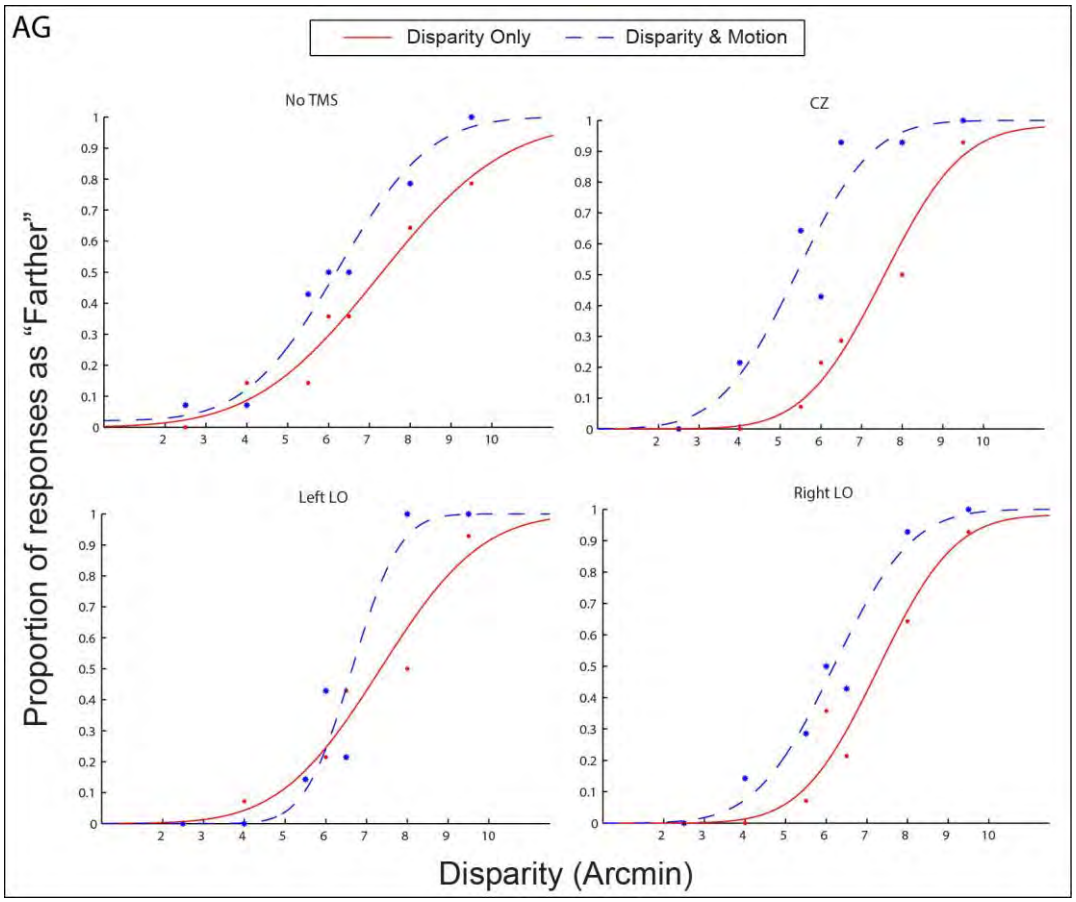

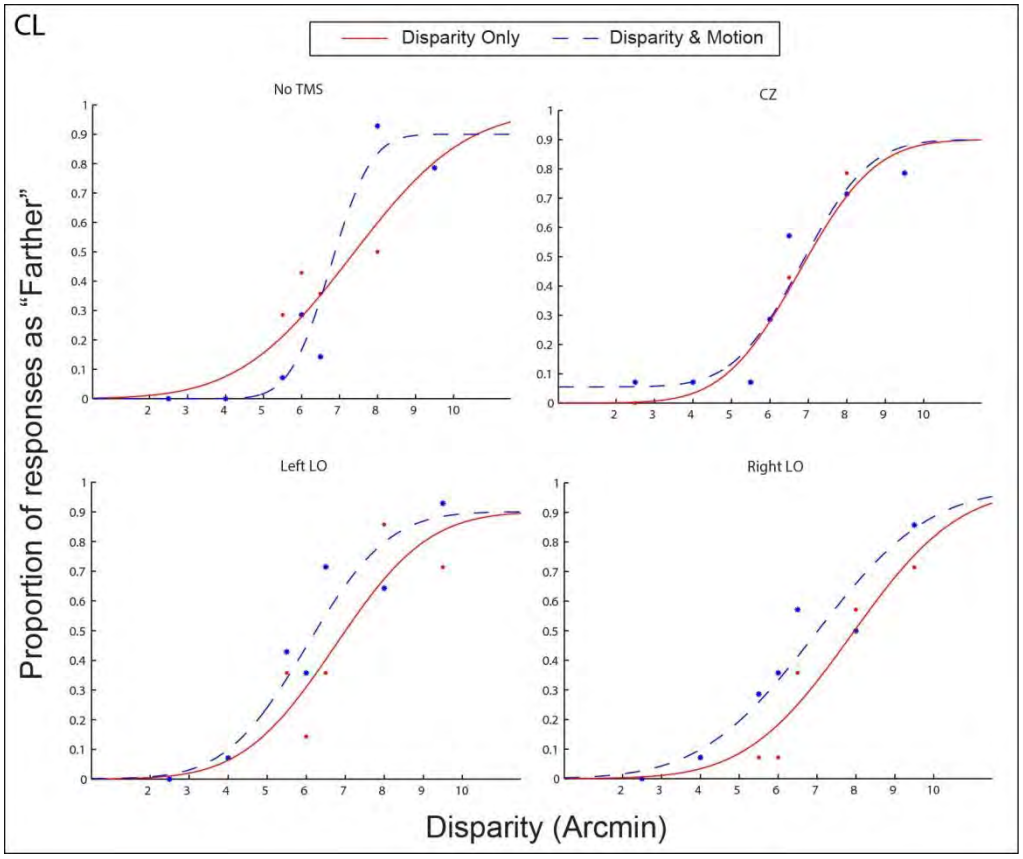
CL
Disparity Only
Disparity & Motion
No TMS
CZ
Left LO
Right LO
Proportion of responses as "Farther"
Disparity (Arcmin)

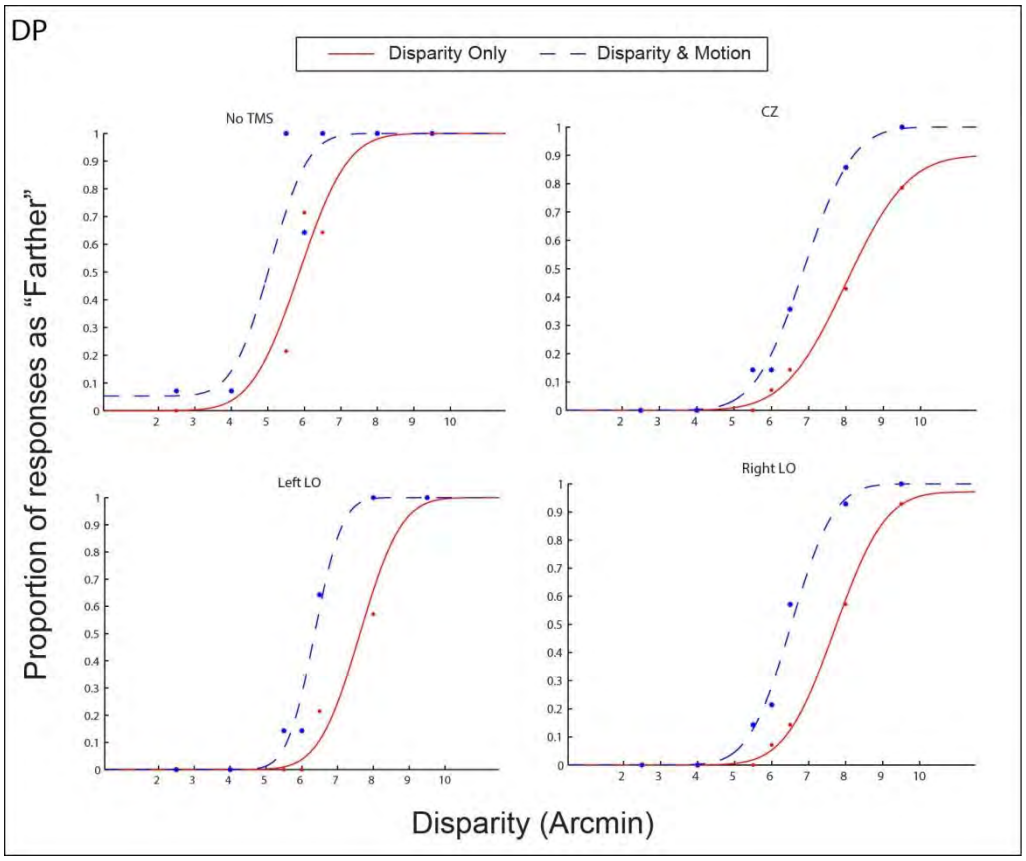
DP
Disparity Only
Disparity & Motion
No TMS
CZ
Left LO
Right LO
Proportion of responses as "Farther"
Disparity (Arcmin)

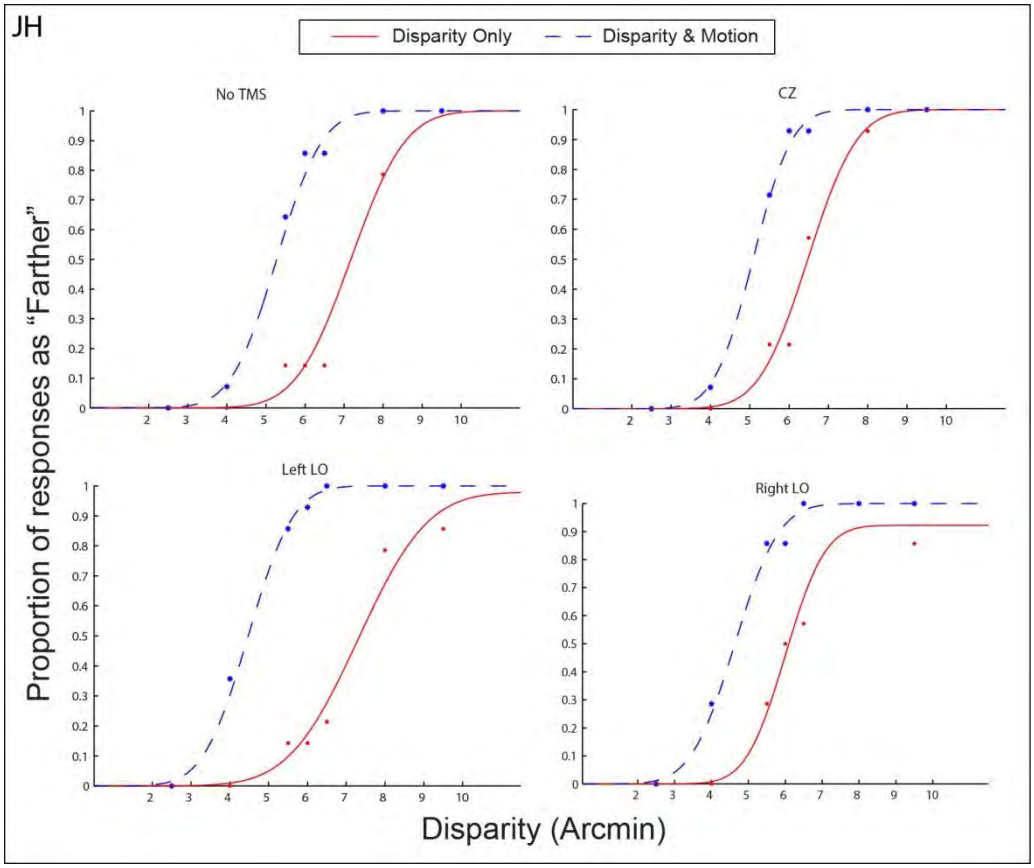
JH
Disparity Only
Disparity & Motion
No TMS
CZ
Left LO
Right LO
Proportion of responses as "Farther"
Disparity (Arcmin)

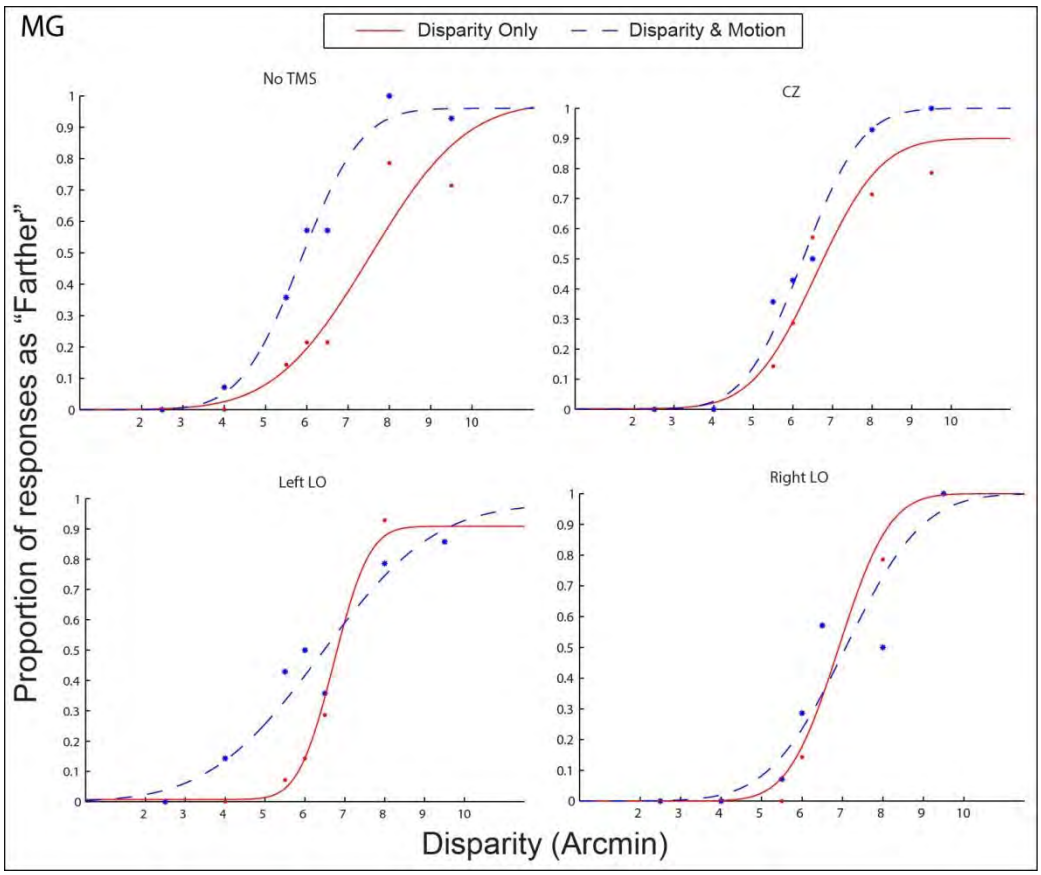
MG
Disparity Only
Disparity & Motion
No TMS
CZ
Left LO
Right LO
Proportion of responses as "Farther"
Disparity (Arcmin)

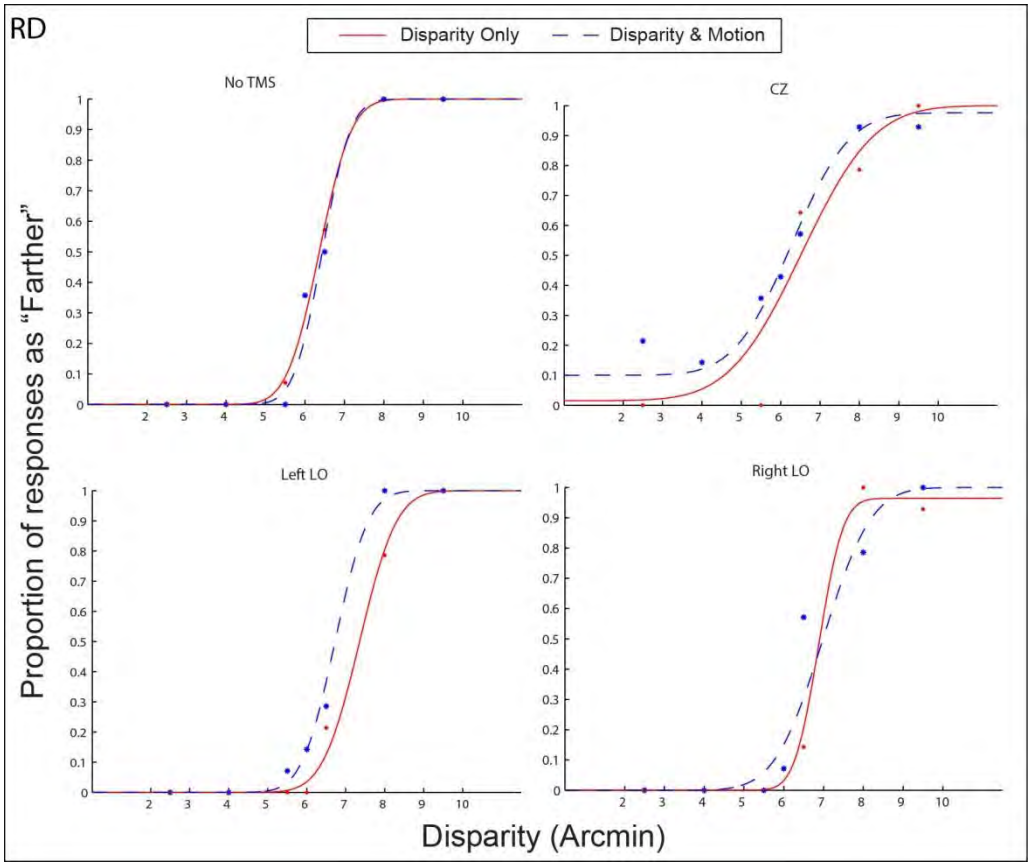
RD
Disparity Only
Disparity & Motion
No TMS
CZ
Left LO
Right LO
Proportion of responses as "Farther"
Disparity (Arcmin)

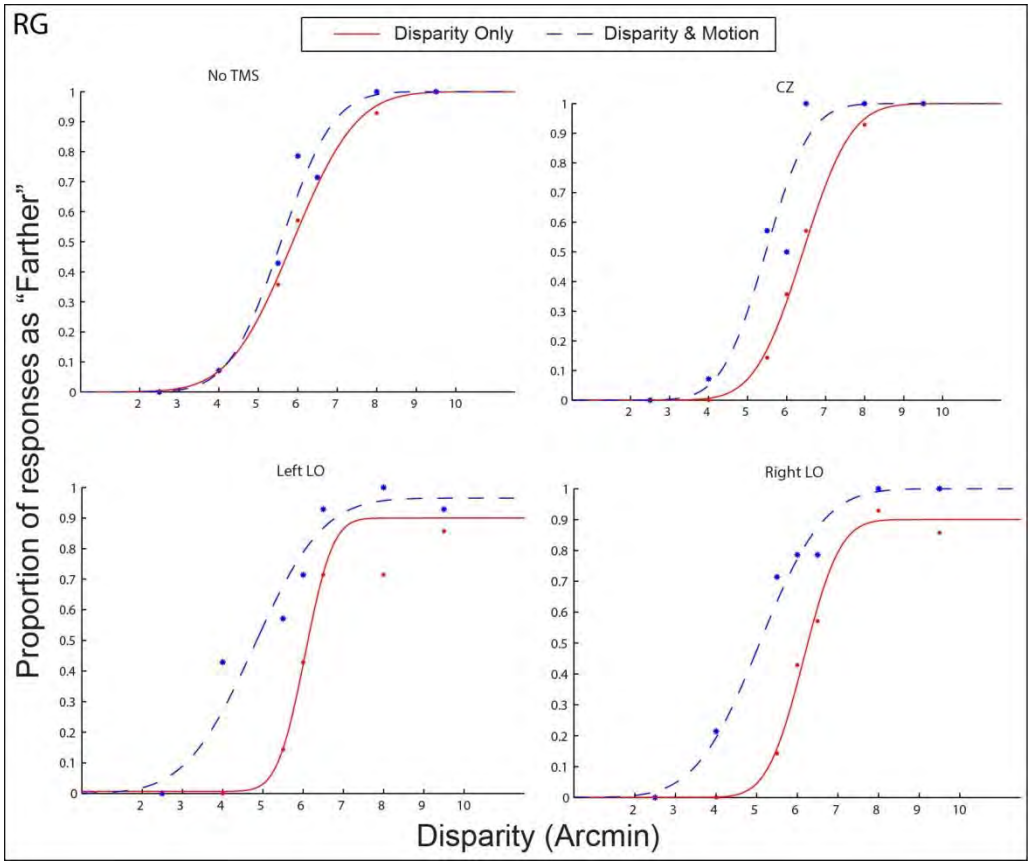
RG
Disparity Only
Disparity & Motion
No TMS
CZ
Left LO
Right LO
Proportion of responses as "Farther"
Disparity (Arcmin)

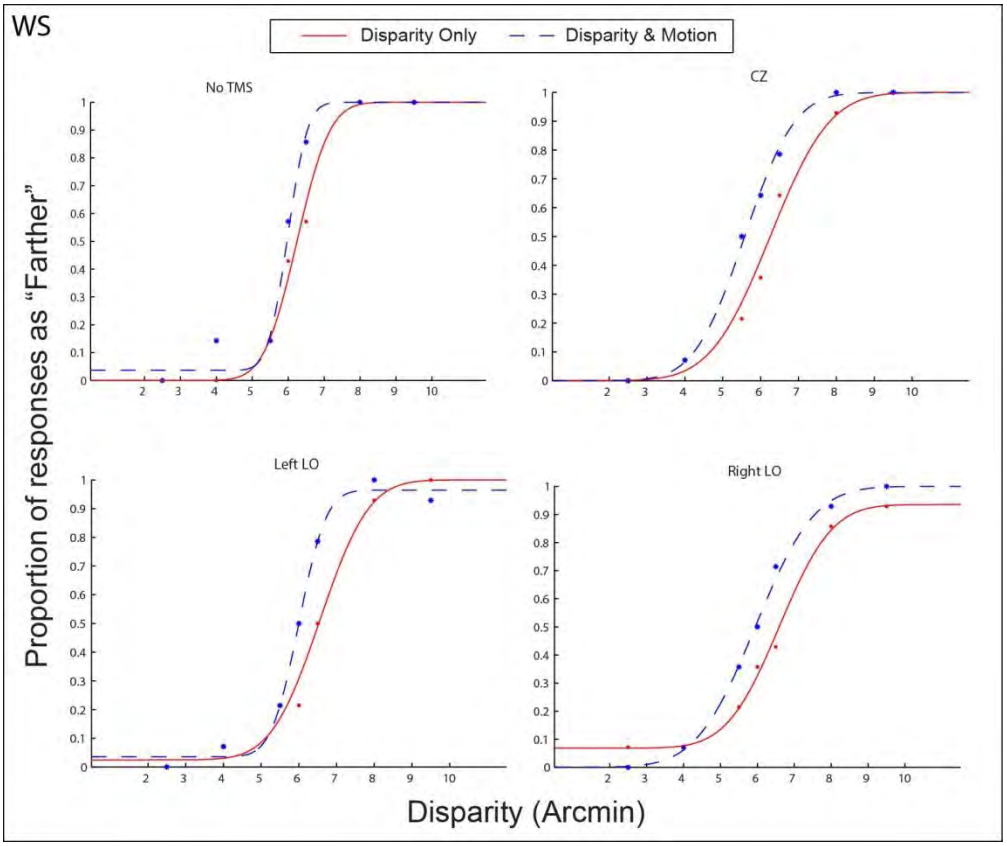
WS
Disparity Only
Disparity & Motion
No TMS
CZ
Left LO
Right LO
Proportion of responses as "Farther"
Disparity (Arcmin)

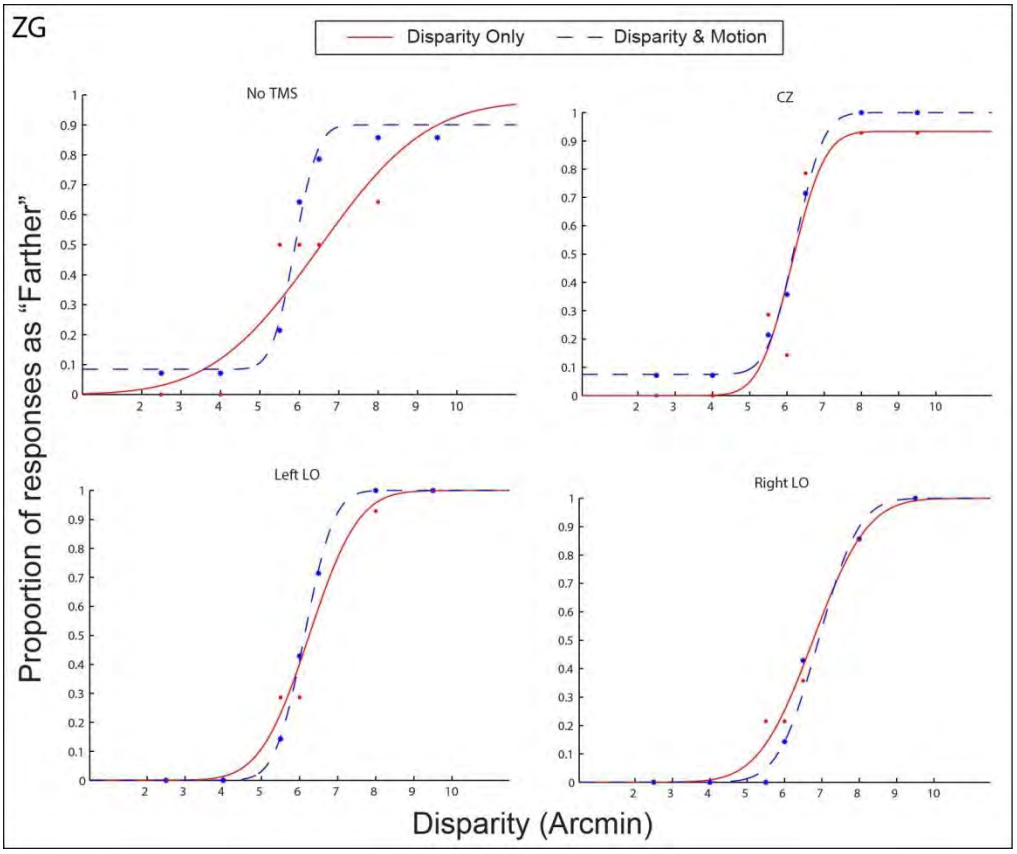
ZG
Disparity Only
Disparity & Motion
No TMS
CZ
Left LO
Right LO
Proportion of responses as "Farther"
Disparity (Arcmin)

5. Learning generalisation across visual features in dorsal visual cortex

Abstract

Recent studies in both the human and the monkey suggest that, within depth paradigms, the benefits of training on a feature difference discrimination task generalise to signal in noise discrimination tasks and the (otherwise) important contribution of the dorsal cortex to signal in noise extraction diminishes. Here, I explored whether such a 'neural shift' during learning generalisation occurs not within the same visual feature (i.e., depth) only, but across different visual features (orientation/depth) as well. The study consisted of three phases: in the 'pre-training' phase, participants were tested on a (either orientation or depth) signal in noise discrimination task while repetitive transcranial magnetic stimulation (rTMS) was applied over the left posterior parietal cortex (P3), right PPC (P4) and area CZ, over three separate days. In the second phase, training with feedback, on a task (or visual feature) other than the one used in the first phase took place over three days. Finally, the 'post-training' phase was identical to the first one. In my first experimental group, participants (n=9) were tested with rTMS on a signal in noise orientation discrimination task and trained on a feature difference depth discrimination task. In the second group, participants (n=7) were tested on signal in noise depth and trained on feature difference orientation. In the third group (n=8), testing was on signal in noise depth and training on signal in noise orientation. I found that, before training, processing in P3 is necessary for the execution of a signal in noise task. After training, however, P3's contribution decreases dramatically. These results indicate that the dorsal neural circuit that supports performance in signal in noise changes in favour of transferring training benefits.

5.1 Introduction

The training effect analysis of the slant discrimination project in chapter 3 showed that the extensive training on the 3D task with feedback resulted in the improvement of participants' performance across TMS testing days. On the other hand, the cue integration experiments in chapter 4, in light of the Ban et al.'s (2012) findings, highlighted the functional dissociation between the ventral and the dorsal visual stream in the processing of binocular disparity. The purpose of the present study was twofold: at first, to investigate visual learning further and decipher the contribution of training to performance; additionally, to examine how learning generalisation is associated with (dorsal) cortical organisation.

Visual learning facilitates recognition and optimizes the tuning of neurons in ventral cortical areas in both the human and the monkey (Adab & Vogels, 2011; Li, et al., 2009; Raiguel, et al., 2006; T. Yang & Maunsell, 2004); see *General Introduction*. On the other hand, as it has been discussed earlier, areas of the dorsal stream encode information during coarse discriminations of absolute disparity embedded in noise, while ventral areas specialise in the processing of feature-difference in the absence of noise ('fine' discriminations). Interestingly, Chowdhury and DeAngelis (2008), after demonstrating a dramatic impairment in performing a signal-in-noise, coarse disparity, task caused by a temporary pharmacological inactivation of MT, trained their animals on a 'fine' depth task. After this training, the researchers found that MT's reversible inactivation had no effects on the 'coarse' (or the 'fine') task anymore. In the human, Chang, Kourtzi, & Welchman (2013) used psychophysics to show that the benefits of visual learning transfer asymmetrically: within the same visual feature (disparity defined depth), training on a feature difference discrimination ('fine') task enhances performance for both the feature difference and a signal-in-noise discrimination task. Interestingly, however, training on the signal-in-noise task facilitates performance only for the signal-in-noise but not the feature difference one. In a second experiment, where multiple visual features (depth, motion and orientation) were considered, Chang et al. (2013) showed that training on the signal-in-noise task of one

visual feature promotes performance facilitation for the signal-in-noise tasks of all the other features, but the benefits of training on the feature difference task do not transfer to the feature difference tasks of the other visual features.

Using rTMS, Chang et al. (2014) employed a disparity defined depth task of near/far discrimination to show that, once learned, discrimination of feature differences in depth boosts the cortical processing of disparity in the ventral stream (LO) and this processing substitutes the otherwise critical role of the left parietal cortex in a depth signal-in-noise discrimination task. Taken together, these recent studies in Welchman's group suggest that, within depth paradigms, training on feature difference discrimination generalises at the behavioural (learning benefits transfer to both feature difference and signal-in-noise discriminations; Chang et al., 2013) and the neural level (dorsal areas are not necessary anymore for signal-in-noise discrimination; Chang et al., 2014).

However, it remains unknown whether generalisation of learning 'at the neural level' (e.g., a potential reduced contribution of the dorsal areas to signal-in-noise discrimination due to training) exists not only within depth paradigms, but across visual features (orientation/depth) as well. Chang et al. (2013) did examine learning's generalisation across visual features, but always within the same type of task (either signal-in-noise or feature difference alone). Here, I used rTMS to explore the neural basis of visual learning generalisation across different tasks (signal-in-noise/feature difference) and across visual features (orientation/depth).

5.2 Methods

In order to evaluate performance in these experiments, I have compared discrimination thresholds (acquired while repetitive magnetic stimulation was applied over the dorsal areas of interest) between before- and after- training phases. I sought to reveal the extent

to which neural processing in dorsal areas is necessary for 'coarse' discriminations of signal embedded in noise both within and across different visual feature paradigms. Firstly, I examined whether, apart from its high contribution within paradigms involving depth judgments (e.g., Minini, et al., 2010), neural processing in the dorsal stream is also necessary in orientation discrimination informed by glass patterns. In particular, in experiment 1, I evaluated whether training on a fine disparity task (small differences in the depth plane in the absence of noise) discrimination can transfer its benefits and promote performance in the signal-in-noise discrimination of orientation (Dosher & Lu, 2005). For a description of all the experiments, see *Experimental groups & participants*.

5.2.1 Apparatus

I used the same laboratory stereo set up as in chapters 3 and 4, where the two eyes viewed separate LCD monitors from a distance of 50 cm through a mirror stereoscope. However, screens had a resolution of 1280 x 1024 pixels here, and a refresh rate of 120 Hz.

5.2.2 Stimuli and tasks

The stimuli were adopted from Chang et al. (2014) study. Stimuli were circular random-dot stereograms depicting a 14 x 19 degrees surface ("surround") whose central part (7 x 7 degree) ("target") was either horizontally/vertically oriented (glass pattern/orientation experiments) and/or extended in near/far depth (depth experiments) with respect to the surround (**figure 5.1**). Stimulus presentation time was 300 ms. The profiles of the stimuli and each task's difficulty varied depending on the type of task (signal-in-noise/feature difference) and the type of visual feature (depth/orientation judgments). Specifically, the stimuli I used can be categorised as follows:

1. Signal-in-noise depth: Target's disparity, in 100% signal, was fixed at ± 6 arcmin. However, on each trial, the proportion of dots having this disparity/signal varied relative to noise dots which had a random disparity within ± 12 arcmin. The range of target's signal was set at 0, 0.2, 0.3, 0.4, 0.5, 0.7, 1 coherence and the signal assigned on each trial was controlled by two interleaved staircases. Apart from the proportion of disparity signal, the orientation of the target was another variable to define stimuli in the signal-in-noise disparity task: the glass pattern dipoles (target's dot pairs) were either horizontally or vertically oriented. However, the proportion of signal dipoles (dipoles with the same -horizontal or vertical- orientation) against noise dipoles (which had a randomly chosen orientation 0-180 degrees) varied within a range of 0, 0.1, 0.2, 0.25, 0.3, 0.4, 0.7 signal. On each trial, a randomly chosen proportion of signal dipoles was assigned. The participants' task was to indicate, by keyboard pressing, whether the target was nearer or farther than the surround [two-alternative forced-choice (2AFC) design].

2. Signal-in-noise orientation, defined by glass pattern dipoles: Here, the proportion of signal dipoles (dipoles with the same -horizontal or vertical- orientation against noise dipoles) that assigned on each trial was controlled by two interleaved staircases, while the proportion of disparity signal on each trial was randomly chosen from the disparity signal range (0, 0.2, 0.3, 0.4, 0.5, 0.7, 1 coherent signal). Participants were asked to indicate whether the target was vertically or horizontally oriented.

3. Depth defined by fine disparity in the absence of noise: The surround surface had a fixed ± 12 arcmin disparity, but the disparity of the target differed with respect to the surround in fine steps. The range of target's disparity was set at 0.0167, 0.1, 0.3, 0.4, 0.5, 1, 4 arcmin and the value assigned on each trial was controlled by two interleaved staircases. Apart from this difference in disparity, the orientation profile of the target was another variable to define stimuli in the present feature difference task: the direction difference (clockwise or anti-clockwise) between the target and the surround varied within a range of 0, 6, 12, 18, 24, 30, 40 degree difference. On each trial, a randomly chosen

direction difference was assigned. Participants were required to indicate whether the target was nearer or farther than the surround.

4. ‘Fine’ orientation in the absence of noise, defined by glass pattern dipoles: Here, the direction difference (clockwise or anti-clockwise) between the target and the surround assigned on each trial was controlled by two interleaved staircases, while the target’s disparity difference on each trial was randomly chosen from the disparity difference range (0.0167, 0.1, 0.3, 0.4, 0.5, 1, 4 arcmin). The participants’ task was to indicate whether the target was clockwise or anti-clockwise oriented relative to the orientation of the surround.

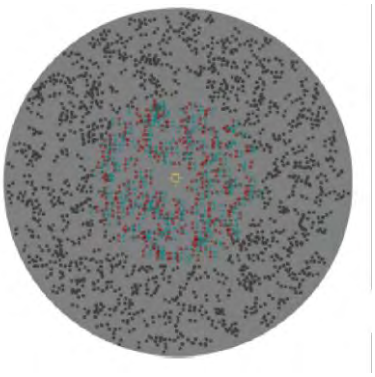

Figure 5.1: Red-cyan anaglyphic stereogram to illustrate a sample signal-in-noise stimulus.

Table 5.1: Summary of the experimental design.

Experiment	Task	Disparity Profile	Orientation Profile	2AFC Task
Depth (Disparity)	Signal-in-noise discrimination	Proportion of disparity signal controlled by 2 interleaved staircases.	On each trial, a proportion of GP signal randomly assigned.	The target is nearer or farther than the surround?
	Feature difference discrimination	Disparity difference controlled by 2 interleaved staircases.	On each trial, a direction difference randomly assigned.	
Orientation (Glass pattern)	Signal-in-noise discrimination	On each trial, a proportion of disparity signal randomly assigned.	Proportion of GP signal controlled by 2 interleaved staircases.	The target is vertically or horizontally oriented?
	Feature difference discrimination	On each trial, a disparity difference randomly assigned.	Direction difference controlled by 2 interleaved staircases.	The target is clockwise or anti-clockwise oriented relative the surround?

5.2.3 Procedure

a. Psychophysics general training session

Because all participants were not used to psychophysical experiments, before starting the main experimental phase, I sought to familiarise them with the rationale of a forced-choice psychophysical experiment. To this end, they completed two brief blocks of a simple 2IFC psychophysical task: they were required to judge whether the first or the second of two sequentially presented pairs of separated lines was more distant. Further participation on the main experiments was decided on the basis of participants' performance on this simple

psychophysical set up. All of the observers tested showed a reasonable and reliable performance on this preliminary/pilot session.

b. Main experiments

The main experiments consisted of three phases. During all phases and experiments, each experimental block consisted of 13 repetitions X 2 (depth: near/far) X 2 (orientation: horizontal/vertical) X 2 (staircases) = 104 trials. The first ('pre-training') phase carried over three separate days. On each day, rTMS over a separate brain area was applied: left posterior parietal cortex (P3), right posterior parietal cortex (P4) or CZ (as a control site) while participants were tested in two blocks (208 trials in total) without feedback. The second ('training') phase carried over three days, when participants were trained with feedback on a different task than the one completed in the first phase. Training did not involve any TMS, and feedback was provided for correct and wrong answers in 21 blocks of 104 trials (2184 trials in total). Finally, in the third ('post-training') phase, rTMS was applied over P3, P4 and CZ in three separate days, while participants attended the same task and experimental protocol (number of trials, lack of feedback etc) as in phase one.

5.2.4 TMS protocol

I applied three experimental rTMS conditions, each in a separate session: rTMS over the left posterior parietal cortex (P3), the right posterior parietal cortex (P4) and area CZ. The three sessions involving TMS took place in a random order, each on a separate day of the pre-training and the post-training phases of the study.

In light of recent evidence that training can dramatically alter the contribution of cortical areas to fine and signal-in-noise stereopsis tasks (Chowdhury & DeAngelis, 2008; Raiguel, et al., 2006; T. Yang & Maunsell, 2004), I was interested in the bilateral stimulation of the posterior parietal cortex to examine its functional necessity in discrimination tasks

involving the extraction of signal in noise, before and after extensive behavioral training. Area CZ was stimulated as a control for the possibility of nonspecific effects associated with rTMS experiments, such as the sound generated by the TMS pulse administration and the tactile-muscle stimulation artifacts. On each trial, 5 successive pulses at 10 Hz (i.e. each pulse lasting for 100 ms) administered simultaneously with the visual stimulus onset. Both the PPC and CZ were identified and guided through the 10-20 EEG coordinate system (see *General Methods*). None of the participants reported the perception of phosphenes. After response, there was a 2500 ms interval before the next trial. Each 208-trial TMS session was accomplished in two blocks (104 trials each) in the intermission of which, I replaced the TMS coil.

5.2.5 Experimental groups & participants

I used the above protocol to assess the neural circuits supporting visual discrimination before and after visual learning. Participants were divided in separate groups and each group was tested in a single combination of task type and visual feature.

Thresholds were calculated using staircase methodology to obtain the 82% threshold (Leek, 2001). Each session's threshold was the average of the 4 staircases (2 staircases in each of the 2 blocks). The criteria I set in order to establish the valid blocks (and participants) for statistical analysis were a) the two staircase algorithms to converge to produce reasonable thresholds (I visually inspected the raw staircase plots of every single block of each participant to address whether this criterion is met) and b) the calculated threshold not to exceed the 85% of stimulus intensity. If any of the above criteria was not met, I excluded the corresponding staircase so that it would not contribute to the averaged threshold for the corresponding session. For representative examples of excluded and valid blocks/participants, see **figures 5.3, 5.6** and **5.9**. Participants were students or post-docs at

the University of Cambridge participating for money compensation. The experimental combinations of the study were the following:

1. Experiment 1: signal-in-noise orientation – feature difference depth - signal-in-noise orientation: before and after training on the feature difference / fine disparity task, rTMS was applied in three separate days while participants (N=9; 6 female, 3 male) completed the signal-in-noise orientation task. The aim of this protocol was to examine whether training can generalise not only between task/discrimination types (from feature difference to signal-in-noise) but across tasks defined by different visual features (orientation) as well. Critically, I was interested in examining whether the contribution of dorsal areas to executing the signal-in-noise orientation task at the post-training phase decreases as a result of training on fine disparity in the absence of noise. The data from one participant were excluded from statistical analysis because of very poor performance across almost all the blocks and sessions: the two staircase algorithms either failed to converge to produce reasonable thresholds, or the calculated thresholds exceeded the 85% of stimulus intensity. (For representative examples of this participant's raw staircase performance, see **figure 5.3**).

2. Experiment 2: signal-in-noise depth - feature difference orientation - signal-in-noise depth: participants (N = 7; 6 female, 1 male) detected the depth signal embedded in noise while rTMS was applied during the pre- and post-training phases. In between, they were trained with feedback on the feature difference orientation task. Similarly to experiment 1, I was interested in examining whether the parietal cortex eliminates its involvement in the estimation of depth embedded in noise as a result of training on orientation estimation in the absence of noise. The data from one participant were excluded from statistical analysis because they showed no improvement across the testing runs of the training phase and also the thresholds during the TMS phases were unreasonably high (exceeding the 85% of stimulus intensity, see **figure 5.6**).

3. Experiment 3: signal-in-noise depth - signal-in-noise orientation - signal-in-noise depth: this experiment used 8 participants (7 female, 1 male) and aimed to explore whether training on a signal-in-noise task, apart from generalising its benefits across visual features psychophysically (Chang et al., 2013; experiment 2), is also accompanied by a switch in the cortical circuits that support the execution of the post-training task. The data from two participants were excluded from statistical analysis because of very poor performance across almost all sessions and blocks: the two staircase algorithms either failed to converge to produce reasonable thresholds, or the calculated thresholds exceeded the 85% of stimulus intensity (**figure 5.9**).

5.3 Results

5.3.1 Experiment 1: signal-in-noise orientation - feature difference depth - signal-in-noise orientation

To quantify performance, I measured thresholds determined at 82%-correct level (see above). Before training, the signal-in-noise orientation raw discrimination thresholds were increased under stimulation of the left posterior parietal cortex (P3) and the right PPC (P4) compared to CZ. Interestingly, after training on the fine disparity task, this difference was eliminated and performance among the three stimulation areas became almost equal (**figure 5.2a**). A 2-way ANOVA on the difference between each PPC area and CZ (ΔCZ), with area-hemisphere (P3/P4) and learning (before/after training) as factors, showed a non-significant main effect of the hemisphere of stimulation [$F(1,7) < 1$, $p = .740$, partial $\eta^2 = .017$, power ($1-\beta$) = 0.05] and a non-significant main effect of learning [$F(1,7) = 2.025$, $p = .198$, partial $\eta^2 = .224$, power ($1-\beta$) = 0.23]. Nevertheless, simple effects revealed that thresholds under P3 stimulation were significantly elevated relative to CZ [$t(7) = 2.7$, $p = .031$] before training, but not after training [$t(7) = -.107$, $p = .92$]. These results suggest that the disruptive effects of rTMS over P3 in signal-in-noise orientation estimation before training

were eliminated as a result of training on the estimation of fine disparity in the absence of noise.

In order to remove the variability in overall thresholds between participants, I normalized (per participant) the data by dividing the threshold for each stimulation site by the mean performance of each individual across all three stimulation sites (**figure 5.2b**). However, the increment of P3 and P4 thresholds compared to CZ before training and their equalisation after training failed, again, to reach statistical significance [$F(1,7) < 1$, $p = .567$, partial $\eta^2 = .049$, power $(1-\beta) = 0.05$].

Finally, **figure 5.4** shows the performance on the discrimination of depth feature difference task during behavioural training for two representative participants. A clear decrease in the discrimination thresholds is depicted across the different trial runs and days. A similar learning effect was profound for all the participants, providing reassurance that the training phase of the study was effective.

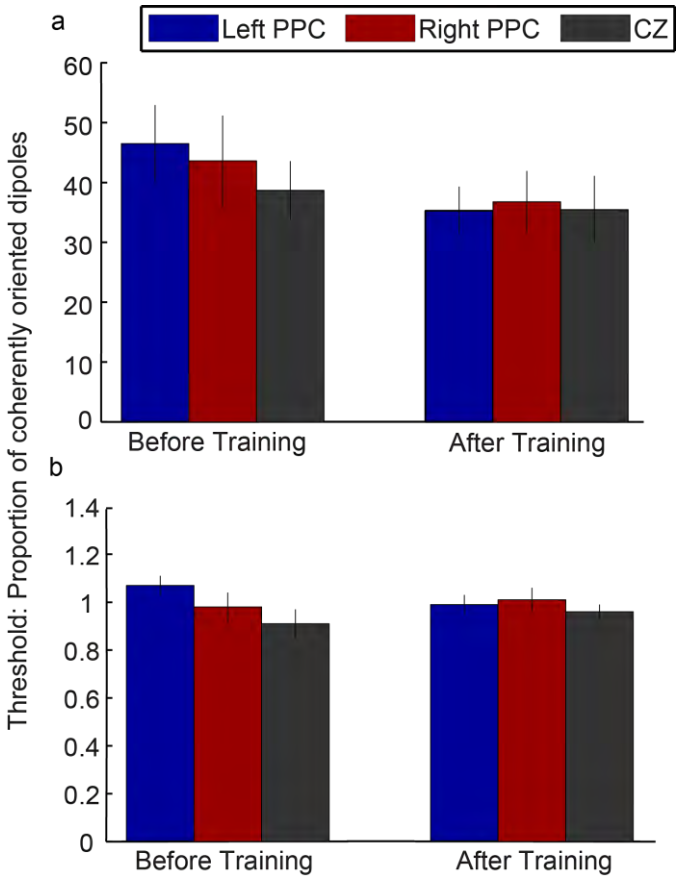

Figure 5.2: Experiment 1: **(a)** Raw threshold data as obtained in the signal-in-noise orientation task before and after training on the feature difference depth (fine disparity) task. **(b)** Normalised thresholds by dividing performance on each condition by the average threshold across all three stimulation sites for each participant. Error bars indicate standard error of the mean.

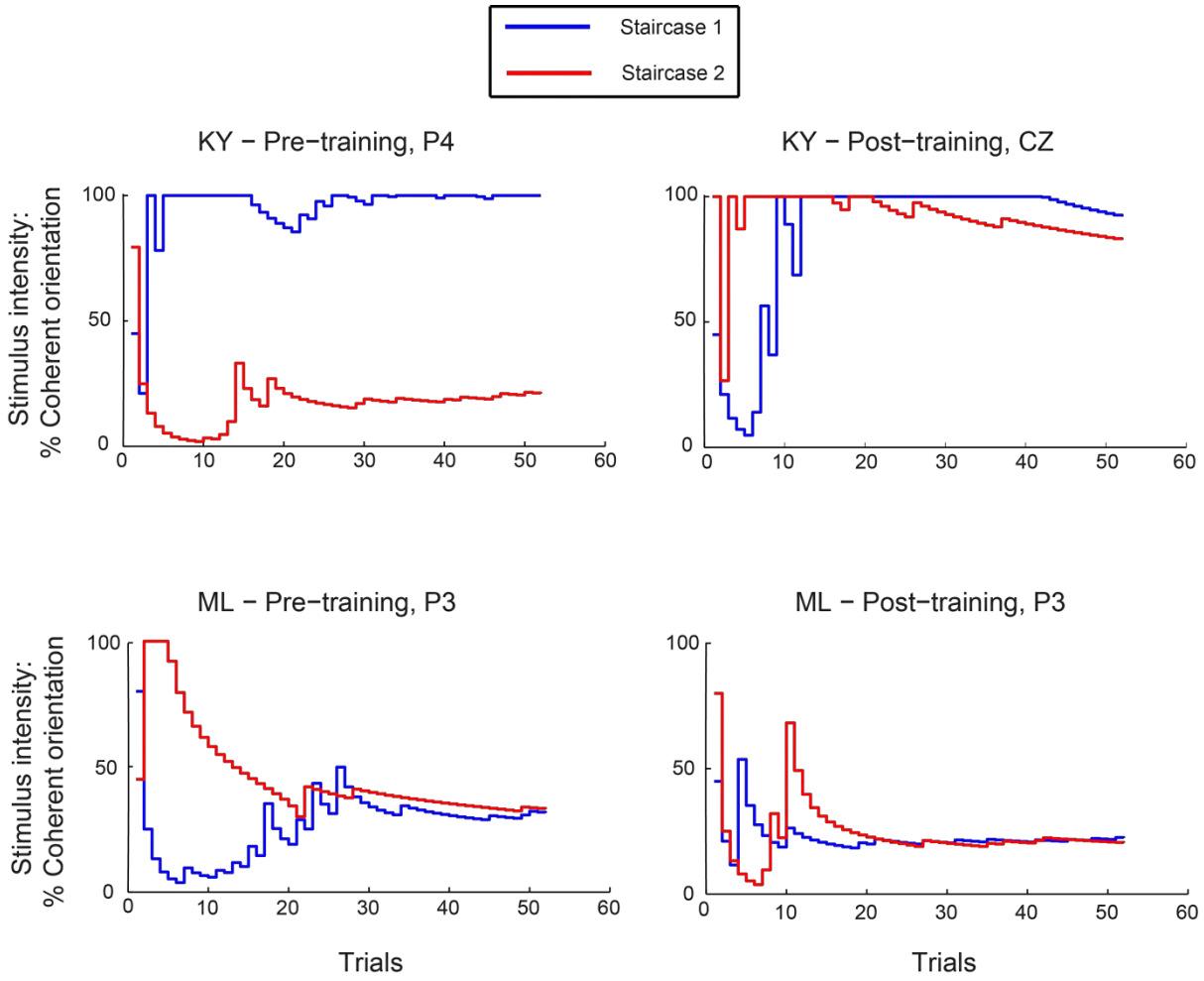

Figure 5.3: Indicative examples of performance on the signal-in-noise orientation task of experiment 1 for two participants. The two interleaved staircases (consisted of 52 trials each) in each block are plotted separately. **Top panel:** Performance of participant KY (the one who was excluded from statistical analysis) under P4 stimulation before training and CZ stimulation after training. As the graphs show, thresholds were either too high (around 100% of stimulus intensity), or not properly converged to produce a reasonable detection threshold. **Bottom panel:** Performance of participant ML under P3 stimulation before training and P3 stimulation after training. Here, performance improved as a function of trials, as expected. Also, the two staircases were properly converged to produce reasonable thresholds.

a. (SM)

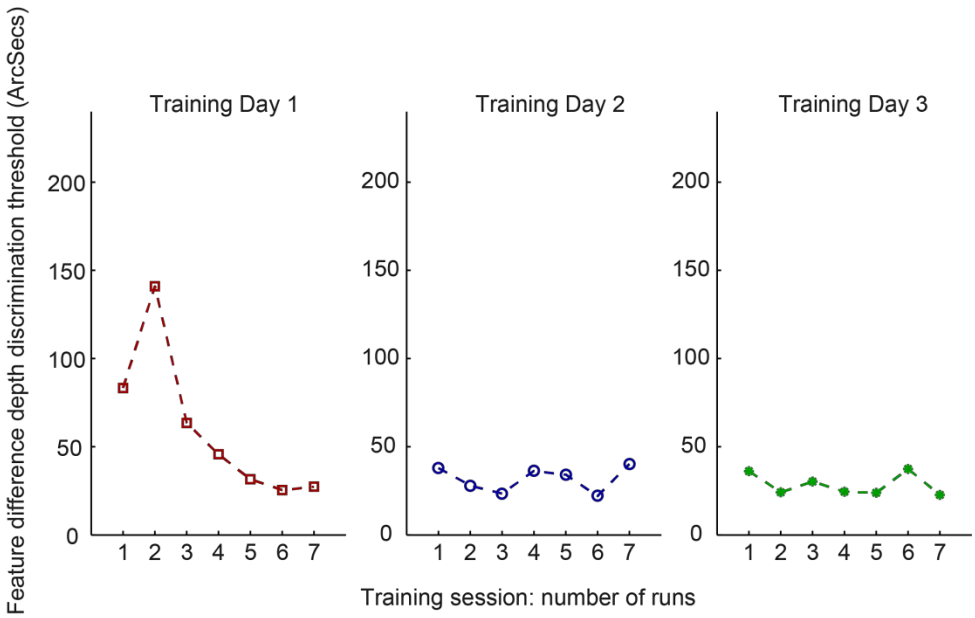

b. (JG)

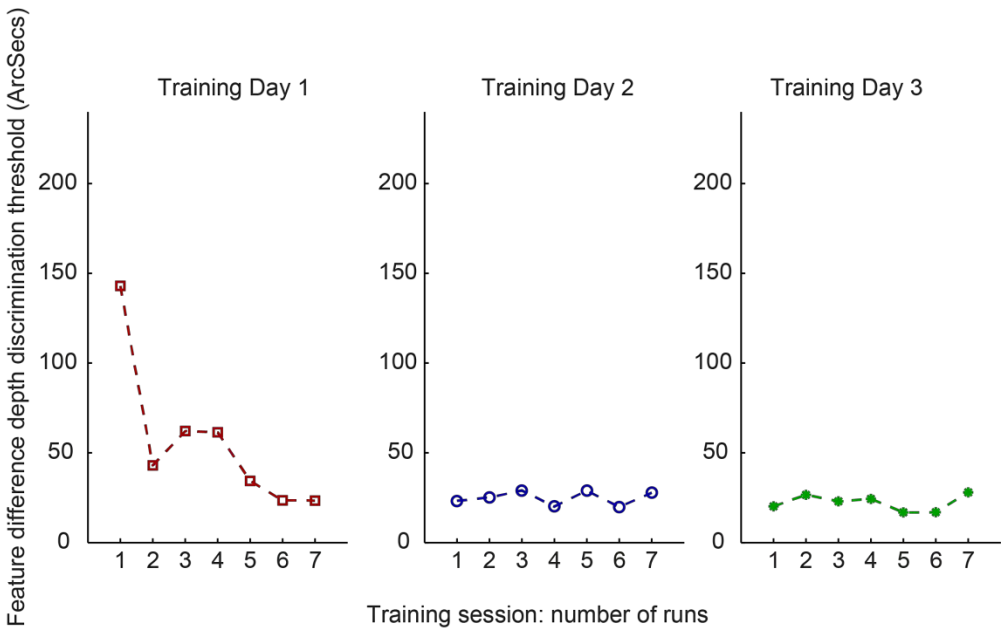

Figure 5.4: Thresholds as obtained for participants SM and JG across the runs and days of training on the feature difference/fine disparity discrimination for experiment 1. There is a clear improvement in performance as a function of the behavioural run and this was the case for all the participants.

5.3.2 Experiment 2: Signal-in-noise depth - feature difference orientation - signal-in-noise depth

Before training, raw depth discrimination thresholds increased under stimulation of the left posterior parietal cortex (P3) and the right PPC (P4) compared to CZ. Interestingly, this difference was eliminated after training on feature difference / 'fine' orientation (**figure 5.5a**). However, a 2-way ANOVA on ΔCZ revealed that this pattern was not specific in the hemisphere of stimulation (neither P3, nor P4 were significantly different than CZ [$F(1,5) < 1$, $p = .524$, partial $\eta^2 = .086$, power $(1-\beta) = 0.07$]. Also, there was a non-significant main effect of learning [$F(1,5) = 1.89$, $p = .227$, partial $\eta^2 = .275$, power $(1-\beta) = 0.25$] (but see paragraph 5.3.4 for a mixed design analysis).

I clustered PPC data (areas P3 and P4 pooled together) and compared them with the clustered CZ (before- and after-training CZ pooled together). This comparison showed that the increment of the concatenated PPC thresholds before training was significant (p =.001) indicating a disrupted performance in signal-in-noise depth estimation before training. Interestingly, there was a non-significant difference between PPC and CZ thresholds after training, suggesting that the disruptive effects of rTMS over PPC in signal-in-noise depth estimation were eliminated as a result of training on feature difference orientation estimation.

However, since there was no main effect in the individual raw data, I normalized the data per participant (as in experiment 1), to remove the variability in overall thresholds (**figure 5.5b**). ΔCZ failed again to reach statistical significance for the hemisphere [$F(1,5) < 1$, $p = .841$, partial $\eta^2 = .009$, power $(1-\beta) = 0.05$] and the learning [$F(1,5) = 1.59$, $p = .264$, partial $\eta^2 = .241$, power $(1-\beta) = 0.20$] factors.

Data in **figure 5.7** show threshold decrement as the behavioural training was progressing for two representative participants. Most of the participants showed similar learning effects (except for participant CM who showed no improvement across the testing

runs of the training and was excluded from the analysis) providing reassurance that the training phase of the study was effective.

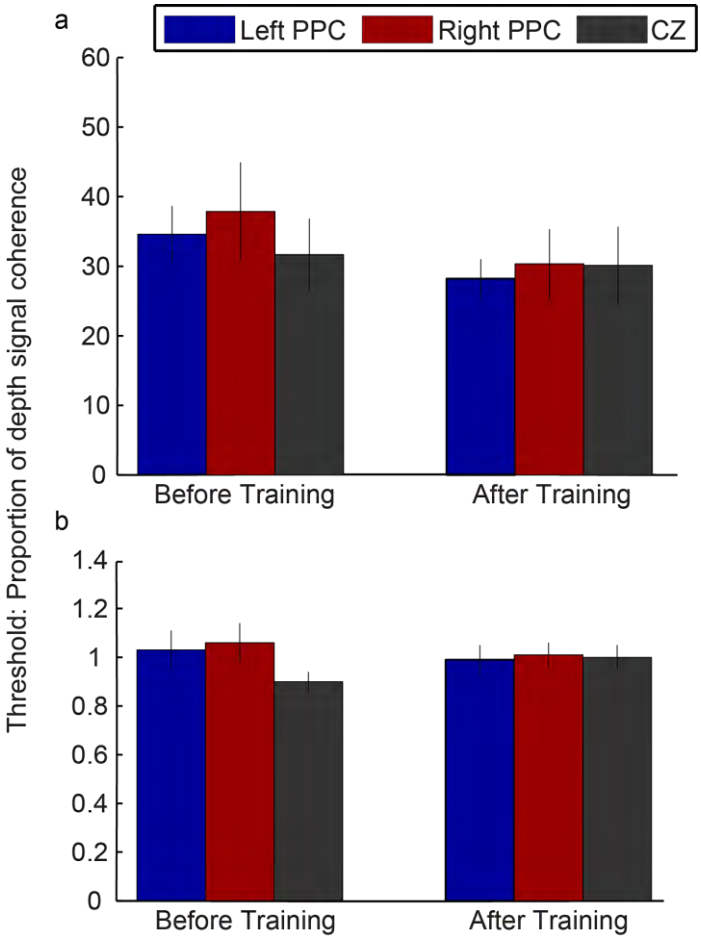

Figure 5.5: Experiment 2: **(a)** Raw threshold data as obtained in the signal-in-noise depth task before and after training on the feature difference orientation task. **(b)** Normalised thresholds by dividing performance on each condition by the average threshold across all three stimulation sites for each participant. Error bars indicate standard error of the mean.

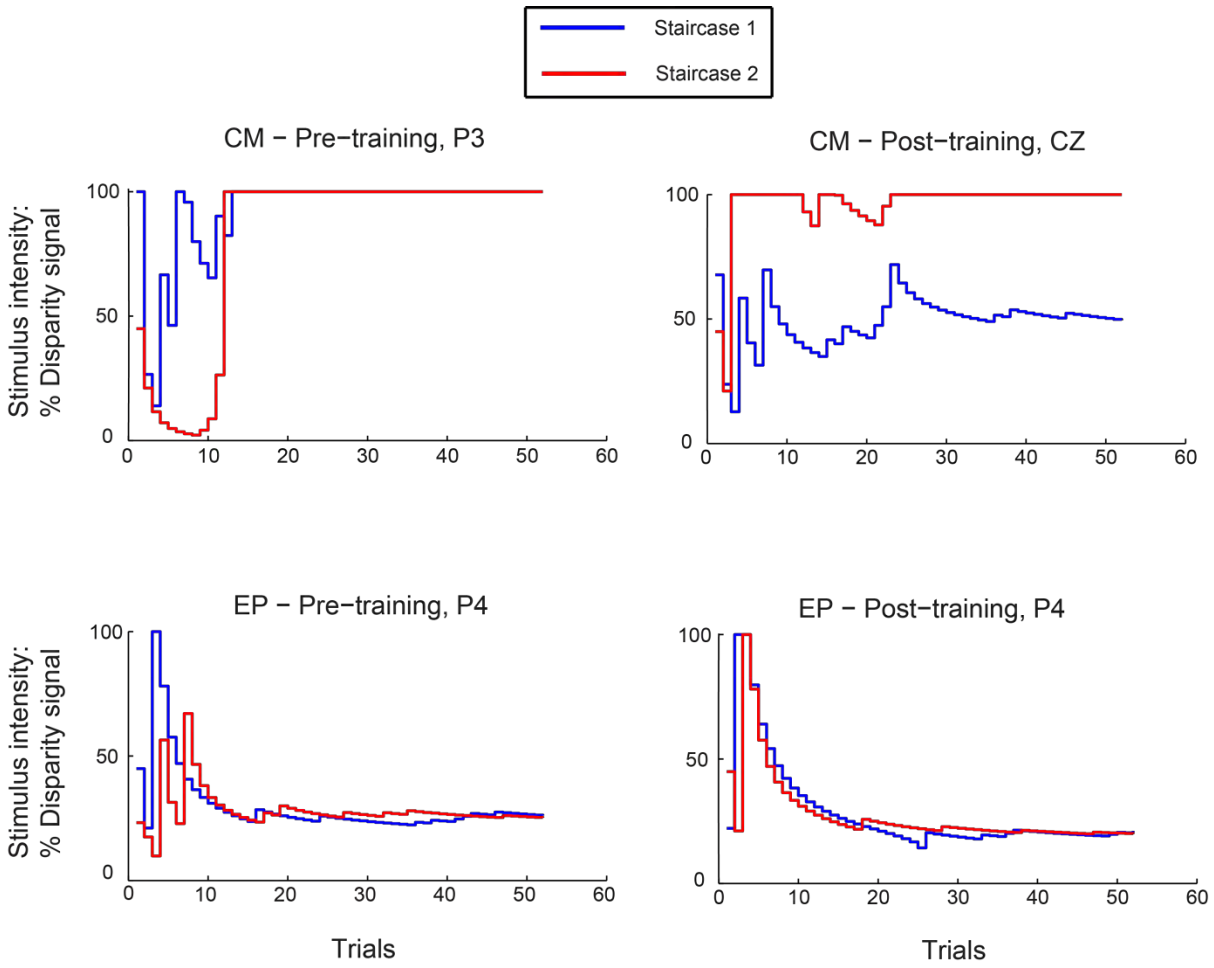

Figure 5.6: Indicative examples of performance on the signal-in-noise depth task of experiment 2 for two participants. The two interleaved staircases (consisted of 52 trials each) in each block are plotted separately. **Top panel:** Performance of participant CM (the one who was excluded from statistical analysis) under P3 stimulation before training and CZ stimulation after training. As the graphs show, thresholds were either too high (even at 100% of stimulus intensity), or not properly converged to produce a reasonable threshold. **Bottom panel:** Performance of participant EP under P4 stimulation before training and P4 stimulation after training. Here, performance improved as a function of trials, as expected. Also, the two staircases were properly converged to produce reasonable thresholds.

a. (CH)

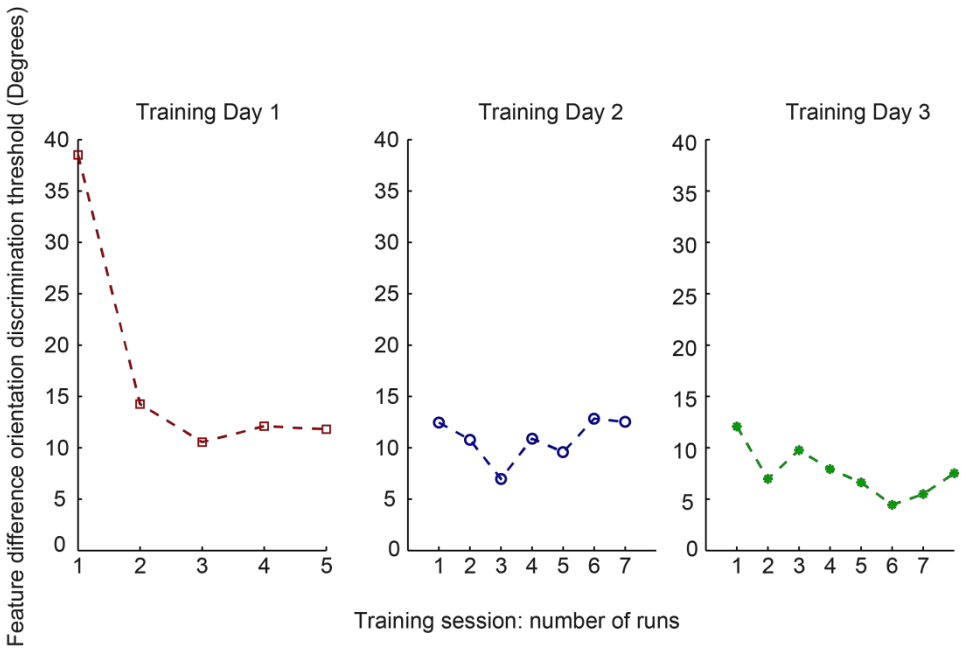

b. (MR)

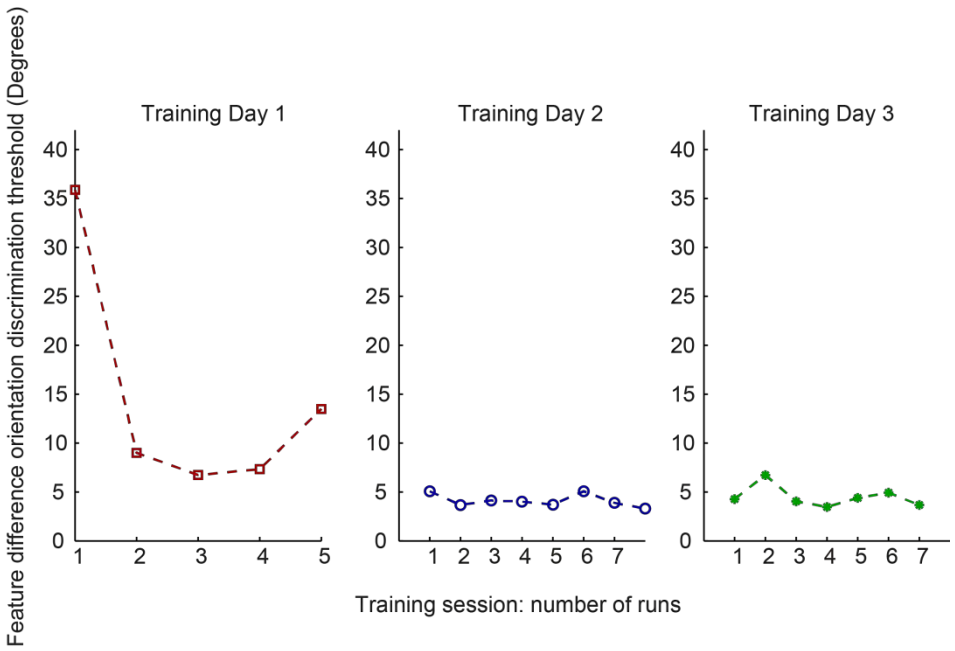

Figure 5.7: Threshold data as obtained for participants CH and MR across the runs and days of training on the feature difference orientation task for experiment 2. There is a clear improvement in performance as a function of training and this was the case for all the participants included in the analysis.

5.3.3 Experiment 3: signal-in-noise depth - signal-in-noise orientation - signal-in-noise depth

In the present experiment, I sought to examine whether training benefits can transfer across visual features (orientation to depth) but within the same (signal-in-noise) discrimination task. Results showed that before training, raw discrimination thresholds increased under stimulation of the left posterior parietal cortex (P3) and the right PPC (P4) compared to CZ. Importantly, though, this difference diminished after training (**figure 5.8a**). This observation was supported by a 2-way ANOVA which revealed a significant main effect of learning (before vs after training, [$F(1,5) = 11.396$, $p = .020$, partial $\eta^2 = .695$, power ($1-\beta$) = 0.90]. The effect, however, was not specific to any hemisphere, as the lack of a main effect of the hemisphere [$F(1,5) < 1$, $p = .635$, partial $\eta^2 = .049$, power ($1-\beta$) = 0.05] suggests. However, simple main effects showed that the difference between P3 and CZ was significant before training [$t(5) = 3.4$, p = .019], while none of the comparisons were significant after training. Finally, a main effect of learning [$F(1,5) = 13.061$, $p = .015$, partial $\eta^2 = .723$, power ($1-\beta$) = 0.92] was also found after normalising the data (**figure 5.8b**).

The above results suggest that the disruptive effects of rTMS over PPC in the signal-in-noise depth estimation task before training were eliminated as a result of training on the signal-in-noise orientation task. **Figure 5.10** depicts the performance on the signal-in-noise orientation task during behavioural training for two representative participants. All the participants included in the analysis showed similar reasonable learning effects.

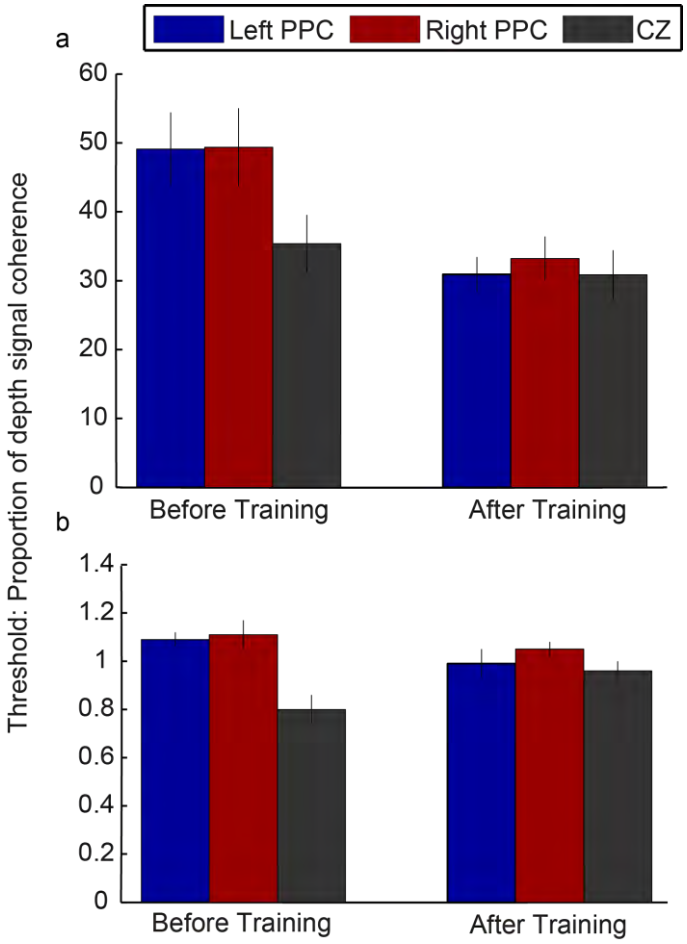

Figure 5.8: Experiment 3: **(a)** Raw threshold data as obtained in the signal-in-noise depth task before and after training on the signal-in-noise orientation task. **(b)** Normalised thresholds by dividing performance on each condition by the average threshold across all three stimulation sites for each participant. Error bars indicate standard error of the mean.

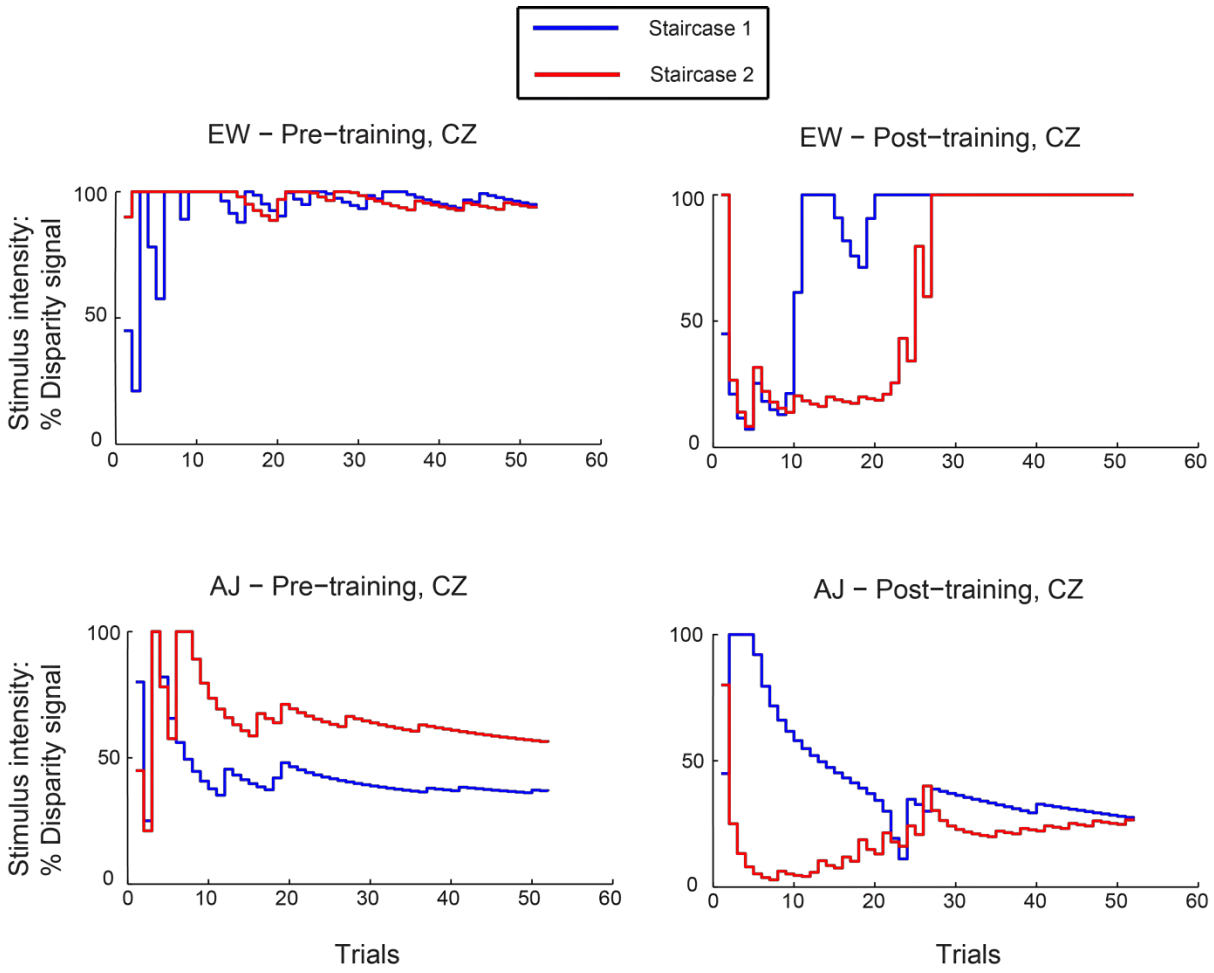

Figure 5.9: Indicative examples of performance on the signal-in-noise depth task of experiment 3 for two participants. The two interleaved staircases (consisted of 52 trials each) in each block are plotted separately. **Top panel:** Performance of participant EW (who was excluded from statistical analysis) under CZ stimulation before training and CZ stimulation after training. As the graphs show, thresholds were too high (at almost 100% of stimulus intensity) for most of EW's sessions and areas of stimulation. **Bottom panel:** Performance of participant AJ under CZ stimulation before training and CZ stimulation after training. Here, performance improved as a function of trials, as expected. Also, the two staircases were properly converged to produce reasonable thresholds.

a. (AJ)

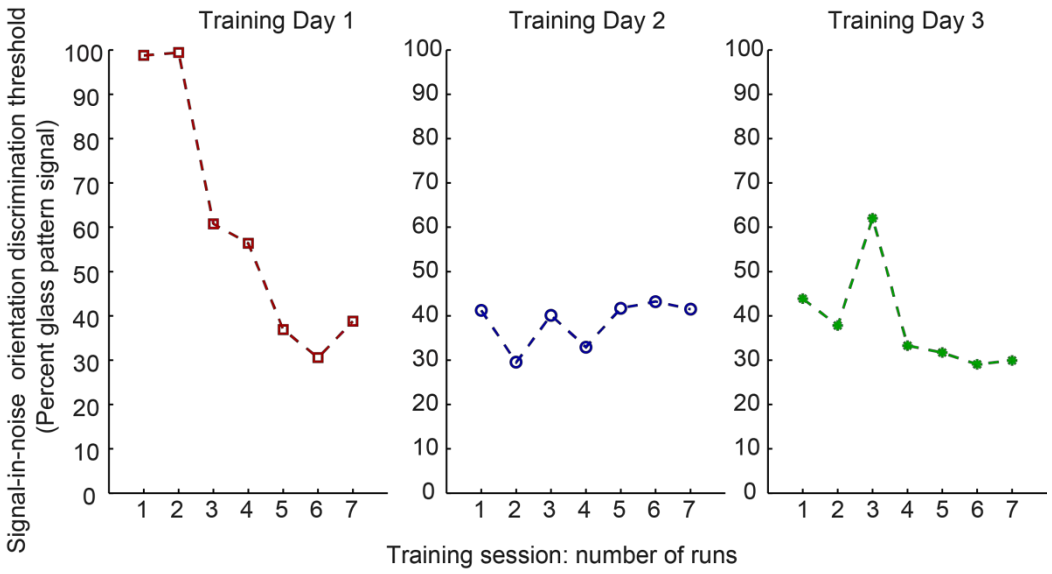

b. (BK)

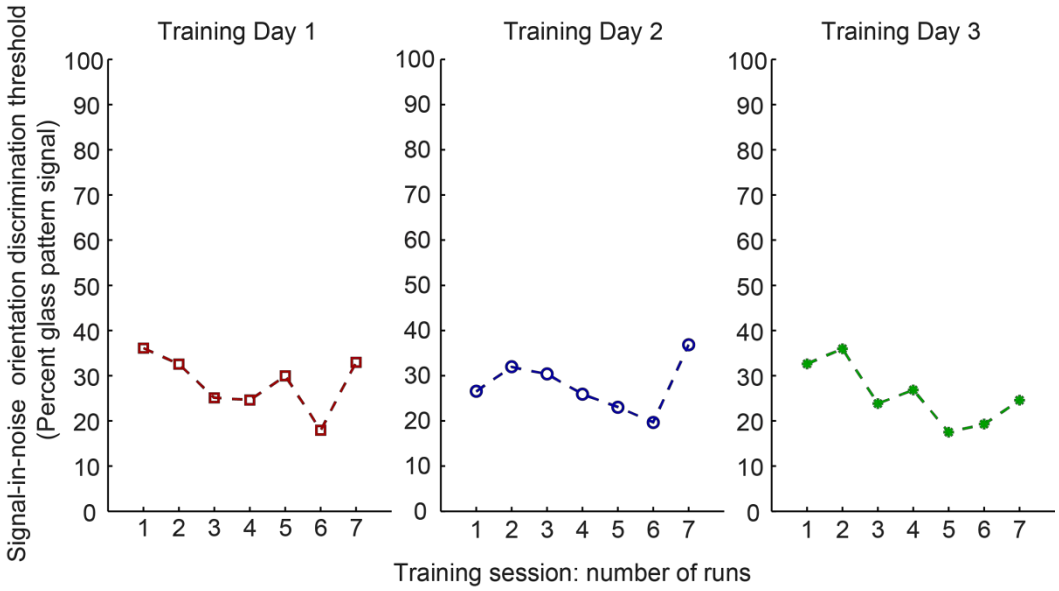

Figure 5.10: Threshold data as obtained for participants AJ and BK across the runs and days of training on the signal-in-noise orientation task for experiment 3. There is an improvement in performance as a function of training and this was the case for most of the participants.

5.3.4 Experiments 2 and 3: mixed design analysis

The only difference between experiments 2 and 3 was the type of training participants received: in experiment 2, participants were trained on feature difference orientation, while in experiment 3, training was on signal-in-noise orientation. Other than that, in both experiments, participants were tested in the same signal-in-noise depth task. Therefore, I analysed the data from the two experiments further: I merged participants from the two experiments to increase statistical power and evaluate the main effect that training on each orientation task had. A mixed design ANOVA with the hemisphere (P3/P4) and learning (before/after) ΔCZ as within subject variables and the group in each experiment as between subject factor showed that there was a significant main effect of learning for both groups [$F(1,10) = 11.073$, $p = .008$, partial $\eta^2 = .525$, power $(1-\beta) = 0.99$]. There was a non-significant interaction effect between the variables, suggesting that this significant difference between before and after training did not differ between the hemispheres or the group. There was a non-significant effect of the hemisphere, suggesting that the main effect of learning was not specific to area P3 or P4. Finally, there was a non-significant main effect of the group [$F(1,10) = 3.008$, $p = .114$, partial $\eta^2 = .231$, power $(1-\beta) = 0.61$] indicating that no matter the type of training, estimation of disparity-defined depth embedded in noise was not different between the two groups.

5.4 Discussion

The data obtained from this study showed that disruptive rTMS over the posterior parietal cortex, compared to rTMS over the control area CZ, resulted in elevated thresholds for discriminating orientation and disparity signals embedded in noise. Interestingly, this PPC contribution to the discrimination of signal-in-noise was eliminated after 3 days of training, but proper statistical analysis did not always provide full support to this observation.

In particular, experiment 1 assessed the effect of feature difference (fine) disparity training on the parietal cortex's contribution to signal-in-noise orientation discrimination. Compared to control stimulation, stimulation over the PPC resulted in the elevation of thresholds for discriminating signal-in-noise orientation before training, but this PPC contribution vanished after training. However, this neural reorganisation was not supported statistically, since ANOVA failed to show a significant main effect of learning. Nevertheless, simple effect analysis showed that the observed difference between before and after training in discriminating thresholds was more specific to P3. Experiment 2, similarly, compared the involvement of the parietal cortex in the discrimination of disparity-defined depth embedded in noise, between before and after training on feature difference orientation. Visual inspection of the data suggests that, before training, the thresholds for discriminating signal-in-noise depth increased under PPC stimulation compared to control stimulation. Interestingly, this difference was eliminated after training, but statistical analysis confirmed neither a main effect of learning (before vs after), nor a main effect of hemisphere. Experiment 3 examined the effect of signal-in-noise orientation discrimination training on the parietal cortex's contribution to the discrimination of signal-in-noise depth. A 2-way ANOVA showed that, before training, thresholds for discriminating disparity-defined depth embedded in noise were significantly elevated under PPC stimulation compared to control stimulation. Intriguingly, however, this significant PPC contribution was eliminated after training on signal-in-noise orientation. Although the ANOVA failed to point to a

particular hemisphere for the specificity of this effect, simple main effects analysis showed that it was the left PPC, area P3, that showed the greatest difference compared to CZ.

Chang et al. (2014) found that, after training on the discrimination of fine disparity in the absence of noise, it was area LO -and not the PPC- that was disrupted by neural stimulation during signal-in-noise depth discrimination. With experiments 1 and 2 here, I sought to investigate whether a similar neural shift in the circuit that supports the transfer of training benefits exists, not only within depth, but across visual features. My data indicate that training on feature difference discrimination within either depth (experiment 1) or orientation (experiment 2) visual features did result in the weakening of dorsal contribution to the execution of a signal-in-noise task of the opposite visual feature. These findings, although not supported by analysis of variance, were supported by the less strict t-tests. A possible explanation for this might be that the data were underpowered due to the relatively small sample of participants. Since visual learning has been shown to facilitate recognition and optimize the tuning of neurons in ventral cortical areas in both the human (Li, et al., 2009) and the monkey (Adab & Vogels, 2011; Raiguel, et al., 2006; T. Yang & Maunsell, 2004), it is possible that the extensive three-day training of the participants shifted the contribution of the cortical areas from dorsal (normally important for signal-in-noise and coarse discriminations) to ventral cortex. It would thus be reasonable to assume that a similar cortical shift from dorsal to ventral areas is the case not only when both training and test tasks involve discriminations in depth (Chang et al., 2014), but also when the training benefits generalise across visual features. However, since I did not test participants' performance during any ventral area stimulation, and also given that my findings failed to reach proper statistical support (probably due to insufficient statistical power as the post-hoc power analyses revealed –see *Results*), I cannot elaborate further on this issue.

An inspection of the present data challenges the psychophysical evidence from the first experiment of Chang et al. (2013) which suggested that training on a feature difference task does not generalise to other visual features, but instead promotes its benefits to a feature difference or a signal-in-noise task of the same visual feature only. This does not seem to be the case at the neural level, as the findings from experiments 1 and 2 of the present study suggest: the parietal cortex modulates its contribution to a signal-in-noise discrimination task after training on a feature difference task of the opposite visual feature. However, since these findings are supported by t-tests only, the novel finding of the present study remains that of experiment 3: before training, PPC neural processing was causally related to the discrimination of depth embedded in noise. However, after training on signal-in-noise orientation, that causal relationship vanished. This finding somehow accords with Chang et al.'s (2013) second experiment which showed that training on a signal-in-noise task can promote its benefits to the signal-in-noise task of a different visual feature.

In all three experiments, thresholds decreased under PPC (as well as CZ) stimulations after training. This observation indicates that rTMS efficacy to disrupt performance declined as a result of training. Therefore, one might suggest that, during training, participants became familiar with the spatial characteristics of the stimuli (for instance the arrangements and spatial relationship of the pairs of dots), and not with the type of task *per se*. In other words, it could be the case that performance, and the accompanied cortical involvement, were affected by the low-level aspects of the stimuli, and not by the specific task or training session *per se*. Although this could be a reasonable speculation, on the other hand, the same stimuli and visual features were present in all the experiments and tasks of the present study. That is, orientation experiments were informed also by (randomly chosen) disparity and disparity experiments were informed also by (randomly chosen) orientation. This experimental manipulation provides reassurance that, since the same low-level characteristics of the stimuli were present in all different conditions, it is the condition (i.e., the type of task) that determined the results.

5.5 Appendix for chapter 5: eye movement data

The PPC has been reported to be involved in the control of vergence eye movements (e.g., Gnadt & Beyer, 1998; Q. Yang & Kapoula, 2004). In order to control for the possibility of TMS-induced disruptions of vergence, similarly to chapter 3, I have recorded eye movements online with the TMS experiments reported above. In this section, I present representative graphs depicting vergence eye movement data for a few participants. I obtained vergence movements by substracting the left eye's horizontal position from the right eye's horizontal position with regard to the centre of the screen. Hence, negative vergence values correspond to eye positioning for near stimuli (being closer than the fixation point at the centre of the screen - on the screen's plane). Vergence during posterior parietal cortex (P3 or P4) stimulation, and CZ (or no TMS) as controls, are plotted as a function of time. The graphs presented in the first section of the appendix refer to vergence data averaged across all trials within each session and, as shown on the graphs, refer to 100 ms before rTMS stimulation onset and last for some 150 ms following the last TMS pulse. The highlighted gray areas correspond to the stimulus presentation on screen (300 ms; dark gray) and the entire duration of rTMS stimulation (500 ms; dark and light gray).

As the graphs show, vergence eye movements followed similar fluctuation patterns between PPC stimulation sessions and the control sessions. Visual inspection of the graphs for the majority of the trials for all the participants showed no systemic differences in vergence across the experimental sessions. However, eye movements were more noisy overall than those reported in chapter 3. This is not surprising given the fact that the stimuli used here (in both the orientation and the depth signal-in-noise settings) contained a certain amount of noise. It is thus expected that viewers would explore the stimulus with more vivid eye movements in order to detect the coherent signal embedded in noise.

5.5.1 Data averaged across trials

5.5.1.1 Eye movements in signal-in-noise orientation discrimination (experiment 1)

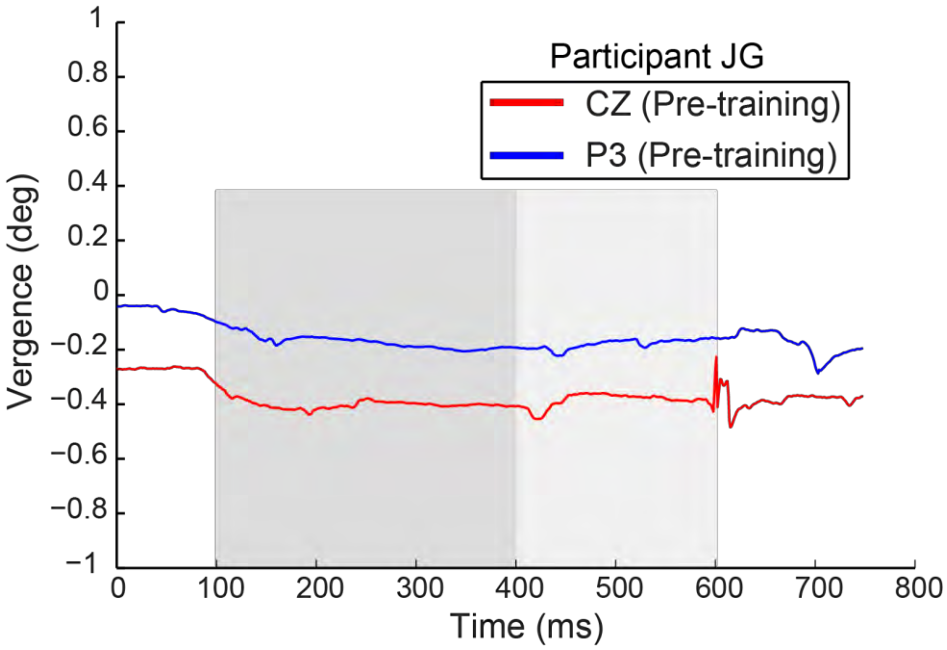

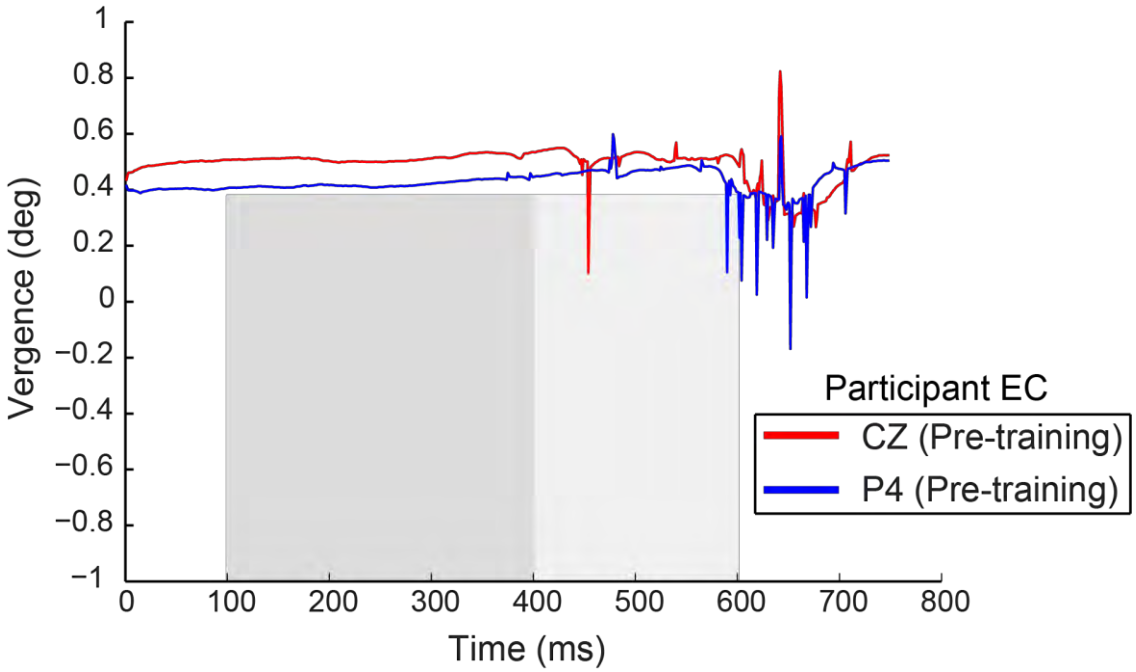

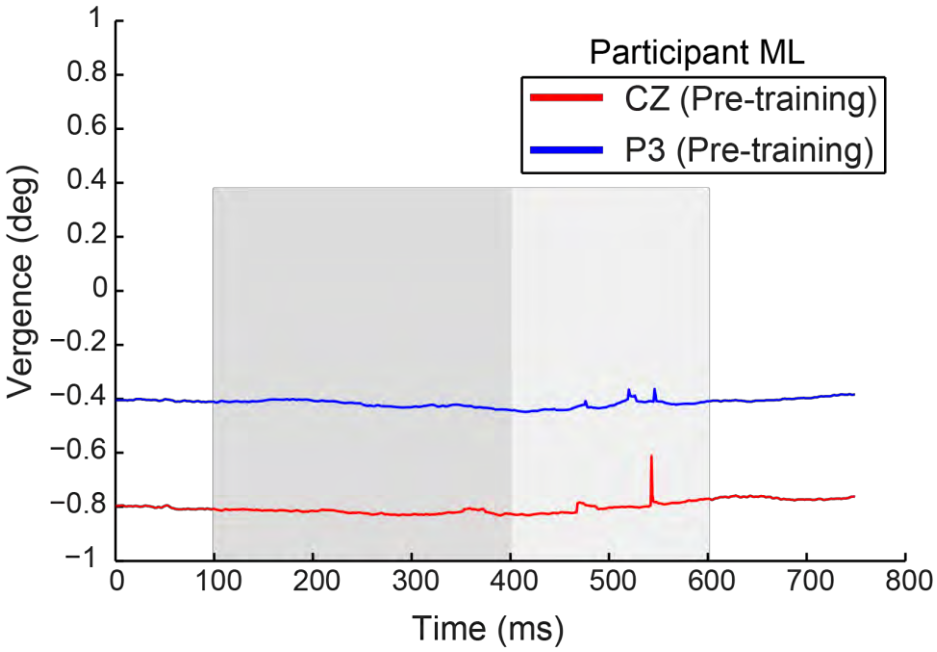

5.5.1.2 Eye movements in signal-in-noise depth discrimination (experiments 2-3)

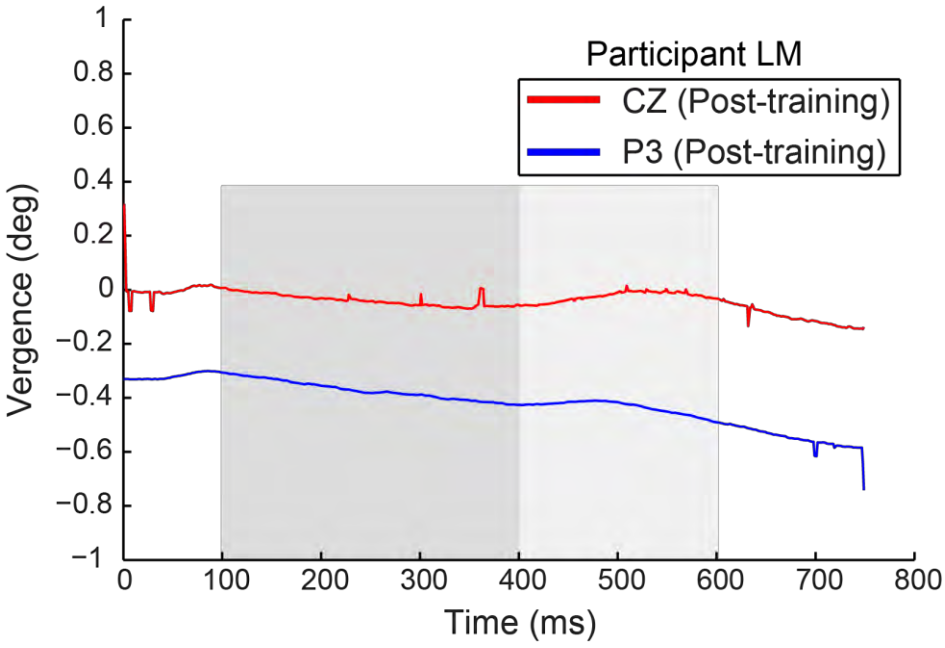

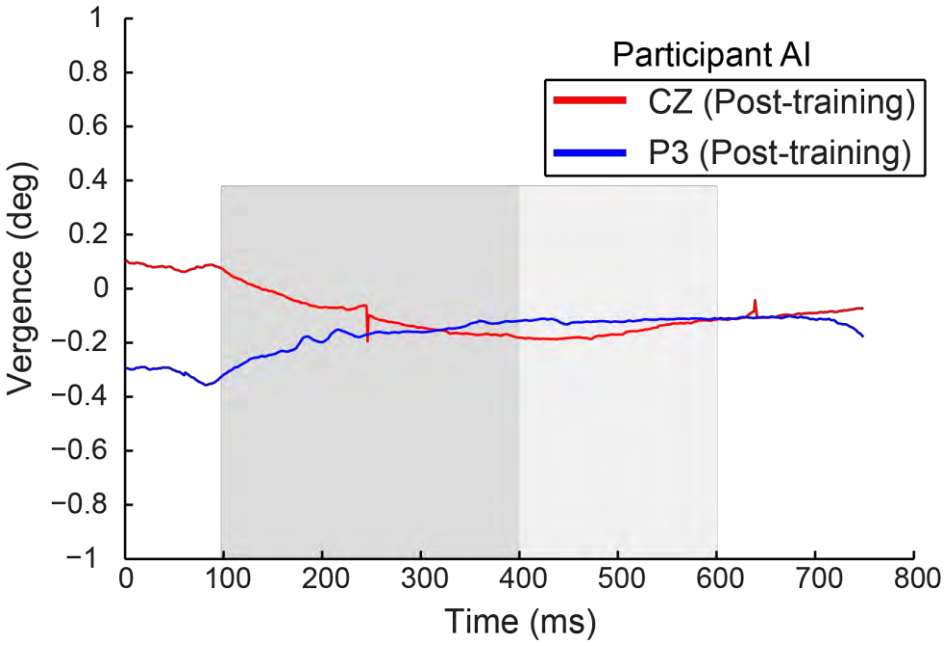
Participant AI
CZ (Post-training)
P3 (Post-training)
Vergence (deg)
Time (ms)
1
0.8
0.6
0.4
0.2
0
−0.2
−0.4
−0.6
−0.8
−1
0
100
200
300
400
500
600
700
800

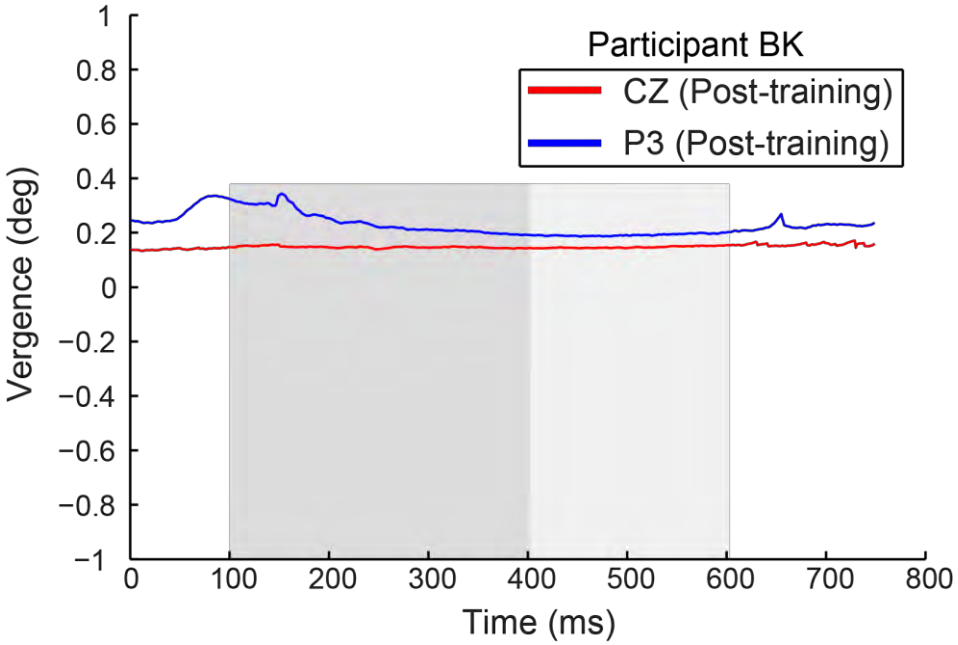
Participant BK
CZ (Post-training)
P3 (Post-training)
Vergence (deg)
Time (ms)
1
0.8
0.6
0.4
0.2
0
−0.2
−0.4
−0.6
−0.8
−1
0
100
200
300
400
500
600
700
800

5.5.2 Single trial raw data

Since the data presented above are averaged across tens of trials, it is reasonable to assume that the overall variability between trials has been defused due to averaging. However, the majority of the raw eye movement data derived from individual trials indicate that vergence followed similar flactuation patterns across different sessions anyway. Below, I present a few representative graphs from individual trials.

5.5.2.1 Eye movements in signal-in-noise orientation discrimination (experiment 1)

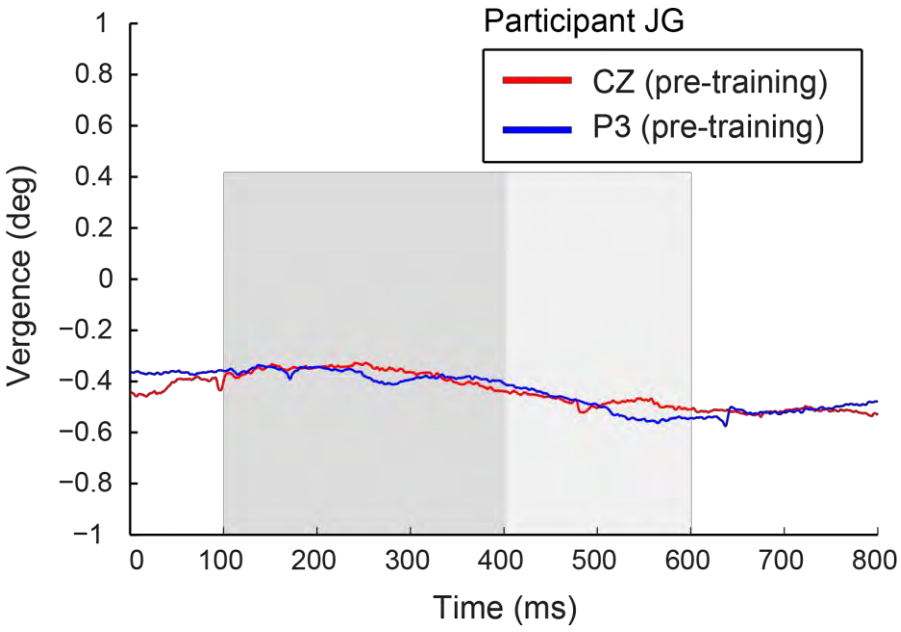

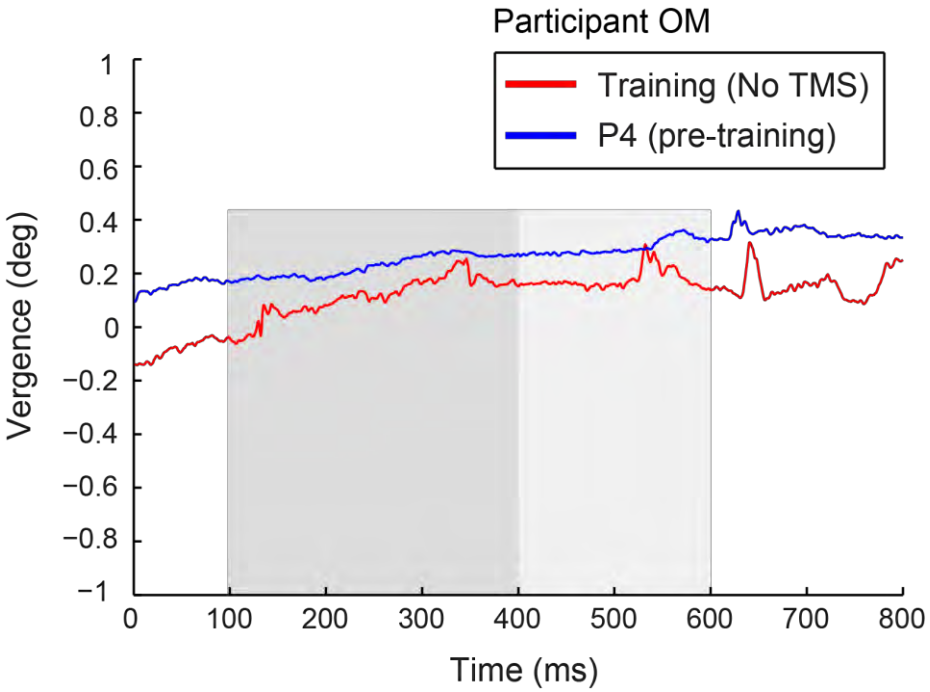

5.5.2.2 Eye movements in signal-in-noise depth discrimination (experiments 2-3)

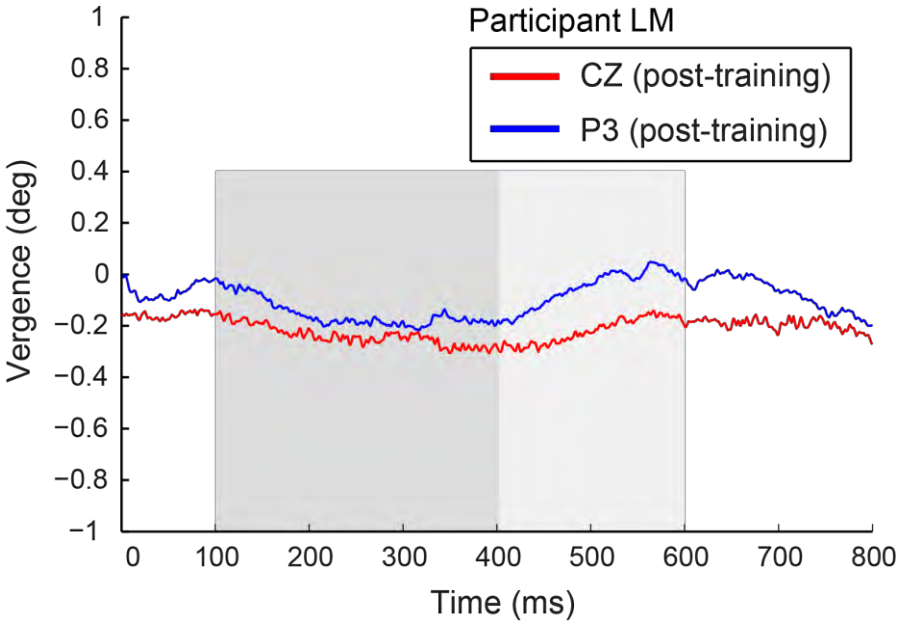

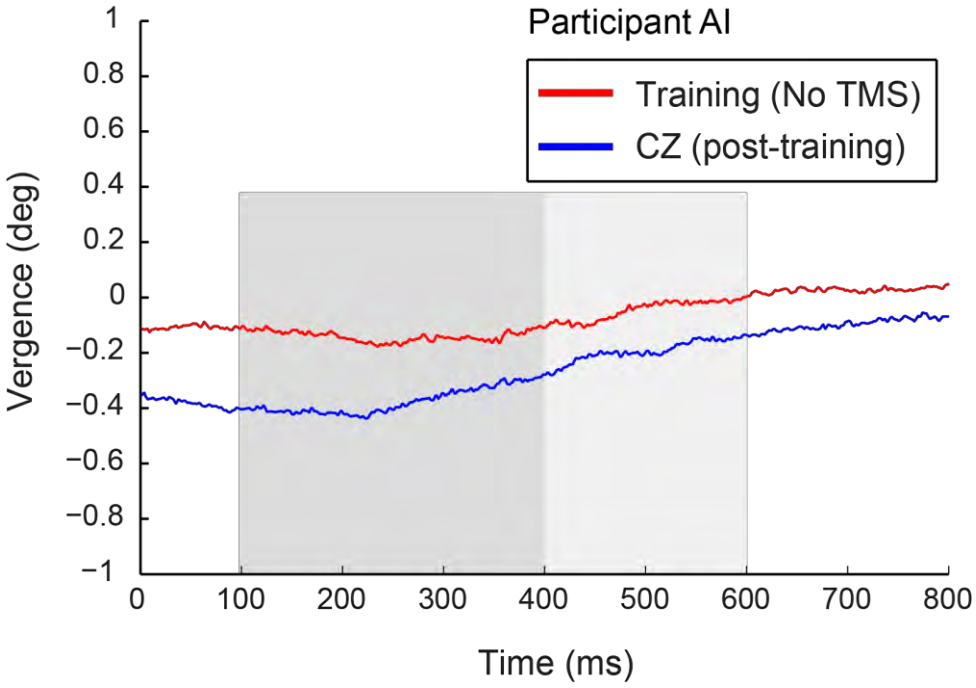
Participant AI
Training (No TMS)
CZ (post-training)
Vergence (deg)
Time (ms)
1
0.8
0.6
0.4
0.2
0
−0.2
−0.4
−0.6
−0.8
−1
0
100
200
300
400
500
600
700
800

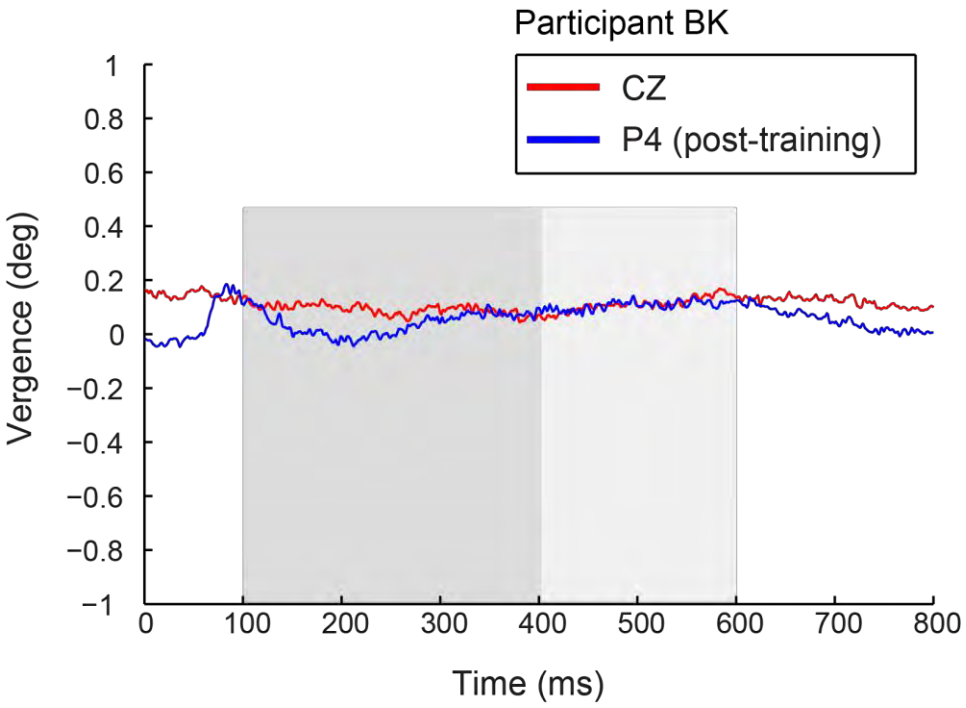
Participant BK
CZ
P4 (post-training)
Vergence (deg)
Time (ms)
1
0.8
0.6
0.4
0.2
0
−0.2
−0.4
−0.6
−0.8
−1
0
100
200
300
400
500
600
700
800

6. Brightness masking is modulated by disparity structure[3]

Abstract

The luminance contrast at the borders of a surface strongly influences surface's apparent brightness, as demonstrated by a number of classic visual illusions. Such phenomena are compatible with a propagation mechanism believed to spread contrast information from borders to the interior. This process is disrupted by masking, where the perceived brightness of a target is reduced by the brief presentation of a mask (Paradiso & Nakayama, 1991, Vision Research, 31, 1221-1236), but the exact visual stage this happens remains unclear. In the present study, I examined whether brightness masking occurs at a monocular-, or a binocular-level of the visual hierarchy. I used backward masking, whereby a briefly presented target stimulus is disrupted by a mask coming soon afterwards, to show that brightness masking is affected by binocular stages of the visual processing. I manipulated the 3D configurations (slant direction) of the target and mask and measured the differential disruption that masking causes on brightness estimation. I found that the masking effect was weaker when stimuli had a different slant. This finding suggests that brightness masking is partly mediated by mid-level neuronal mechanisms, at a stage where binocular disparity edge structure has been extracted.

[3] This chapter has been published in its current form as: Pelekanos, V., Ban, H., & Welchman, A. E. (2015). Brightness masking is modulated by disparity structure. *Vision Res, 110*(Pt A), 87-92.

6.1 Introduction

The perceived brightness of a surface differs substantially from its photometric luminance. A number of classic visual illusions demonstrate the important role that contrast edges play in the visual appearance of an enclosed surface (see *General Introduction*). For instance, when viewing the Craik-O'Brien-Cornsweet illusion, observers interpret isoluminant areas as having different brightness due to the luminance intensity ramps at their edges. The spatial influence of such contrast edge effects can be extensive (for example, Adelson, 2000; Komatsu, 2008).

Such phenomena can be understood in terms of the operation of spatial filtering processes that act at very early stages (pre-cortical) of visual processing (Blakeslee & McCourt, 1999; McArthur & Moulden, 1999; Otazu, Vanrell, & Alejandro Parraga, 2008; Watt & Morgan, 1985). Alternatively, higher-level explanations have been offered on the basis that the brain employs propagation mechanisms ("filling-in" –see *General Introduction*), whereby attributes encoded at one portion of the scene (e.g., contrast edges) influence the perceptual appearance of stimulus attributes that the visual system appears less ready to encode (e.g., regions of homogenous intensity) or unable to sense (e.g., due to the retinal blind spot) (Anstis, 2010; Komatsu, 2006; Pessoa, et al., 1998). Electrophysiological recordings from the visual cortex provide some support for the notion that neural activity spreads across the cortex during presentation of displays that involve filling-in effects (De Weerd, et al., 1995; Lamme, Rodriguez-Rodriguez, & Spekreijse, 1999). This lateral spreading of activity may provide part of explanation for the absence of 'missing' information in our perceptual interpretation of the world, and is compatible with psychophysical evidence for the lateral spread of contrast information across the cortical surface (Davey, Maddess, & Srinivasan, 1998).

One means of studying the mechanisms of brightness perception is to interfere with the putative filling-in mechanisms that may support it. Paradiso and Nakayama (1991)

developed such an approach using metacontrast masking, reasoning that if brightness estimation involves the spread of activity from the border of a surface towards its interior, then it should be possible to interrupt it. Specifically, they hypothesized that if contrast information is propagated from contrast edges, the subsequent presentation of new border signals should interfere with the filling-in process before it was completed. They found that the brightness at the center of a uniform target was considerably reduced when followed (50-100 ms) by a briefly presented circular mask (concentric with the target). Moreover, they observed a trade-off between the distance between the edges of the target and mask and the time at which the mask had a suppressive effect on brightness, which they suggested was compatible with a filling-in process where spreading of activity occurred at around 130 deg/s. They further observed that masking was greater under dichoptic presentation (target and mask presented to different eyes) than under monoptic presentation: in the former case, dramatic brightness suppression occurred even with simultaneous presentation of target and mask. This indicates that binocular processes are involved in the estimation of brightness, indicating contributions at the cortical level, although effects of rivalry or binocular summation could not be separated.

Information about three-dimensional scene structure has previously been suggested to be important for brightness estimation. For instance, computational models of early visual processing and brightness estimation (Grossberg & Mingolla, 1985; Grossberg & Todorovic, 1988) posit a role for disparity signals in constraining filling-in mechanisms for brightness (Kelly & Grossberg, 2000). Moreover, high-level theories of brightness (Adelson, 1993) and lightness (e.g., Anderson & Winawer, 2005; Gilchrist, 1977; Knill & Kersten, 1991) incorporate information about the three-dimensional scene structure that is available from the image.

Here I sought to test the contribution of disparity-defined three-dimensional scene information in guiding the impression of brightness by employing a modified version of the paradigm developed by Paradiso and Nakayama. In particular, I asked whether the

brightness reduction induced by a mask was affected by the depth configuration of the target and mask. I reasoned that if brightness estimation takes place at a low level of processing (i.e., before depth estimation has occurred) I would find no change in the effect of a briefly presented mask when the mask and target had the same or opposite disparity-defined slants. However, if brightness estimation involves binocular disparity edge information, I anticipated that masking would be greatest when the target and mask where spatially coincident. In the first experiment, I considered the effects of opposite slants for the target and mask. In experiment two, I then examined the sensitivity of the masking effect to gradations of slant differences between the target and mask.

6.2 Methods

6.2.1 Participants and apparatus

Eleven participants took part in Experiment 1 (mean age = 27.7, *SD* = 4.58; 3 female, 8 male) and nine in Experiment 2 (mean age = 27.4, *SD* = 4.67; 1 female, 8 male). All participants were naïve to the purpose of the study and were recruited from staff and students at the University of Birmingham and the University of Cambridge. All had normal or corrected to normal vision, and provided written informed consent. They were screened to ensure they could reliably discriminate depth positions defined by at least 1 arcmin of horizontal disparity. The protocols for the experiment were approved by the University of Birmingham's STEM ethics committee. The work was carried out in accordance with the Code of Ethics of the World Medical Association (Declaration of Helsinki).

Stimuli were viewed through a mirror stereoscope, where the two eyes viewed separate gamma corrected CRT (ViewSonic FB2100X) monitors from a distance of 50 cm. Screen resolution was 1600 x 1200 pixels at 100 Hz. Luminance calibration was achieved by linearizing grey-level values using a Minolta LS110 photometer. Presentation monitors

were recalibrated regularly to ensure that stimulus luminance was constant for different participants and across experiments.

6.2.2 Stimuli and procedure

The stimuli were circular target disks (diameter = 12 deg) and a mask which was an unfilled circle (diameter = 5.2 deg; line width = 0.4 deg) (**figure 6.1**). One of the targets (the reference; 'target 1' in **figure 6.1c**) was a uniform disk (luminance of 101.7 cd/m^2) while the other target (the test; 'target 2' in **figure 6.1c**) had a centre-surround configuration with a blurred interior boundary (see **figure 6.1b**). The diameter of the centre portion was 5.2 deg, and I applied blur to the boundary using a 2D Gaussian-kernel of FWHM = 0.2 deg. The luminance of the centre portion of the disk in the test target was controlled by an adaptive staircase and varied from 101.7 to 135 cd/m^2; the surround had a constant luminance of 101.7 cd/m^2.

Prior to taking part in the experiment, participants were dark adapted for 5 minutes, followed by two minutes of passive viewing on a mid-level gray patch of 67.8 cd/m^2 (this corresponded to the background luminance during stimulus presentation). Brightness judgments were measured using a two-interval forced-choice paradigm where the inter-stimulus interval (ISI) was 800ms. During the reference interval, a single disc with a uniform luminance of 101.7 cd/m^2 was presented for 60ms. During the test interval, a target disc (with variable luminance at its centre) was followed by the mask after a pre-defined time interval (stimulus onset asynchrony). The order of the reference and test stimulus presentation was randomised. I measured luminance increment thresholds, defined as the just noticeable difference. In particular, participants judged whether the first or the second target had a brighter centre. Thresholds were calculated using the QUEST staircase method (Watson & Pelli, 1983) to obtain the 82% threshold (see also Leek, 2001).

Luminance decreased after three successive correct responses, but increased after one incorrect response (i.e., '3-up and 1-down' staircase).

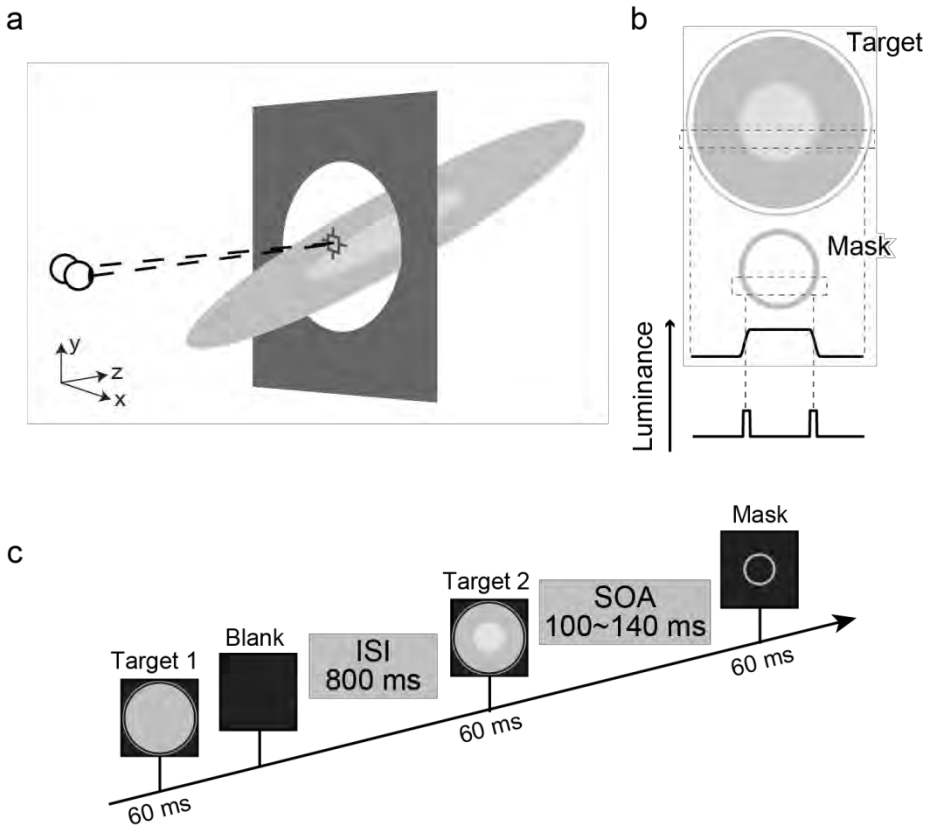

Figure 6.1: (a) A cartoon illustration of the target and its depth configuration. The target and masking stimuli were slanted in depth around a horizontal axis. **(b)** Illustration of the luminance profiles for the stimuli presented in the study. **(c)** The time sequence of stimulus presentation on a typical trial. Stimuli are depicted in the frontal plane for ease of representation; however for Experiment 1 both target and mask stimuli were slanted, and for Experiment 2 the masks were slanted in depth.

6.2.3 Masking properties

For the test interval presentations, a mask was presented after the target stimulus (metacontrast backward masking; see Breitmeyer & Ogmen, 2000; 2006). The mask was centred on the target, and had the same diameter (5.2 deg) as the centre portion of the target. The target and the mask remained on screen for 60 ms each, while the exact

interval (stimulus onset asynchrony) between them was tailored to individual participants (see *Stimulus Onset Asynchrony estimation* below).

6.2.4 Stimulus onset asynchrony (SOA) estimation

Prior to taking part in the main experiments, participants completed a session designed to estimate their stimulus onset asynchrony threshold. It is known that masking is a function of the SOA (Alpern, 1953), with little masking at either very short or long SOAs, but dramatic reductions in target's visibility in-between (see *General Methods*). Paradiso & Nakayama (1991) tested the influence of SOA on brightness masking finding maximal effects for an SOA of 50-100 ms. Other studies on backward masking find SOA time-windows for optimal target suppression vary in the range 30 and 150 ms (Breitmeyer & Ogmen, 2006, p. 38; M. F. Green et al., 2005; Polat, Sterkin, & Yehezkel, 2007), with differences between individual participants. I therefore chose to tailor the maximal masking effect by identifying optimal values for each participant.

The SOA-estimation session consisted of three blocks of 50 trials. Stimuli were orientated in the fronto-parallel plane. The participants' task was to indicate which interval had the brighter centre, and I estimated the SOA threshold using the QUEST method. Specifically, the QUEST algorithm was searching for the SOA duration that could give the maximum masking effect (set as a 10 cd/m^2 difference). In other words, I set a criterion that the SOA threshold for a given participant should be the SOA that would result in the test target's luminance increment of 10 candelas, relative to the reference target, in order for the test to be reported as brighter than the reference. The results from the main experiment (having revealed a just noticeable difference of 12.5 cd/m^2 -see below) confirmed that the 10 cd/m^2 criterion was a reasonable one for sufficient masking. I found that estimated SOA thresholds for two participants exceeded 250 ms, which is outside the range expected for genuine metacontrast masking. I retested these (naïve) participants in a second session

and again found SOA thresholds in excess of 250 ms. I therefore excluded them from further study. For the remaining nine participants, the mean estimated SOA was 116.7 ms (*SEM* = 4.4).

6.2.5 Main experimental conditions

In Experiment 1, I tested how the relationship between the slant of the target and the mask affects brightness estimation. I presented targets and masks that were slanted in depth (±45 deg) with respect to the fronto-parallel plane (**figure 6.2a** provides stereograms for cross-fusion). I varied whether the target and the mask had the same or opposite slants, resulting in four different stimulus configurations (**figure 6.2b**). I measured thresholds by averaging over ten blocks (three participants) or four blocks (six participants) of 200 trials each. The different conditions were randomly interleaved during an individual run.

To ensure that any possible differences in masking were due to the slant of the surface, I included a control condition in which I measured masking for binocular presentation of the images viewed by the left eye in the main experiment 1. In particular, the disparity applied to the stimuli would create small offsets between the edges of the mask and target when they had binocularly specified opposite slants while edges would be aligned for stimuli with the same slant. Thus, I measured whether differential masking caused by these small, monocularly available signals might affect masking for 'same' and 'opposite' slant conditions. As the identical images were presented to both eyes in this condition, the stimuli had no binocular disparity and appeared flat. Thresholds were calculated as mean performance over ten blocks for three observers and over four blocks for six observers.

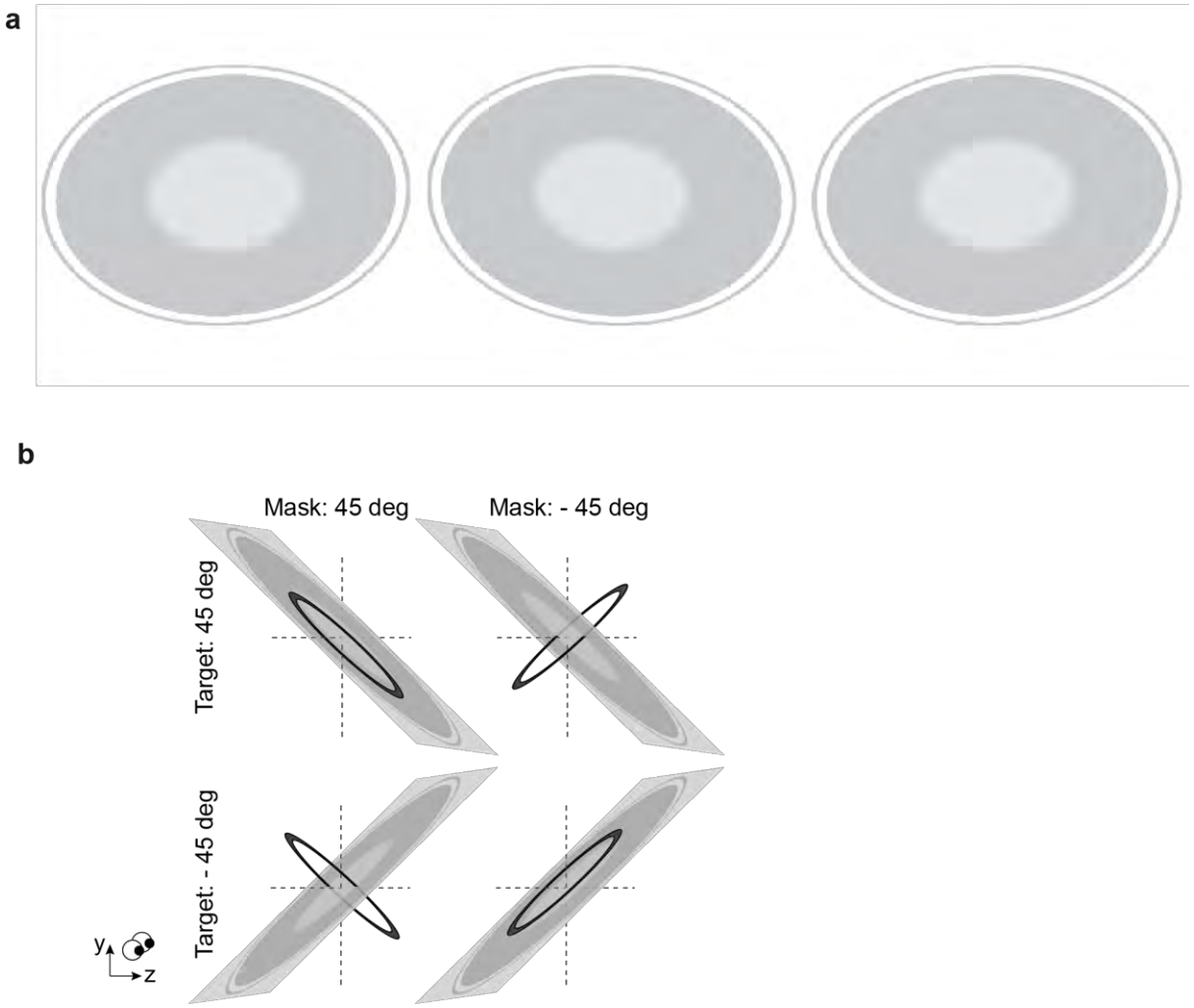

Figure 6.2: (a) Stereogram illustrating a sample of the monocular views of the stimuli of experiment 1. **(b)** Illustration of the target and mask configurations for Experiment 1. The control experiment consisted of the same conditions, but the stimuli had no binocular disparity/3D information, since each eye viewed the same stereo half image.

6.3 Results

6.3.1 Experiment 1

In experiment 1, I was interested in examining whether brightness masking would be stronger when the target and mask shared the same 3D orientation. I measured just noticeable difference thresholds for the central portion of the target disc. Raw (luminance measured in cd/m^2) data for each participant are shown in **figure 6.3a**. Although there is variability between individuals, these data reveal that for 7 out of the 9 participants,

thresholds were elevated (stronger brightness masking) in the 'same' condition where the target and the mask shared 3D orientations, compared to the orthogonal conditions. In order to remove the variability in overall thresholds between participants, I normalized (per participant) the data by dividing each luminance threshold for the experimental conditions by the mean luminance thresholds measured in the no-disparity control conditions.

The average (normalised) discrimination thresholds from Experiment 1 are shown in **figure 6.3b**. I found that thresholds were higher in the conditions where the target and mask had the same slant orientations, compared to the conditions where their slants were orthogonal. In particular, using a 2 (slant congruence: same vs. orthogonal) x 2 (slant sign: positive vs. negative) repeated-measures ANOVA, I found that there was a main effect of target-mask congruence ($F(1,8) = 6.06$, $p = .039$, partial $\eta^2 = .431$, power $(1-\beta) = 0.71$), but no effect of slant sign ($F(1,8) = 1.35$, $p = .278$, partial $\eta^2 = .145$, power $(1-\beta) = 0.13$) and no interaction ($F(1,8) < 1$, $p = .730$, partial $\eta^2 = .016$, power $(1-\beta) = 0.05$).

Considering data from the control condition, in which there was no difference in the slant of the target and mask (the stimuli appeared frontoparallel), I found no effect of slant congruence on the extent of masking ($F(1,8) < 1$, $p = .935$, partial $\eta^2 = .001$, power $(1-\beta) = 0.05$), nor slant sign ($F(1,8) < 1$, $p = .881$, partial $\eta^2 = .003$, power $(1-\beta) = 0.05$) or an interaction ($F(1,8) < 1$, $p = .935$, partial $\eta^2 = .001$, power $(1-\beta) = 0.05$). This suggests that the masking effect observed in the stereoscopically defined condition could not be attributed to subtle differences in the monocular images, but, rather, is due to the extraction of binocular signals.

In addition, to evaluate the effectiveness of masking *per se* in my paradigm, I conducted another control, no-masking, experiment on three participants. I preserved the standard experimental configurations of the target (-45 and 45 deg slants) and also presented a flat condition (target appearing with zero slant), where none of the targets/conditions was followed by mask. The mean increment thresholds in this no-

masking control was 105.4 cd/m^2, i.e., the just noticeable difference (jnd) was 3.7 cd/m^2 (reference target's luminance being 101.7 cd/m^2). In contrast, in the main experiment, the mean threshold was 114.2 cd/m^2, (jnd of 12.5 cd/m^2).

Inspecting **figure 6.3a** and comparing the results from the 'same' condition in the main experiment (± 45 deg slant) and the 'same' condition in the no-disparity control condition (frontoparallel stimuli), might suggest that brightness masking is slightly higher for slanted targets. However, there was no reliable difference between the two conditions (mean threshold in main condition = 114.2 cd/m^2 vs. 114.9 cd/m^2 in the control condition). A repeated-measures ANOVA confirmed that there were no statistically significant differences ($F(1,8) < 1$, $p = .57$, partial $\eta^2 = .042$, power $(1-\beta) = 0.05$).

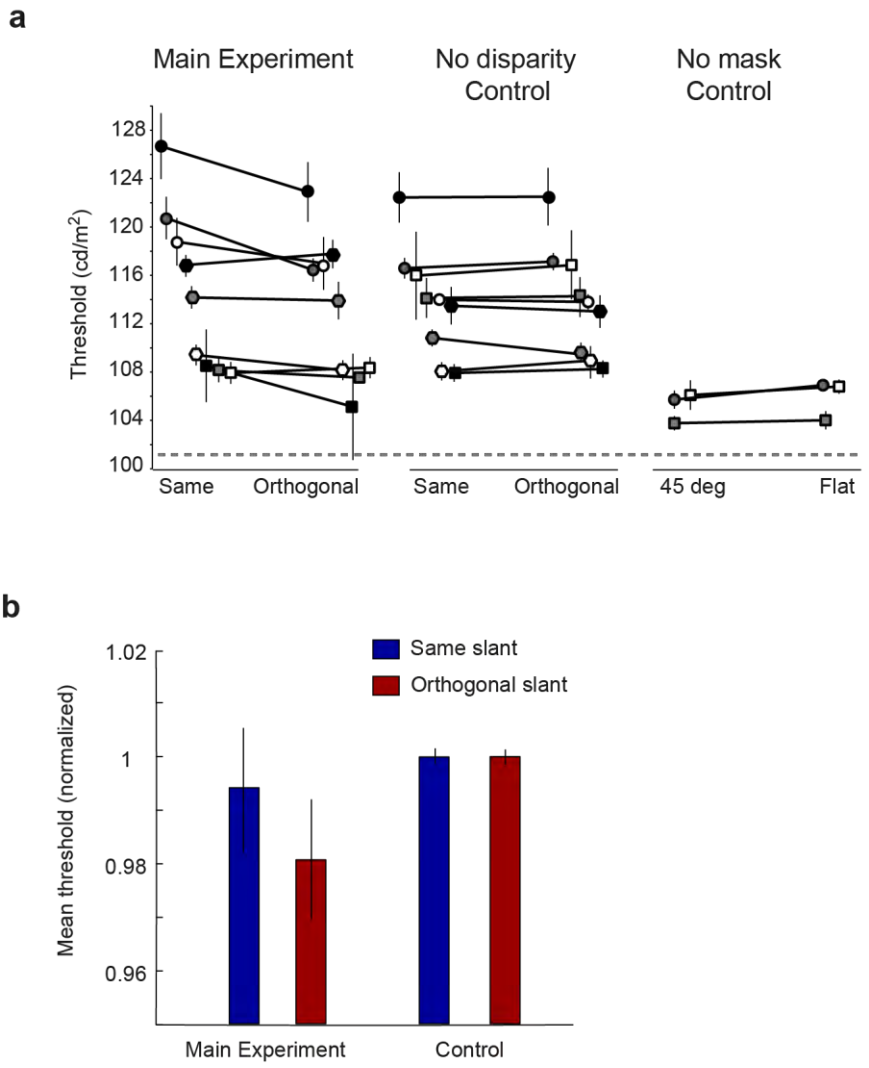

Figure 6.3: (a) Raw discrimination thresholds across the 'same' and 'orthogonal' stimuli configurations for the main and the no-disparity control experiments for all nine participants (left panels). Raw thresholds for the three additional participants across the 45 deg slants and the flat conditions for the no-masking control (right panel). The dotted continuous line represents the constant luminance of the reference target surface whose brightness was compared with the test target throughout the experimental conditions. Individual participants are indicated by each plotting symbol. **(b)** Average discrimination thresholds as a function of stimulus configurations for the main experiment and the no-disparity control conditions. Threshold values here are normalized by dividing each luminance (cd/m^2) value by the mean luminance measured in the control conditions, for each participant. Error bars show the between-subjects standard error of the mean.

6.3.2 Experiment 2

In experiment 2, I sought to determine whether the mask interferes with the target only when stimuli share the same slant, or whether interference occurs when the target and mask are slightly misaligned. I therefore presented a frontoparallel (0 deg angle) target stimulus, and then masks of different slant angles with respect to it (0, $\pm$22.5 or $\pm$45 deg; **figure 6.4a**). I measured thresholds by averaging over four blocks of 250 trials each, while conditions in each block were randomly interleaved. A repeated-measures ANOVA showed that masking was stronger (higher thresholds; see **figure 6.4b**) when the mask and target shared the same frontoparallel orientation compared to the slanted conditions of the mask [$F(4,32) = 5.12$, $p < .01$, partial $\eta^2 = .39$, power $(1-\beta) = 0.48$].

I normalised the data to remove between participant variability (as described for Experiment 1), and grouped opposing slant values (**figure 6.4c**). I found an effect of slant on brightness masking: a one-way ANOVA (with 45, 22.5 and zero deg conditions as factors) showed a significant effect of magnitude [$F(2,16) = 8.87$, $p < .01$, partial $\eta^2 = .526$, power $(1-\beta) = 0.63$]. Post-hoc analysis, using Bonferroni correction for multiple comparisons, indicated a significant difference between zero and 45 deg slant ($p < .01$), but not between zero and 22.5 deg ($p = .087$), or between 45 and 22.5 deg conditions ($p = .557$). These results indicate that masking is weakest (decreased thresholds) when the target and mask have the greatest spatial misalignment (45 deg slant of the mask).

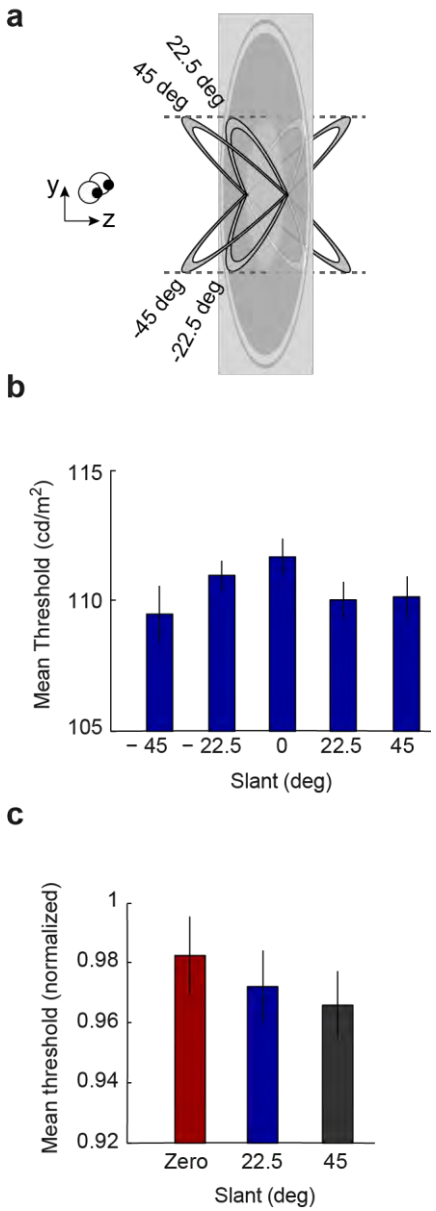

Figure 6.4: (a) Illustration of the stimulus configuration for experiment 2. The target had zero disparity, appearing flat, across all the conditions. The mask had different slants with respect to the target (0, ±22.5 and ±45 deg) resulting in five target-mask configurations. As the figure shows, I controlled the spatial extensions of the masks so that they cover the same spatial extent irrespectively of their slant. **(b)** Between-subjects average thresholds in the five individual experimental conditions expressed in measured luminance. **(c)** Average normalized thresholds data for the different slant levels. Error bars show the between-subjects standard error of the mean.

6.4 Discussion

In the present study, I investigated whether brightness estimation incorporates the 3D information of disparity-defined slanted surfaces. I used a masking paradigm to examine whether the disruption of brightness estimation from backward masking is modulated by the slant configurations of target and mask stimuli. I report an influence of surface slant on brightness masking. Specifically, in experiment 1, I found targets and masks that shared the same 3D orientation produced a greater attenuation of brightness. Moreover, a no-disparity control condition indicated that this difference could not be explained by subtle image differences at the monocular level. Experiment 2 examined how sensitive this effect was to the precise 3D orientation of the masking surfaces. While I found an influence of mask orientation on brightness, I did not observe a tight tuning of the effect to the precise slant angle. More generally, it is important to note that the modulation of masking by changes in surface slant was small. Thus, it is likely that brightness estimation involves a substantial monocular component, with a relatively minor contribution from disparity-defined surface structure information. These results suggest that brightness estimation is at least partially mediated by mid-level neuronal mechanisms where disparity edge signals have been extracted.

While my approach is grounded in the work of Paradiso and Nakayama (1991) it is important to note the differences existing in the stimulus configuration between the two studies: Paradiso and Nakayama used uniform surfaces and asked participants to make brightness matches using the method of adjustment. Here, I used a centre-surround configured test target (‘target 2’ in **figure 6.1c**) whose central area, without masking, appeared brighter than the surround. I asked participants whether this central area was brighter than the corresponding area of the reference target (‘target 1’ in **figure 6.1c**). The test target was followed by a mask, whereas the reference was followed by no mask and also had uniform and constant luminance. Thereby, I sought to use a staircase procedure to quantify the masking effects. My approach of using a bipartite stimulus may be

responsible for the relatively modest masking effects I observed. Paradiso and Nakayama reported masking effects that could approach two orders of magnitude (although their stimuli were considerably more luminous than I could achieve on my setup). It is possible that backward masking was weaker in my study because brightness propagation could have started inside the masked region from the central portion of the disk. My use of blurred boundaries between the two portions of the disk was intended to attenuate any such effect, and it is important to consider that while this effect may have been present at the start of an experimental session (i.e., large luminance difference between centre and surround), the contribution of an interior boundary signal would be considerably reduced as the luminance contrast between the centre and surround was adaptively reduced by the staircase algorithm.

My data suggest that binocular disparity edges modulate the degree of disruption that backward masking causes to the estimation of a surface's brightness. Apparent brightness has been strongly associated with a propagation (filling-in) process. Previous work suggests that active filling-in processes are unlikely to explain the perceptual filling-in of motion and depth information (but see also Welchman & Harris, 2003a) given lower spatial resolution of these signals. Nevertheless, the current study suggests a modest role for disparity-defined edge structure in modulating brightness estimation. This can be framed within the framework of Grossberg (1994) model according to which, once the boundaries of surfaces are registered, the 3D surfaces are filled-in/generated at a stage not earlier than area V4.

7. General Discussion and Conclusions

The work I have presented in chapters 1-6 used neuromodulation (fMRI-guided TMS) and backward visual masking techniques to temporarily suppress visual stimulus processing and infer the cortical stages that support the perception of 3D surfaces and their associated processes. In the following paragraphs, I outline the main findings of each experimental chapter and discuss how this work advances our understanding of the neural mechanisms engaged in seeing 3D surfaces.

7.1 Summary of main findings

In chapter 3, I used fMRI-guided rTMS to directly probe the cortical areas that support the perception of slanted surfaces. Stimulation over V3A, LO and the posterior parietal cortex failed to reveal a significant contribution to slant estimation, but stimulation of the posterior parietal cortex showed that performance in discriminating surfaces of high slant and surfaces of low slant became similar. This result suggests a minor contribution of the PPC to slant estimation and possibly to the encoding of spatial information, such as stimuli's aspect ratios, but the effect did not reach statistical significance due to insufficient statistical power.

Following a similar methodological approach, in chapter 4, I used rTMS to temporarily suppress the function of the functionally-localized are LO, to directly investigate the area's contribution to 3D surface fine discrimination when depth is informed congruently by disparity and motion. I found that stimulation of LO 500 ms before the onset of the visual stimulus attenuates discrimination performance in the disparity & motion fused condition and the integration advantage eliminates. This result highlights that LO supports the integration of different cues to depth and accords with the ventral stream's specialisation in fine stereopsis.

In chapter 5, I examined the involvement of the dorso-parietal cortex in tasks requiring the discrimination of signal embedded in noise. Also, I tested how this involvement may change as a function of training. Using disruptive rTMS, I first found that extracting both depth and orientation signals embedded-in-noise causally relates to processing in the posterior parietal cortex. However, this relationship diminished after training on a visual feature other than the one used during the rTMS testing. This result confirms the contribution of dorso-parietal circuits to signal-in-noise discriminations of absolute disparity and further suggests that the underlying neuronal architecture can change due to learning.

In chapter 6, I used metacontrast backward masking and manipulated whether a target surface and a mask had the same or orthogonal slants. I found that masking-induced brightness suppression was greater in the condition where target and mask shared the same slant (experiment 1), but the effect was not sensitive to the precise angle of the mask (experiment 2). Altogether, the results indicate that brightness masking incorporates binocular disparity information. The study indirectly suggests, therefore, that brightness estimation occurs at a stage where disparity edge signals have been extracted, after the convergence of binocular signals in V1.

Finally, in chapters 3 and 5, I additionally considered the potential effects of the posterior parietal stimulation on the control of vergence eye movements. Binocular eye movements were measured during rTMS experiments. Data analysis showed that neural stimulation over the PPC did not affect eye movements systematically. These supplementary results provide reassurance that participants' vergence was stable throughout the experiments and there was no stimulation-induced disruption of stereopsis.

7.1.1 Chapter 3: Seeing slanted surfaces: probing the contributions of dorsal and ventral visual brain areas

In the preliminary behavioural experiments of chapter 3, I observed a 'slant oblique effect'. Specifically, the discrimination of surfaces defined by low disparity, slanted close to the frontoparallel, was facilitated compared to the more oblique (and defined by bigger disparity) slants. I applied rTMS over disparity-selective areas of the ventral and dorsal visual stream aiming to investigate the cortical locus of this effect. Data analysis failed to reveal a significant contribution of either V3A or LO to slant perception, but suggested that rTMS over the left PPC slightly attenuated the behavioural difference in discriminating between high and low slants. That is, P3 stimulation resulted in the attenuation of the '10 deg advantage' of the slant oblique effect. Although this finding hints at a functional contribution of the PPC to slant estimation, however, the inferences from this experiment are not conclusive. For instance, it could be the case that PPC stimulation knocked out the salient spatial differences between the high and the low slant. This would indicate the involvement of the PPC in encoding the aspect ratio of the different slant magnitudes (that is, the spatial attributes of different slants) and not in contributing to the fine discrimination of slant *per se*. Such a possibility is in accordance with the specialisation of dorso-parietal areas in the spatial localisation of objects in general (see *General Introduction*). Intriguingly, the study lacked sufficient statistical power. Also, slant discrimination performance improved as the days of experimentation passed. These findings indicate that any speculations on what the acquired data suggest remain incomplete and elusive. Possible alternative experimental methodologies (for example, alternative criteria for choosing the regions of interest, sample size, the TMS protocol and/or the psychophysical parameters) are discussed in detail in chapter 3.

7.1.2 Chapter 4: Integration of motion and disparity cues to depth in ventral visual cortex

In the preliminary behavioural experiments of chapter 4, I observed that perceptual judgments in a fine depth discrimination task were enhanced in the condition where depth was informed by both disparity and motion parallax cues, compared to disparity alone. Subsequently, I conducted two rTMS experiments over area LO and manipulated the timing of the TMS pulses. In experiment 1, the pulses were synchronised with the stimulus onset, while in experiment 2, pulses preceded the stimulus onset. In experiment 2, I found that stimulation of area LO, 500 ms before the stimulus onset, eliminated the behavioural enhancement of the integrated disparity and motion condition significantly. This finding suggests that LO's function contributes to the integration of disparity and motion cues to surface depth and is in accordance with (Welchman, et al. (2005)). These researchers showed fMRI evidence that neural activity in LO supports the combination of disparity and perspective cues to slant, resulting in the perception of global 3D shapes. However, in a study more similar to the present one, Ban et al. (2012) found fMRI evidence that dorsal (in area V3B/KO), rather than ventral, processing supports the integration of motion and disparity cues. The discrepancy between the two studies can be possibly attributed to the different methodologies used (fMRI vs TMS). More importantly though, the two studies employed different discrimination tasks: in Ban et al.'s (2012) study, viewers were asked to make absolute disparity discriminations, while here, viewers made fine discriminations of relative disparity. Both the present and the Ban et al.'s study, therefore, provide further support for the specialisation of the ventral stream in fine stereopsis and the involvemnet of the dorsal stream in coarse stereopsis (see *General Introduction*).

7.1.3 Chapter 5: Learning generalisation across visual features in dorsal visual cortex

Previous studies have shown that the causal contribution of the dorso-parietal visual stream to the discrimination of depth signal embedded in noise vanishes due to training on the discrimination of fine disparity in the absence of noise (see *Introduction*). In chapter 5, I explored whether this change of the parietal engagement can occur even when the test and training phases employ different visual features. In three experiments, I applied disruptive rTMS over the posterior parietal cortex to confirm that neural encoding of information in the PPC is necessary for the execution of a signal-in-noise discrimination task (both in the orientation and depth domains). Interestingly, my results further supported previous findings indicating that this causal involvement decreases dramatically after training. Specifically, in experiments 1 and 2, I observed that the contribution of the PPC to the discrimination of signal-in-noise orientation and depth was eliminated as a result of training on fine disparity and orientation (in the absence of noise) respectively. However, this finding did not receive proper statistical support. In experiment 3, on the other hand, I found that training on signal-in-noise orientation significantly reduced the contribution of the PPC to the discrimination within signal-in-noise depth. This finding indicates that the benefits of training on a signal-in-noise task of one visual feature affect the involvement of the PPC in the execution of a signal-in-noise task of another visual feature. Experiment 3, thus, provides neuromodulation evidence to support previous findings that, behaviourally, training on a signal-in-noise task can promote its benefits to signal-in-noise tasks of different visual features (Chang et al., 2013).

7.1.4 Chapter 6: Brightness masking is modulated by disparity structure

This chapter examined the relationship between brightness perception and 3D surface configuration and sought to infer the stage of the visual pathway where brightness

estimation occurs. I used a centre-surround configured test target which was followed by a mask (backward masking). I asked participants whether the centre of the target was brighter than the corresponding area of a reference (unmasked) target stimulus. I found that the 3D spatial layout affects brightness masking and that the latter incorporates the 3D information of disparity-defined slant. Specifically, in experiment 1, I found that when targets and masks shared the same 3D orientation, a greater disruption of brightness estimation was produced. In experiment 2, I further examined how sensitive this effect was to the precise 3D orientation of the masking stimulus. I found an influence of mask orientation on brightness, but only when the mask had the greatest spatial misalignment relative to the target (45 deg of mask vs 0 deg of the target). All together, these results suggest that the estimation of a surface's brightness is modulated by the surface's disparity-defined edge structure. In particular, brightness masking is at least partially mediated by mid-level neuronal mechanisms, where disparity edge signals have been extracted. Therefore, brightness estimation seems to occur after the combination of the two eyes' signals in V1.

7.2 Contributions to the literature

Directly in chapters 3, 4 and 5 and indirectly in chapter 6, I probed the cortical mechanisms of the visual brain involved in the perception of 3D surfaces. The individual chapters, although using different experimental paradigms and stimulus configurations, all together offer a significant insight into the stages of the visual pathway that contribute to the binocular perception of surfaces in depth.

First, in chapter 3, I found that the behavioural sensitivity for discriminating slant was greater for surfaces slanted close to the frontoparallel (10 deg) than for slants farther away (50 deg). However, this Weber's-law-like salience for the low disparity slants was minimised after TMS-induced disruption over the left posterior parietal cortex, and the '10

deg advantage' of the 'slant oblique effect' attenuated. This finding can be accounted for by the possibility that the PPC encodes the aspect ratio of the different slant magnitudes and contributes to the computation of the salient spatial differences between the high and the low slant. This interpretation of the data does not directly attribute a functional role of the PPC to slant perception. However, it is, still, an interesting speculation that supports previous studies and highlights the significant role of the dorso-parietal stream in the encoding of spatial features and relationships among objects locations (see *General Introduction*).

In chapter 4, I found that TMS-induced disruption over area LO eliminates the behavioural enhancement observed in depth discrimination when disparity and motion cues congruently inform depth. More specifically, I found that stimulation 500 ms before the stimulus onset eliminates the cue integration advantage for fine depth judgments when the depth of the surface is informed by both disparity and motion parallax, compared to disparity alone. This study extends the findings by Ban et al. (2012) and highlights that, apart from the dorsal, the ventral visual stream is also important for the integration of qualitatively different cues to depth. Given that participants in chapter 4 discriminated fine differences of surface depth (contrary to Ban et al.'s where participants made 'more coarse' judgments of absolute disparity), the present finding is additionally interesting and provides further evidence for the specialisation of the ventral stream in fine stereopsis (see *General Introduction*). Moreover, experiment 1 in chapter 4 showed that the delivery of TMS pulses concurrently with the stimulus onset did not result in an attenuation of the 'integration advantage'. Rather, stimulation before the stimulus onset, in experiment 2, was effective. This is an important finding that elucidates between different TMS protocols and suggests that the elimination of the cue integration advantage depends on the timing of the TMS stimulation.

In the third experiment of chapter 5, I found rTMS evidence that the discrimination of depth embedded in noise causally relates to the neural processing in the PPC. Specifically,

I found discrimination impairment under P3 stimulation, compared to control stimulation. Interestingly enough, this causal relation vanished after participants were extensively trained to discriminate signal-in-noise orientation. This finding, at first, further supports previous studies which suggest that neural processing in dorsal cortex is necessary for the detection of disparity signals embedded in noise. Additionally, the current results accord with a recent study by Chang et al. (2014) in that training can change the neuronal architecture that supports signal-in-noise depth estimation. More importantly though, the present finding provides strong evidence that this neuronal re-organisation occurs not only when the same visual feature is employed during both testing and training, but also when different visual features are considered. That is, the benefits of training on signal-in-noise discrimination influence the signal-in-noise discrimination in another domain (e.g., from orientation to depth) at the behavioural (Chang et al., 2013) as well as the neural level.

In chapter 6, I showed that the disruption that masking induces in the estimation of brightness is influenced by the 3D configuration of the target and the mask. This indicates that brightness masking incorporates binocular disparity information and occurs within a 3D framework where binocular signals have been combined to extract disparity edge structure. A 'filling-in' mechanism, suggesting that contrast information at the edge of a surface spreads and influences brightness estimation of the entire surface, has been proposed to account for the estimation of brightness (see *General Introduction*). Since the masking paradigm adopted in chapter 6 is thought to interrupt the spread of activity from the border towards the interior of a surface and highlight the putative filling-in mechanisms that may support it, the findings in chapter 6 shed light on a long-lasting debate regarding the neural basis of filling-in. Specifically, since Paradiso and Nakayama's (1991) study, the exact stage of the visual pathway where brightness filling-in occurs remained unsolved. Chapter 6 offers evidence that brightness filling-in, as disclosed by masking, is mediated by mid-level neuronal mechanisms, where binocular information has been extracted. This important finding contributes to our understanding of the cortical stages related to

brightness perception and completion mechanisms and suggests that brightness filling-in occurs after the convergence of binocular signals in the primary visual cortex.

7.3 Concluding remarks

A primary goal in neuroscience is to designate the relationship between a function and the neuronal substrate that supports it. In visual neuroscience, in particular, the elucidation of the neural pathways engaged in visual perception has been aided the last decades by the major advances in neuroimaging techniques such as fMRI and TMS. In the domain of binocular depth perception, neuroimaging has dramatically advanced our understanding of how the perception of surfaces in depth emerges from the neural processing of cue signals such as binocular disparity. In this PhD dissertation, I benefited from these powerful research tools, which I employed together with classical psychophysics, to contribute to the understanding of some contemporary issues in the field. Considering the relationship between surface 3D configuration and brightness, I found that brightness estimation interferes with surface's slant at early stages of the visual pathway. On the other hand, higher parts of the visual cortex, extending in the dorsal and the ventral pathway, were found to specialise in processes such as the estimation of slant, the integration of different depth cues, the detection of signal embedded in noise and learning generalisation.

References

Abrahamyan, A., Clifford, C. W., Arabzadeh, E., & Harris, J. A. (2011). Improving visual sensitivity with subthreshold transcranial magnetic stimulation. *J Neurosci, 31*(9), 3290-3294.

Adab, H. Z., & Vogels, R. (2011). Practicing coarse orientation discrimination improves orientation signals in macaque cortical area v4. *Curr Biol, 21*(19), 1661-1666.

Adelson, E. H. (1993). Perceptual organization and the judgment of brightness. *Science, 262*(5142), 2042-2044.

Adelson, E. H. (2000). Lightness Perception and Lightness Illusions. In M. Gazzaniga (Ed.), *The New Cognitive Neurosciences* (pp. 339-351). Cambridge: MIT Press.

Ahissar, M., & Hochstein, S. (1997). Task difficulty and the specificity of perceptual learning. *Nature, 387*(6631), 401-406.

Alpern, M. (1953). Metacontrast. *J Opt Soc Am, 43*(8), 648-657.

Anderson, B. L., Singh, M., & Fleming, R. W. (2002). The interpolation of object and surface structure. *Cogn Psychol, 44*(2), 148-190.

Anderson, B. L., & Winawer, J. (2005). Image segmentation and lightness perception. *Nature, 434*(7029), 79-83.

Anstis, S. (2010). Visual filling-in. *Curr Biol, 20*(16), R664-666.

Anstis, S., Verstraten, F. A., & Mather, G. (1998). The motion aftereffect. *Trends Cogn Sci, 2*(3), 111-117.

Anzai, A., & DeAngelis, G. C. (2010). Neural computations underlying depth perception. *Curr Opin Neurobiol, 20*(3), 367-375.

Backus, B. T., Banks, M. S., van Ee, R., & Crowell, J. A. (1999). Horizontal and vertical disparity, eye position, and stereoscopic slant perception. *Vision Res, 39*(6), 1143-1170.

Backus, B. T., Fleet, D. J., Parker, A. J., & Heeger, D. J. (2001). Human cortical activity correlates with stereoscopic depth perception. *J Neurophysiol, 86*(4), 2054-2068.

Bakin, J. S., Nakayama, K., & Gilbert, C. D. (2000). Visual responses in monkey areas V1 and V2 to three-dimensional surface configurations. *J Neurosci, 20*(21), 8188-8198.

Ban, H., Preston, T. J., Meeson, A., & Welchman, A. E. (2012). The integration of motion and disparity cues to depth in dorsal visual cortex. *Nat Neurosci, 15*(4), 636-643.

Ban, H., & Welchman, A. E. (2015). fMRI Analysis-by-Synthesis Reveals a Dorsal Hierarchy That Extracts Surface Slant. *J Neurosci, 35*(27), 9823-9835.

Banks, M. S., Hooge, I. T., & Backus, B. T. (2001). Perceiving slant about a horizontal axis from stereopsis. *J Vis, 1*(2), 55-79.

Barlow, H. B., Blakemore, C., & Pettigrew, J. D. (1967). The neural mechanism of binocular depth discrimination. *J Physiol, 193*(2), 327-342.

Barlow, H. B., & Brindley, G. S. (1963). Inter-ocular transfer of movement after-effects during pressure blinding of the stimulated eye. *Nature, 200*, 1347.

Bartels, A. (2014). Visual perception: early visual cortex fills in the gaps. *Curr Biol, 24*(13), R600-602.

Bell, A. H., Pasternak, T., & Ungerleider, L. G. (2014). Ventral and dorsal cortical processing streams. In J. S. Werner & L. M. Chalupa (Eds.), *In The New Visual Neurosciences* (pp. 227-242). Cambridge, MA: MIT Press.

Blakeslee, B., & McCourt, M. E. (1999). A multiscale spatial filtering account of the White effect, simultaneous brightness contrast and grating induction. *Vision Res, 39*(26), 4361-4377.

Bonneh, Y. S., Cooperman, A., & Sagi, D. (2001). Motion-induced blindness in normal observers. *Nature, 411*(6839), 798-801.

Boring, E. G. (1964). Size-constancy in a picture. *Am J Psychol, 77*, 494-498.

Brainard, D. H. (1997). The Psychophysics Toolbox. *Spat Vis, 10*(4), 433-436.

Breitmeyer, B. G., & Ogmen, H. (2000). Recent models and findings in visual backward masking: a comparison, review, and update. *Percept Psychophys, 62*(8), 1572-1595.

Breitmeyer, B. G., & Ogmen, H. (2006). *Visual masking: Time slices through conscious and unconscious vision* (2nd ed.). Oxford: Oxford University Press.

Breitmeyer, B. G., Ro, T., & Ogmen, H. (2004). A comparison of masking by visual and transcranial magnetic stimulation: implications for the study of conscious and unconscious visual processing. *Conscious Cogn, 13*(4), 829-843.

Campbell, F. W., & Kulikowski, J. J. (1966). Orientational selectivity of the human visual system. *J Physiol, 187*(2), 437-445.

Cavanagh, P. (2011). Visual cognition. *Vision Res, 51*(13), 1538-1551.

Chanes, L., Chica, A. B., Quentin, R., & Valero-Cabre, A. (2012). Manipulation of pre-target activity on the right frontal eye field enhances conscious visual perception in humans. *PLoS One, 7*(5), e36232.

Chang, D. H., Kourtzi, Z., & Welchman, A. E. (2013). Mechanisms for extracting a signal from noise as revealed through the specificity and generality of task training. *J Neurosci, 33*(27), 10962-10971.

Chang, D. H., Mevorach, C., Kourtzi, Z., & Welchman, A. E. (2014). Training Transfers the Limits on Perception from Parietal to Ventral Cortex. *Curr Biol*.

Chowdhury, S. A., & DeAngelis, G. C. (2008). Fine discrimination training alters the causal contribution of macaque area MT to depth perception. *Neuron, 60*(2), 367-377.

Cohen, J. (1988). *Statistical power analysis for the behavioral sciences (2nd ed.)*: Hillsdale, NJ: Erlbaum.

Cornelissen, F. W., Peters, E. M., & Palmer, J. (2002). The Eyelink Toolbox: eye tracking with MATLAB and the Psychophysics Toolbox. *Behav Res Methods Instrum Comput, 34*(4), 613-617.

Cumming, B. G., & Parker, A. J. (1997). Responses of primary visual cortical neurons to binocular disparity without depth perception. *Nature, 389*(6648), 280-283.

Davey, M. P., Maddess, T., & Srinivasan, M. V. (1998). The spatiotemporal properties of the Craik-O'Brien-Cornsweet effect are consistent with 'filling-in'. *Vision Res, 38*(13), 2037-2046.

Davis, N. J., Gold, E., Pascual-Leone, A., & Bracewell, R. M. (2013). Challenges of proper placebo control for non-invasive brain stimulation in clinical and experimental applications. *Eur J Neurosci*.

De Weerd, P., Gattass, R., Desimone, R., & Ungerleider, L. G. (1995). Responses of cells in monkey visual cortex during perceptual filling-in of an artificial scotoma. *Nature, 377*(6551), 731-734.

DeAngelis, G. C. (2000). Seeing in three dimensions: the neurophysiology of stereopsis. *Trends Cogn Sci, 4*(3), 80-90.

DeAngelis, G. C., Cumming, B. G., & Newsome, W. T. (1998). Cortical area MT and the perception of stereoscopic depth. *Nature, 394*(6694), 677-680.

Di Luca, M., Ernst, M. O., & Backus, B. T. (2010). Learning to use an invisible visual signal for perception. *Curr Biol, 20*(20), 1860-1863.

Dosher, B. A., & Lu, Z. L. (1998). Perceptual learning reflects external noise filtering and internal noise reduction through channel reweighting. *Proc Natl Acad Sci U S A, 95*(23), 13988-13993.

Dosher, B. A., & Lu, Z. L. (1999). Mechanisms of perceptual learning. *Vision Res, 39*(19), 3197-3221.

Dosher, B. A., & Lu, Z. L. (2005). Perceptual learning in clear displays optimizes perceptual expertise: learning the limiting process. *Proc Natl Acad Sci U S A, 102*(14), 5286-5290.

Dosher, B. A., Sperling, G., & Wurst, S. A. (1986). Tradeoffs between stereopsis and proximity luminance covariance as determinants of perceived 3D structure. *Vision Res, 26*(6), 973-990.

Dovencioglu, D., Ban, H., Schofield, A. J., & Welchman, A. E. (2013). Perceptual integration for qualitatively different 3-D cues in the human brain. *J Cogn Neurosci, 25*(9), 1527-1541.

Dricot, L., Sorger, B., Schiltz, C., Goebel, R., & Rossion, B. (2008). The roles of "face" and "non-face" areas during individual face perception: evidence by fMRI adaptation in a brain-damaged prosopagnosic patient. *Neuroimage, 40*(1), 318-332.

Faul, F., Erdfelder, E., Buchner, A., & Lang, A. G. (2009). Statistical power analyses using G*Power 3.1: tests for correlation and regression analyses. *Behav Res Methods, 41*(4), 1149-1160.

Faul, F., Erdfelder, E., Lang, A. G., & Buchner, A. (2007). G*Power 3: a flexible statistical power analysis program for the social, behavioral, and biomedical sciences. *Behav Res Methods, 39*(2), 175-191.

Friedman, H. S., Zhou, H., & von der Heydt, R. (2003). The coding of uniform colour figures in monkey visual cortex. *J Physiol, 548*(Pt 2), 593-613.

Frund, I., Haenel, N. V., & Wichmann, F. A. (2011). Inference for psychometric functions in the presence of nonstationary behavior. *J Vis, 11*(6).

Furmanski, C. S., & Engel, S. A. (2000). An oblique effect in human primary visual cortex. *Nat Neurosci, 3*(6), 535-536.

Gibson, E. J. (1953). Improvement in perceptual judgments as a function of controlled practice or training. *Psychol Bull, 50*(6), 401-431.

Gibson, J. J. (1950). The perception of visual surfaces. *Am J Psychol, 63*(3), 367-384.

Gibson, J. J., & Cornsweet, J. (1952). The perceived slant of visual surfaces-optical and geographical. *J Exp Psychol, 44*(1), 11-15.

Gilbert, C. D., Sigman, M., & Crist, R. E. (2001). The neural basis of perceptual learning. *Neuron, 31*(5), 681-697.

Gilchrist, A. L. (1977). Perceived lightness depends on perceived spatial arrangement. *Science, 195*(4274), 185-187.

Gilchrist, A. L. (2006). *Seeing in Black and White*: Oxford University Press.

Gilchrist, A. L. (2007). Lightness and brightness. *Curr Biol, 17*(8), R267-269.

Gnadt, J. W., & Beyer, J. (1998). Eye movements in depth: What does the monkey's parietal cortex tell the superior colliculus? *Neuroreport, 9*(2), 233-238.

Goncalves, N. R., Ban, H., Sanchez-Panchuelo, R. M., Francis, S. T., Schluppeck, D., & Welchman, A. E. (2015). 7 tesla FMRI reveals systematic functional organization for binocular disparity in dorsal visual cortex. *J Neurosci, 35*(7), 3056-3072.

Goodale, M. A., & Milner, A. D. (1992). Separate visual pathways for perception and action. *Trends Neurosci, 15*(1), 20-25.

Green, D. M., & Swets, J. A. (1974). *Signal detection theory and psychophysics*. Huntington, New York: Robert E. Krieger Publishing Company.

Green, M. F., Glahn, D., Engel, S. A., Nuechterlein, K. H., Sabb, F., Strojwas, M., et al. (2005). Regional brain activity associated with visual backward masking. *J Cogn Neurosci, 17*(1), 13-23.

Grill-Spector, K., Kushnir, T., Hendler, T., & Malach, R. (2000). The dynamics of object-selective activation correlate with recognition performance in humans. *Nat Neurosci, 3*(8), 837-843.

Grill-Spector, K., & Malach, R. (2004). The human visual cortex. *Annu Rev Neurosci, 27*, 649-677.

Grossberg, S. (1994). 3-D vision and figure-ground separation by visual cortex. *Percept Psychophys, 55*(1), 48-121.

Grossberg, S., & Mingolla, E. (1985). Neural dynamics of form perception: boundary completion, illusory figures, and neon color spreading. *Psychol Rev, 92*(2), 173-211.

Grossberg, S., & Todorovic, D. (1988). Neural dynamics of 1-D and 2-D brightness perception: a unified model of classical and recent phenomena. *Percept Psychophys, 43*(3), 241-277.

Hallett, M. (2007). Transcranial magnetic stimulation: a primer. *Neuron, 55*(2), 187-199.

Harris, J. A., Clifford, C. W., & Miniussi, C. (2008). The functional effect of transcranial magnetic stimulation: signal suppression or neural noise generation? *J Cogn Neurosci, 20*(4), 734-740.

Haxby, J. V., Grady, C. L., Horwitz, B., Ungerleider, L. G., Mishkin, M., Carson, R. E., et al. (1991). Dissociation of object and spatial visual processing pathways in human extrastriate cortex. *Proc Natl Acad Sci U S A, 88*(5), 1621-1625.

Henderson, J. M. (2006). Eye movements. In C. Senior, T. Russell & M. Gazzaniga (Eds.), *Methods in Mind* (pp. 171-191). Cambridge, MA: MIT Press.

Hillis, J. M., Ernst, M. O., Banks, M. S., & Landy, M. S. (2002). Combining sensory information: mandatory fusion within, but not between, senses. *Science, 298*(5598), 1627-1630.

Howard, I. P., & Rogers, B. J. (2002). *Seeing in depth*. Toronto, Canada.

Hubel, D. H., & Wiesel, T. N. (1962). Receptive fields, binocular interaction and functional architecture in the cat's visual cortex. *J Physiol, 160*, 106-154.

Hubel, D. H., & Wiesel, T. N. (1968). Receptive fields and functional architecture of monkey striate cortex. *J Physiol, 195*(1), 215-243.

Julesz, B. (1971). Foundations of Cyclopean Perception Chicago, IL: University of Chicago Press.

Kanizsa, G. (1979). *Organization in vision: Essays on Gestalt perception*: New York: Praeger.

Kapoula, Z., Isotalo, E., Muri, R. M., Bucci, M. P., & Rivaud-Pechoux, S. (2001). Effects of transcranial magnetic stimulation of the posterior parietal cortex on saccades and vergence. *Neuroreport, 12*(18), 4041-4046.

Kellman, P. J., & Shipley, T. F. (1991). A theory of visual interpolation in object perception. *Cogn Psychol, 23*(2), 141-221.

Kelly, F., & Grossberg, S. (2000). Neural dynamics of 3-D surface perception: figure-ground separation and lightness perception. *Percept Psychophys, 62*(8), 1596-1618.

Knill, D. C., & Kersten, D. (1991). Apparent surface curvature affects lightness perception. *Nature, 351*(6323), 228-230.

Knill, D. C., & Saunders, J. A. (2003). Do humans optimally integrate stereo and texture information for judgments of surface slant? *Vision Res, 43*(24), 2539-2558.

Komatsu, H. (2006). The neural mechanisms of perceptual filling-in. *Nat Rev Neurosci, 7*(3), 220-231.

Komatsu, H. (2008). Lightness Perception and Filling-In. In A. I. Basbaum (Ed.), *The Senses: A Comprehensive Reference* (pp. 45-52). New York: Academic Press.

Kourtzi, Z., Betts, L. R., Sarkheil, P., & Welchman, A. E. (2005). Distributed neural plasticity for shape learning in the human visual cortex. *PLoS Biol, 3*(7), e204.

Kourtzi, Z., Erb, M., Grodd, W., & Bulthoff, H. H. (2003). Representation of the perceived 3-D object shape in the human lateral occipital complex. *Cereb Cortex, 13*(9), 911-920.

Kourtzi, Z., & Kanwisher, N. (2001). Representation of perceived object shape by the human lateral occipital complex. *Science, 293*(5534), 1506-1509.

Lamme, V. A., Rodriguez-Rodriguez, V., & Spekreijse, H. (1999). Separate processing dynamics for texture elements, boundaries and surfaces in primary visual cortex of the macaque monkey. *Cereb Cortex, 9*(4), 406-413.

Landy, M. S., Maloney, L. T., Johnston, E. B., & Young, M. (1995). Measurement and modeling of depth cue combination: in defense of weak fusion. *Vision Res, 35*(3), 389-412.

Leek, M. R. (2001). Adaptive procedures in psychophysical research. *Percept Psychophys, 63*(8), 1279-1292.

Li, S., Mayhew, S. D., & Kourtzi, Z. (2009). Learning shapes the representation of behavioral choice in the human brain. *Neuron, 62*(3), 441-452.

Livingstone, M., & Hubel, D. (1988). Segregation of form, color, movement, and depth: anatomy, physiology, and perception. *Science, 240*(4853), 740-749.

Lugtigheid, A. J., Wilcox, L. M., Allison, R. S., & Howard, I. P. (2014). Vergence eye movements are not essential for stereoscopic depth. *Proc Biol Sci, 281*(1776), 20132118.

Maeda, F., Keenan, J. P., Tormos, J. M., Topka, H., & Pascual-Leone, A. (2000). Interindividual variability of the modulatory effects of repetitive transcranial magnetic stimulation on cortical excitability. *Exp Brain Res, 133*(4), 425-430.

Malach, R., Reppas, J. B., Benson, R. R., Kwong, K. K., Jiang, H., Kennedy, W. A., et al. (1995). Object-related activity revealed by functional magnetic resonance imaging in human occipital cortex. *Proc Natl Acad Sci U S A, 92*(18), 8135-8139.

Maunsell, J. H., & Van Essen, D. C. (1983). Functional properties of neurons in middle temporal visual area of the macaque monkey. II. Binocular interactions and sensitivity to binocular disparity. *J Neurophysiol, 49*(5), 1148-1167.

McArthur, J. A., & Moulden, B. (1999). A two-dimensional model of brightness perception based on spatial filtering consistent with retinal processing. *Vision Res, 39*(6), 1199-1219.

McKeefry, D. J., Gouws, A., Burton, M. P., & Morland, A. B. (2009). The noninvasive dissection of the human visual cortex: using FMRI and TMS to study the organization of the visual brain. *Neuroscientist, 15*(5), 489-506.

Mevorach, C., Humphreys, G. W., & Shalev, L. (2006). Opposite biases in salience-based selection for the left and right posterior parietal cortex. *Nat Neurosci, 9*(6), 740-742.

Mevorach, C., Humphreys, G. W., & Shalev, L. (2009). Reflexive and preparatory selection and suppression of salient information in the right and left posterior parietal cortex. *J Cogn Neurosci, 21*(6), 1204-1214.

Meyer, B. U., Diehl, R., Steinmetz, H., Britton, T. C., & Benecke, R. (1991). Magnetic stimuli applied over motor and visual cortex: influence of coil position and field polarity on motor responses, phosphenes, and eye movements. *Electroencephalogr Clin Neurophysiol Suppl, 43*, 121-134.

Milner, A. D., & Goodale, M. A. (2008). Two visual systems re-viewed. *Neuropsychologia, 46*(3), 774-785.

Minini, L., Parker, A. J., & Bridge, H. (2010). Neural modulation by binocular disparity greatest in human dorsal visual stream. *J Neurophysiol, 104*(1), 169-178.

Miniussi, C., Ruzzoli, M., & Walsh, V. (2010). The mechanism of transcranial magnetic stimulation in cognition. *Cortex, 46*(1), 128-130.

Mishkin, M., Ungerleider, L. G., & Macko, K. A. (1983). Object vision and spatial vision: two cortical pathways. *Trends Neurosci, 6*, 414-417.

Morgan, M. J. (1992). On the scaling of size judgements by orientational cues. *Vision Res, 32*(8), 1433-1445.

Morgan, M. J., Watamaniuk, S. N., & McKee, S. P. (2000). The use of an implicit standard for measuring discrimination thresholds. *Vision Res, 40*(17), 2341-2349.

Murakami, I. (1995). Motion aftereffect after monocular adaptation to filled-in motion at the blind spot. *Vision Res, 35*(8), 1041-1045.

Murphy, A. P., Ban, H., & Welchman, A. E. (2013). Integration of texture and disparity cues to surface slant in dorsal visual cortex. *J Neurophysiol, 110*(1), 190-203.

Nachmias, J. (2006). The role of virtual standards in visual discrimination. *Vision Res, 46*(15), 2456-2464.

Nadler, J. W., Angelaki, D. E., & DeAngelis, G. C. (2008). A neural representation of depth from motion parallax in macaque visual cortex. *Nature, 452*(7187), 642-645.

Nadler, J. W., Nawrot, M., Angelaki, D. E., & DeAngelis, G. C. (2009). MT neurons combine visual motion with a smooth eye movement signal to code depth-sign from motion parallax. *Neuron, 63*(4), 523-532.

Neri, P., Bridge, H., & Heeger, D. J. (2004). Stereoscopic processing of absolute and relative disparity in human visual cortex. *J Neurophysiol, 92*(3), 1880-1891.

Nguyenkim, J. D., & DeAngelis, G. C. (2003). Disparity-based coding of three-dimensional surface orientation by macaque middle temporal neurons. *J Neurosci, 23*(18), 7117-7128.

Otazu, X., Vanrell, M., & Alejandro Parraga, C. (2008). Multiresolution wavelet framework models brightness induction effects. *Vision Res, 48*(5), 733-751.

Paradiso, M. A., & Nakayama, K. (1991). Brightness perception and filling-in. *Vision Res, 31*(7-8), 1221-1236.

Parducci, A. (1959). An adaptation-level analysis of ordinal effects in judgment. *J. Exp. Psychol., 58*, 239-246.

Parker, A. J. (2007). Binocular depth perception and the cerebral cortex. *Nat Rev Neurosci, 8*(5), 379-391.

Pasalar, S., Ro, T., & Beauchamp, M. S. (2010). TMS of posterior parietal cortex disrupts visual tactile multisensory integration. *Eur J Neurosci, 31*(10), 1783-1790.

Patten, M. L., & Murphy, A. P. (2012). Relative disparity processing in the dorsal visual pathway. *J Neurosci, 32*(16), 5353-5355.

Pelekanos, V., Ban, H., & Welchman, A. E. (2015). Brightness masking is modulated by disparity structure. *Vision Res, 110*(Pt A), 87-92.

Pelli, D. G. (1997). The VideoToolbox software for visual psychophysics: transforming numbers into movies. *Spat Vis, 10*(4), 437-442.

Pessoa, L., & Neumann, H. (1998). Why does the brain fill in? *Trends Cogn Sci, 2*(11), 422-424.

Pessoa, L., Thompson, E., & Noe, A. (1998). Finding out about filling-in: a guide to perceptual completion for visual science and the philosophy of perception. *Behav Brain Sci, 21*(6), 723-748; discussion 748-802.

Pierrot-Deseilligny, C., Rivaud, S., Gaymard, B., Muri, R., & Vermersch, A. I. (1995). Cortical control of saccades. *Ann Neurol, 37*(5), 557-567.

Poggio, G. F., & Fischer, B. (1977). Binocular interaction and depth sensitivity in striate and prestriate cortex of behaving rhesus monkey. *J Neurophysiol, 40*(6), 1392-1405.

Polat, U., Sterkin, A., & Yehezkel, O. (2007). Spatio-temporal low-level neural networks account for visual masking. *Adv Cogn Psychol, 3*(1-2), 153-165.

Press, W. A., Brewer, A. A., Dougherty, R. F., Wade, A. R., & Wandell, B. A. (2001). Visual areas and spatial summation in human visual cortex. *Vision Res, 41*(10-11), 1321-1332.

Preston, T. J., Li, S., Kourtzi, Z., & Welchman, A. E. (2008). Multivoxel pattern selectivity for perceptually relevant binocular disparities in the human brain. *J Neurosci, 28*(44), 11315-11327.

Raiguel, S., Vogels, R., Mysore, S. G., & Orban, G. A. (2006). Learning to see the difference specifically alters the most informative V4 neurons. *J Neurosci, 26*(24), 6589-6602.

Ramachandran, V. S. (1992). Filling in the blind spot. *Nature, 356*(6365), 115.

Ramachandran, V. S., & Gregory, R. L. (1991). Perceptual filling in of artificially induced scotomas in human vision. *Nature, 350*(6320), 699-702.

Rambo, W. W. (1961). Effect of order of presentation of stimuli upon absolute judgments. *Psychological Reports, 8*, 219-224.

Roe, A. W., Parker, A. J., Born, R. T., & DeAngelis, G. C. (2007). Disparity channels in early vision. *J Neurosci, 27*(44), 11820-11831.

Rogers, B., & Collett, T. S. (1989). The appearance of surfaces specified by motion parallax and binocular disparity. *Q J Exp Psychol A, 41*(4), 697-717.

Rogers, B., & Graham, M. (1982). Similarities between motion parallax and stereopsis in human depth perception. *Vision Res, 22*(2), 261-270.

Rubens, M. T., & Zanto, T. P. (2012). Parameterization of transcranial magnetic stimulation. *J Neurophysiol, 107*(5), 1257-1259.

Ruzzoli, M., Abrahamyan, A., Clifford, C. W., Marzi, C. A., Miniussi, C., & Harris, J. A. (2011). The effect of TMS on visual motion sensitivity: an increase in neural noise or a decrease in signal strength? *J Neurophysiol, 106*(1), 138-143.

Ruzzoli, M., Marzi, C. A., & Miniussi, C. (2010). The neural mechanisms of the effects of transcranial magnetic stimulation on perception. *J Neurophysiol, 103*(6), 2982-2989.

Sack, A. T., Kohler, A., Linden, D. E., Goebel, R., & Muckli, L. (2006). The temporal characteristics of motion processing in hMT/V5+: combining fMRI and neuronavigated TMS. *Neuroimage, 29*(4), 1326-1335.

Sasaki, Y., Nanez, J. E., & Watanabe, T. (2010). Advances in visual perceptual learning and plasticity. *Nat Rev Neurosci, 11*(1), 53-60.

Sasaki, Y., Rajimehr, R., Kim, B. W., Ekstrom, L. B., Vanduffel, W., & Tootell, R. B. (2006). The radial bias: a different slant on visual orientation sensitivity in human and nonhuman primates. *Neuron, 51*(5), 661-670.

Schenk, T., & McIntosh, R. D. (2010). Do we have independent visual streams for perception and action? *Cogn Neurosci, 1*(1), 52-62.

Schiller, P. H., Slocum, W. M., Jao, B., & Weiner, V. S. (2011). The integration of disparity, shading and motion parallax cues for depth perception in humans and monkeys. *Brain Res, 1377*, 67-77.

Sereno, M. I., Dale, A. M., Reppas, J. B., Kwong, K. K., Belliveau, J. W., Brady, T. J., et al. (1995). Borders of multiple visual areas in humans revealed by functional magnetic resonance imaging. *Science, 268*(5212), 889-893.

Shiozaki, H. M., Tanabe, S., Doi, T., & Fujita, I. (2012). Neural activity in cortical area V4 underlies fine disparity discrimination. *J Neurosci, 32*(11), 3830-3841.

Silvanto, J., & Pascual-Leone, A. (2008). State-dependency of transcranial magnetic stimulation. *Brain Topogr, 21*(1), 1-10.

Sinha, P., & Adelson, E. H. (1993). *Recovering Reflectance and Illumination in a World of Painted Polyhedra*. Paper presented at the Fourth International Conference on Computer Vision.

Sousa, R., Brenner, E., & Smeets, J. B. (2009). Slant cue are combined early in visual processing: evidence from visual search. *Vision Res, 49*(2), 257-261.

Stevens, K. A. (1983). Surface tilt (the direction of slant): a neglected psychophysical variable. *Percept Psychophys, 33*(3), 241-250.

Tsao, D. Y., Vanduffel, W., Sasaki, Y., Fize, D., Knutsen, T. A., Mandeville, J. B., et al. (2003). Stereopsis activates V3A and caudal intraparietal areas in macaques and humans. *Neuron, 39*(3), 555-568.

Tyler, C. W., Likova, L. T., Kontsevich, L. L., & Wade, A. R. (2006). The specificity of cortical region KO to depth structure. *Neuroimage, 30*(1), 228-238.

Uka, T., & DeAngelis, G. C. (2003). Contribution of middle temporal area to coarse depth discrimination: comparison of neuronal and psychophysical sensitivity. *J Neurosci, 23*(8), 3515-3530.

Uka, T., & DeAngelis, G. C. (2006). Linking neural representation to function in stereoscopic depth perception: roles of the middle temporal area in coarse versus fine disparity discrimination. *J Neurosci, 26*(25), 6791-6802.

Uka, T., Tanabe, S., Watanabe, M., & Fujita, I. (2005). Neural correlates of fine depth discrimination in monkey inferior temporal cortex. *J Neurosci, 25*(46), 10796-10802.

Ungerleider, L. G., & Mishkin, M. (1982). Two Cortical Visual Systems. In D. J. Ingle, Goodale, M. A. & Mansfield, R. J. W. (Ed.), *Analysis of Visual Behavior* (pp. 549-586). Boston: MIT Press.

Van Oostende, S., Sunaert, S., Van Hecke, P., Marchal, G., & Orban, G. A. (1997). The kinetic occipital (KO) region in man: an fMRI study. *Cereb Cortex, 7*(7), 690-701.

Vreven, D. (2006). 3D shape discrimination using relative disparity derivatives. *Vision Res, 46*(25), 4181-4192.

Walsh, V., & Cowey, A. (1998). Magnetic stimulation studies of visual cognition. *Trends Cogn Sci, 2*(3), 103-110.

Walsh, V., & Cowey, A. (2000). Transcranial magnetic stimulation and cognitive neuroscience. *Nat Rev Neurosci, 1*(1), 73-79.

Wandell, B. A., Dumoulin, S. O., & Brewer, A. A. (2007). Visual field maps in human cortex. *Neuron, 56*(2), 366-383.

Watson, A. B., & Pelli, D. G. (1983). QUEST: a Bayesian adaptive psychometric method. *Percept Psychophys, 33*(2), 113-120.

Watt, R. J., & Morgan, M. J. (1985). A theory of the primitive spatial code in human vision. *Vision Res, 25*(11), 1661-1674.

Weil, R. S., & Rees, G. (2011). A new taxonomy for perceptual filling-in. *Brain Res Rev, 67*(1-2), 40-55.

Welchman, A. E., Deubelius, A., Conrad, V., Bulthoff, H. H., & Kourtzi, Z. (2005). 3D shape perception from combined depth cues in human visual cortex. *Nat Neurosci, 8*(6), 820-827.

Welchman, A. E., & Harris, J. M. (2003a). Is neural filling-in necessary to explain the perceptual completion of motion and depth information? *Proc Biol Sci, 270*(1510), 83-90.

Welchman, A. E., & Harris, J. M. (2003b). Task demands and binocular eye movements. *J Vis, 3*(11), 817-830.

Wheatstone, C. (1838). Contributions to the physiology of vision: I. On some remarkable and hitherto unobserved phenomena of binocular vision. *Philos. Trans. R. Soc. London*(128), 371–394.

Wohlgemuth, A. (1911). On the after-effect of seen movement. *British Journal of Psychology*(1), 1-117.

Xu, Y., & Chun, M. M. (2006). Dissociable neural mechanisms supporting visual short-term memory for objects. *Nature, 440*(7080), 91-95.

Yang, Q., & Kapoula, Z. (2004). TMS over the left posterior parietal cortex prolongs latency of contralateral saccades and convergence. *Invest Ophthalmol Vis Sci, 45*(7), 2231-2239.

Yang, T., & Maunsell, J. H. (2004). The effect of perceptual learning on neuronal responses in monkey visual area V4. *J Neurosci, 24*(7), 1617-1626.

Zeki, S., Perry, R. J., & Bartels, A. (2003). The processing of kinetic contours in the brain. *Cereb Cortex, 13*(2), 189-202.

Zeki, S., Watson, J. D., Lueck, C. J., Friston, K. J., Kennard, C., & Frackowiak, R. S. (1991). A direct demonstration of functional specialization in human visual cortex. *J Neurosci, 11*(3), 641-649.